Investigating the interaction between the *Xenopus laevis* protein p43 and 5S rRNA

by

Heather V. Croft
B.Sc., University of Victoria, 2001

A Thesis Submitted in Partial Fulfillment of the
Requirements of the Degree of

MASTER OF SCIENCE

In the Department of Biochemistry and Microbiology

© Heather V. Croft, 2004
University of Victoria
All rights reserved. This thesis may not be reproduced in whole or on part, by photocopy or other means, without the permission of the author.

Supervisor: Dr. Paul Romaniuk

ABSTRACT

The p43 protein is a major component of the 42S ribonucleoprotein (RNP) storage particle found in the cytoplasm of immature oocytes from the African clawed frog, *Xenopus laevis*. p43 has nine tandemly repeated zinc fingers that are nearly identical with respect to size and spacing of the archetypal C2H2 zinc finger protein, TFIIIA. Although both of these proteins bind to the same natural ligand, 5S rRNA, biochemical evidence suggests that each protein binds the RNA in a unique way.

More is known about the interaction of TFIIIA with 5S rRNA than is known about the interaction of p43 with this RNA. Therefore, the experiments conducted in this thesis focused on the molecular interactions between p43 and 5S rRNA. The binding affinities and contact sites of mutant p43 proteins to 5S rRNA were studied.

A yeast three-hybrid system was one approach used to probe the interactions between p43 and 5S rRNA. In this system, the expression of the *HIS3* and *beta-galactosidase* genes relies upon an interaction between the protein and the RNA of interest. Random mutations were introduced into wild type p43 cDNA by error-prone PCR. The yeast *Saccharomyces cerevisiae* was co-transformed with the PCR products and a linearized plasmid which, following homologous recombination, grew on histidine-deficient medium. Colonies that demonstrated histidine prototrophy were studied further for the strength of the RNA-protein interaction by assaying for beta-galactosidase activity. From a pool of approximately 1300 colonies, 152 colonies that expressed putative p43 mutants exhibiting reduced 5 S RNA binding activity were identified. Fifteen of these 152 colonies were demonstrated by Western blotting to express a protein

with an apparent molecular weight equal to wild type p43. Nine of these 15 colonies had cDNAs that were shown by DNA sequencing to contain actual mutations. Three of these p43 mutants were characterized by *in vitro* 5 S RNA binding assays. None of the mutants characterized exhibited a significant decrease in 5S rRNA binding activity in this assay. Possible reasons for this discrepancy between the *in vivo* and *in vitro* results are discussed.

To identify the specific amino acid residues of p43 involved in 5S rRNA binding, a series of finger swap and deletion mutants were constructed by PCR. These mutants were characterized by *in vitro* 5 S RNA binding assays. The results from these studies indicate that the specific protein-nucleic acid interactions in the biological pathway of 5 S rRNA use a mechanism that, in the case of p43, may involve the C-terminal region of the protein and inter-finger interactions.

TABLE OF CONTENTS

LIST OF TABLES

LIST OF FIGURES

LIST OF ABBREVIATIONS

3-AT	3-amino-1,2,4-triazole
A650	Absorbance at 650 nm
bp	base pair
BSA	bovine serum albumin
cDNA	complementary deoxyribonucleic acid
cpm	counts per minute
d	day (s)
D. radiodurans	*Deinococcus radiodurans*
dNTP	deoxyribonuceotide triphosphate
	dATP deoxyadenosine triphosphate
	dCTP deoxycytidine triphosphate
	dGTP deoxyguanosine triphosphate
	dTTP deoxythymidine triphosphate
DEPC	diethyl pyrocarbonate
dH_2O	deionized water
DNA	deoxyribonucelic acid
DTT	dithiothreitol
E. coli	*Escherichia coli*
EDTA	ethylenediamine-tetraacetic acid
HIV	human immunodeficiency virus
HIV Rev	nuclear export factor for unspliced viral RNA
HIV RRE	RNA region bound by Rev

H. marismotui	*Halobacterium marismotui*	
ICR	internal control region	
IPTG	isopropyl-β-D-thiogalactopyranoside	
KDa	kilodalton	
LB	Luria-Bertani broth	
mRNA	messenger ribonucleic acid	
mw	molecular weight	
NC	nucleocapsid	
nt	nucleotide	
nucleotide bases	A	adenine
	C	cytosine
	G	guanine
	T	thymidine
	U	uracil
	N	either A, C, G or T
nucleotide triphosphates		
	ATP	adenosine triphosphate
	CTP	cytosine triphosphate
	GTP	guanine triphosphate
	UTP	uracil triphosphate
p	probability	
PAGE	polyacrylamide gel electrophoresis	
PCR	polymerase chain reaction	

PMSF	phenylmethylsulfonyl fluoride
poly d(IC)	poly deoxyinosine deoxycytosine
RNA	ribonucleic acid
rRNA	ribosomal ribonucleic acid
RNase	ribonuclease
S	Svedberg unit
SDS	sodium dodecyl sulfate
SFR1	spinyfren receptor 1
t	t-test score
Taq	*Thermus aquaticus*
TBE	Tris base, borate, EDTA
TFIIIA	transcription factor IIIA
TFIIIB	transcription factor IIIB
TFIIIC	transcription factor IIIC
U	unit (s)
T. flavus	*Talaromyces flavus*
T. thermophilus	*Thermus thermophilus*
tRNA	transfer ribonucleic acid
Tris-HCl	tris-(hyrdoxymethyl) aminomethane hydrochloride
UTR	untranscribed region
Xlo	*Xenopus laevis* oocyte
Xls	*Xenopus laevis* somatic

ACKNOWLEDGEMENTS

Many people have been a part of my graduate education, as friends, teachers, and colleagues. Paul Romaniuk, first and foremost, has been all of these. Thank you for pushing me. Time after time, his easy grasp of biochemistry at its most fundamental level helped me in the struggle for my own understanding. I was also fortunate to have been a member of the Romaniuk lab at UVic. Paul, Cheng Yang, Jennifer Campbell, Ioana Rosu, Kate Yakimow, Anna Isbister, Megumi Takiguchi, Frances van der Quack, Julie Foster, Chelsea Patrick and Tristen Weiss were an incredible group, with whom I had many productive scientific discussions.

In addition to the people in the Romaniuk lab, I have been lucky enough to have had the support of many good friends in the Biochemistry Department. Life would not have been the same without my classmates Emily Jansen, Liz Ficko-Blean, Alicia Lammerts-van Bueren and Deanna Dryhurst.

Finally, I would like to thank those closest to me, whose presence helped make the completion of my graduate work possible. I am thankful to Duncan Hogg, who shared my happiness, and made me happy. Thanks for the love, patience and understanding. Most of all, I would like to thank my family, and especially my parents, Tom and Jill Croft, for their absolute confidence in me - it is to them that this thesis is dedicated.

1. OVERVIEW AND INTRODUCTION

The interactions of ribonucleic acids (RNAs) with their protein partners in the cell play diverse and essential roles in many fundamental biological processes including splicing, translational control and transport to specific compartments (Jaeger *et al.*, 2004). The ongoing discovery of structurally well-defined RNAs that participate in functional roles has firmly established RNA as a pivotal character in many cellular processes accomplished by ribonucleoprotein complexes in which RNAs interact permanently or transiently with proteins (Hermann, 2003).

The following examples underscore and illustrate the biological importance of RNA-protein interactions:

1. The RNA targets of the protein p210 BCR/ABL, whose expression is activated in the most malignant disease stage of chronic myelogenous leukemia, have been identified (Perrotti & Calabretta, 2004). Two mRNA targets of this RNA binding protein, c/ebp α and mdm2, are directly relevant for the altered differentiation and survival of leukemic cells (Perrotti & Calabretta, 2004);
2. The mammalian protein CPSF-30 and its homologues in yeast, *Drosophila melanogaster* and *Thermus thermophilus* all contain a zinc finger motif associated with nucleolytic activity (Boysen & Hearn, 2001, Zarudnaya *et al.*, 2002). CPSF-30 and its homologues were found to be the nucleases directly responsible for the cleavage of pre-mRNA in the process of polyadenylation (Zarudnaya *et al.*, 2002);

3. The critical nature of protein-RNA interactions is further illustrated by the transfer-RNA mimicry of viral RNAs that partner with both the translation and replication machinery of host cells (Giege, 1996);
4. Two zinc finger proteins, TFIIIA and p43, store ribosomal 5S rRNA in separate storage particles in the previtellogenic oocytes of amphibians and fish (Joho *et al.*, 1990). A complete explanation for the existence of the two modes of storage for 5S rRNA has yet to be elucidated.

In the absence of a final structural solution for the 42S ribonucleoprotein (RNP) particle, the complex that contains both p43 and 5S rRNA, investigators must rely on chemical and enzymatic probing of these complexes or systematic mutational analyses of the RNA or protein components. Further investigation into a possible role of p43 in the transcription of 5S rRNA genes has been neglected because of an inability of 42S particles to provide proteins that bind 5S rRNA genes and influence their transcription *in vitro* (Hamilton *et al.*, 2001). The interaction between TFIIIA and its RNA ligand is well characterized (reviewed by Pieler, 1994). The difference between the binding specificities of p43 and TFIIIA for 5S rRNA provides an excellent system for investigating the differences in the molecular basis for RNA recognition. It is hypothesized that specific amino acid residues of p43 are involved in 5S rRNA binding. It should be possible to mutate these residues such that the zinc finger domains of p43 remain intact yet binding to 5S rRNA is ablated, thus leading to the identification of the precise amino acid residues of p43 involved in specific 5S rRNA binding.

The subsequent sections will be structured as follows: the molecular details of both the zinc finger protein p43 and its RNA ligand will be explored; the *Xenopus laevis*

system will be described and finally the experimental techniques unique to this project will be presented.

1.1 ZINC FINGER PROTEINS

Zinc finger proteins have roles in diverse cellular processes including DNA recognition for replication and repair, RNA packaging during transcription, protein folding and assembly during translation, signaling via lipid binding and regulation of both cell proliferation and apoptosis (Krishna *et al.*, 2003, Laity *et al.*, 2001). Zinc fingers typically function as interaction modules and bind to a wide variety of compounds such as nucleic acids, proteins and small molecules (Krishna *et al.*, 2003).

Initially used to define a repeated zinc-binding motif with DNA-binding properties in *Xenopus laevis* transcription factor IIIA (TFIIIA), the term "zinc finger" is now largely used to identify any small domain stabilized by a zinc ion (Krishna *et al.*, 2003). A zinc finger is defined as a small, functional, independently folded domain that requires coordination of one or more zinc ions to stabilize its structure (Laity *et al.*, 2001). Illustrated in Figure 1, the zinc finger was first recognized as a repeat of approximately 30 amino acids in *Xenopus* TFIIIA, containing conserved cysteine and histidine ligands that made up a zinc-binding motif (Darby & Joho, 1992, Miller *et al.*, 1985). This motif has since been found in many transcription factors and in other nucleic acid binding proteins (Krishna *et al.*, 2003).

C2H2 zinc fingers, in which zinc binding contributes thermal and conformational stability, are the best studied of the metal ion stabilized small domains (Krishna *et al.*, 2003). Zinc fingers of the C2H2 class coordinate a single zinc atom through two invariant

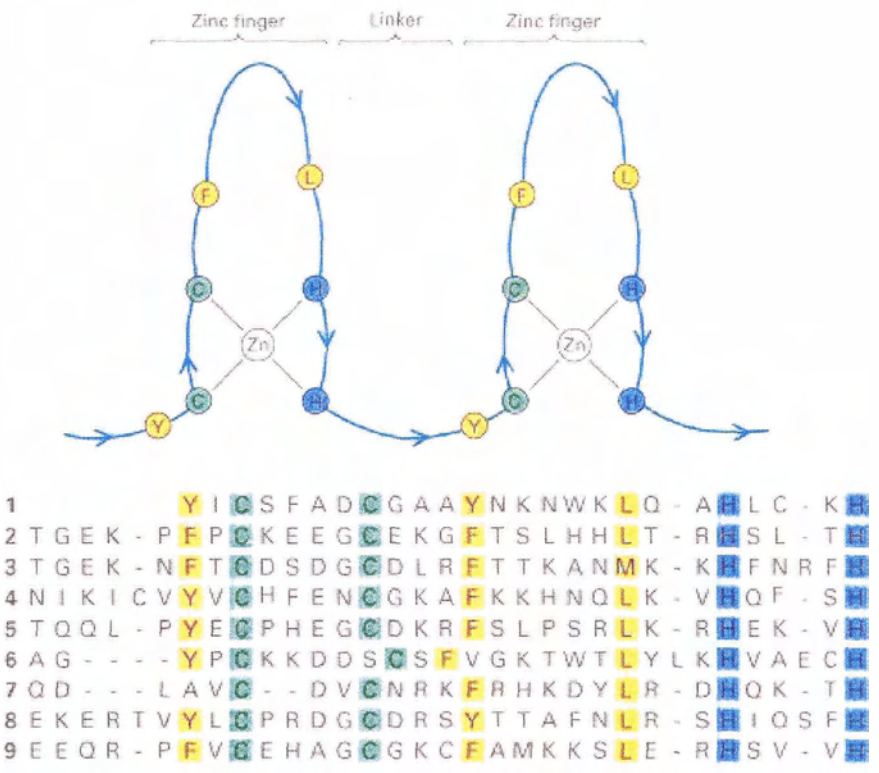

Figure 1. Amino acid sequence of the *Xenopus* zinc finger protein TFIIIA. The repeat of approximately 30 amino acids that comprises the consensus sequence for each of the nine zinc fingers is illustrated. The conserved cysteine and histidine ligands that make up a zinc-binding motif are highlighted in green and blue respectively. Adapted from Stryer (1996).

cysteines, in an antiparallel β sheet, and through two histidines, in an α-helix, illustrated by Figure 2 (Ryan & Darby, 1998). Proteins containing the classical C2H2 zinc finger are among the most abundant proteins in eukaryotic genomes and many putative zinc finger proteins with unknown function have been identified through sequence homology (Darby & Joho, 1992, reviewed by El-Baradi &). However, TFIIIA-like zinc fingers are usually assumed to be transcription factors (Darby & Joho, 1992). Pieler, 1991, Laity *et al.*, 2001).

In addition to the classical C2H2 finger, other combinations of cysteine and histidine as the zinc-chelating residues are possible (Krishna *et al.*, 2003). Domains in the C2H2 zinc finger family contain a β-hairpin followed by an α-helix that forms a left-handed β-β-α unit (Krishna *et al.*, 2003). Two of the zinc ligands are located at the end of the β-hairpin and are contributed by a zinc knuckle, a unique turn with the consensus sequence CPXCG (Krishna *et al.*, 2003). The other two ligands are found at the C-terminal end of the α helix (Krishna *et al.*, 2003). Zinc fingers are commonly arranged in a covalent tandem array of several motifs that function relatively independently of each other (Uil *et al.*, 2003). This arrangement provides the resulting proteins with much greater affinity for their nucleic acid ligands than could be realized with a single zinc finger.

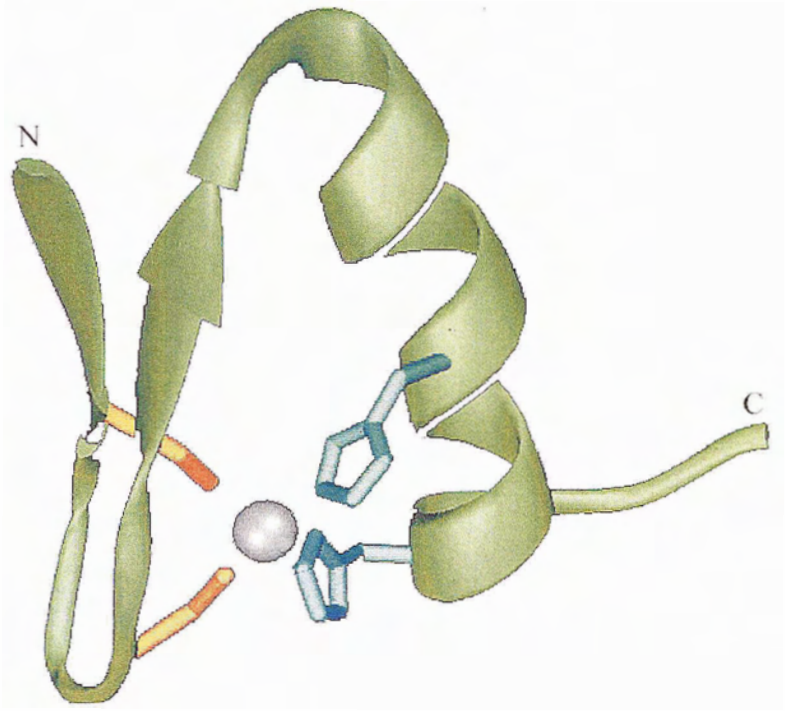

Figure 2. The C2H2 motif is found among many transcription factors and consists of a zinc knuckle and a short beta-hairpin at the N-terminus followed by a small loop and an α-helix. A typical C2H2 zinc figure coordinates a single zinc atom through two invariant cysteines (R groups in orange) in the knuckle of the antiparallel beta sheet and through two histidines (R groups in turquoise) in the C-terminal part of the α helix. Adapted from Bolsover *et al.*, 2004.

1.1.1 RECOGNITION OF NUCLEIC ACIDS BY C2H2 ZINC FINGER DOMAINS

Present in 2 % of all human genes, zinc fingers are by far the most abundant class of nucleic acid-binding domains found in human transcription factors (Jamieson *et al.*, 2003). This large proportional representation of zinc finger-encoding genes reflects a remarkable versatility of this small protein domain for recognizing different nucleic acid base pair sequences. Although regulation of transcription seems to be the most important task performed by C2H2 zinc fingers, recently determined structures of members of this class suggest their roles in mediating protein-protein interactions (Krishna *et al.*, 2003).

1.1.2 RECOGNITION OF DNA BY C2H2 ZINC FINGER DOMAINS

Interactions between C2H2 zinc fingers and DNA have been well studied (Uil *et al.*, 2003). Based on the DNA-binding domain of the 3 finger protein Zif268, binding is believed to occur along one strand of the major groove of the DNA double helix, predominantly via positions –1, 3 and 6 of the N-terminus of the α-helix of each zinc finger, as shown in Figure 3 (Pavletich & Pabo, 1991). Recognition of specific DNA sequences is achieved by the interaction of the DNA bases with the side chains from the surface of the zinc finger's α-helix (Krishna *et al.*, 2003). Attempts to derive a universal rule that relates zinc finger protein sequences to DNA binding site preferences have met with little success (Uil *et al.*, 2003). The lack of a recognition code relating one amino acid to one nucleotide is attributed to the observation that flanking amino acids also play a role in determining DNA base specificity (Uil *et al.*, 2003).

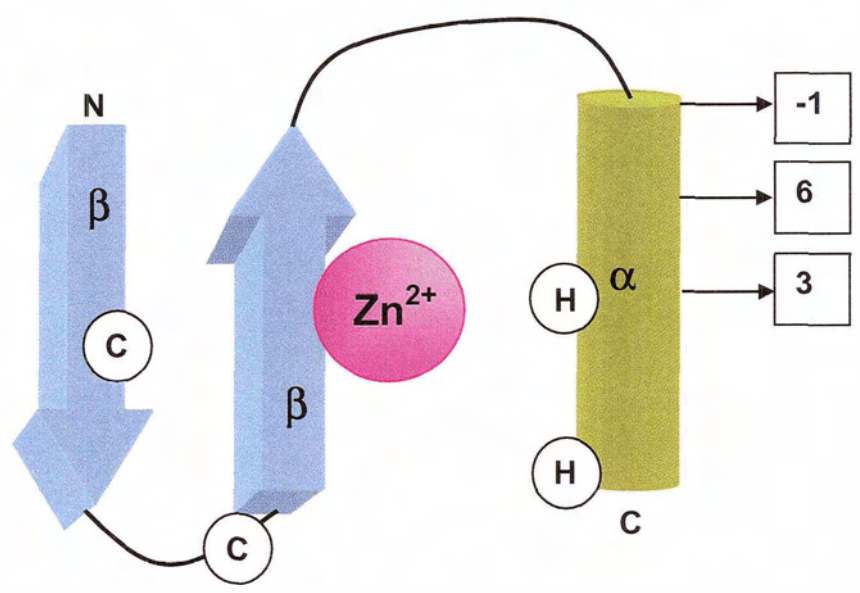

Figure 3. A typical C2H2 zinc finger highlighting the secondary structure motifs; the location of the conserved cysteine and histidine residues that coordinate the zinc ion is indicated. The residues primarily involved in sequence-specific DNA binding are highlighted in the squares. The number in the each square represents the amino acid position relative to the first residue of the □-helix. Adapted from Uil *et al.*, 2003.

1.1.3 RECOGNITION OF RNA BY C2H2 ZINC FINGER DOMAINS

Interactions between RNAs and proteins are fundamental to many cellular processes. The question of how a protein recognizes a specific RNA and which proteins interact with a specific RNA are central to a large number of problems in molecular biology. Like DNA-binding proteins, there is no single archetypal RNA binding site and RNA-binding sites and modes of recognition vary widely. A structural analysis of 32 protein-RNA complexes revealed however that van der Waals interactions are more numerous in protein-RNA complexes than hydrogen bonds (Jones *et al.*, 2001). A preference for proteins making contacts with guanine was observed, and arginine, asparagines, phenylalanine, threonine and tyrosine occurred in RNA-binding sites (Jones *et al.*, 2001).

In the first structural study to describe zinc finger-RNA binding, the three central zinc fingers of the protein TFIIIA were crystallized in a complex with 61 bases of 5S rRNA (Lu *et al.*, 2003). The structure, depicted in Figure 4, revealed two modes of zinc-finger binding. First, the zinc-fingers specifically recognize individual bases that are exposed from the structurally rigid, complicated folded 'loop' regions of the RNA. Second, the zinc-fingers recognize the three-dimensional structures consisting of internal loops and double helices in the RNA. In this latter case, the zinc-finger architecture provides a binding surface where the structure of a regularly folded double-helical region of RNA is recognized. The interaction between TFIIIA zinc finger 5 and 5S rRNA is an example of specific binding by a zinc-finger to double-stranded RNA that is not sequence dependent.

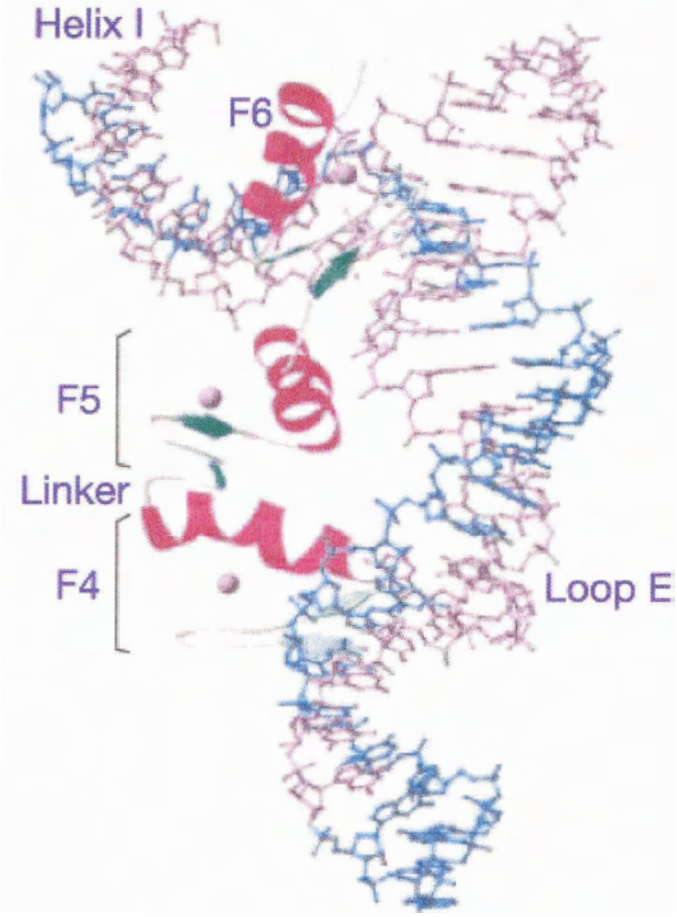

Figure 4. Interactions of a three-zinc finger TFIIIA peptide with a fragment of 5S rRNA. The RNA is represented as a ball-and-stick model with nucleotides 4–82 in purple and nucleotides 83–115 in blue, and the protein is shown as a ribbon model. Purple balls represent zinc ions. Adapted from the crystal structure described by Lu *et al.* (2003).

Combinatorial library experiments have been used to isolate peptide sequences that recognize a given RNA site. In one such study, zinc fingers could only be found to recognize RNA base pair triplets containing G:A or C:A mismatches, consistent with the hypothesis that the α helix of a protein cannot fit into the major groove of an A-form RNA double helix without nearby bulges or mismatches to widen the groove (Weeks & Crothers, 1993). Darby and co-workers (1992) used phage display to isolate zinc fingers that recognize 5S rRNA. In an initial experiment with four randomized positions on one zinc finger helix of the nine-finger TFIIIA protein, 24 peptides were found to bind specifically to the 5S rRNA, all preserving a lysine at a conserved location and a majority preserving a serine at a second conserved site. More recent combinatorial experiments using RNA binding zinc fingers from TFIIIA and the HIV proteins SFR1 and Rev indicate that polar, charged, and hydrophobic contacts can participate in sequence-specific interactions with their respective RNA targets, 5S rRNA and the HIV RRE (Das & Frankel, 2003).

Zinc fingers that interact with RNA are found in the ribosomal proteins from *Halobacterium marismotui*, *Deinococcus radiodurans* and *Thermus thermophilus* (Krishna *et al.*, 2003). These zinc fingers interact mainly at the major groove of RNA, with different parts of the zinc-containing domain making contact with the RNA (Krishna *et al.*, 2003).

1.1.4 EXPLOITING THE SPECIFICITY OF ZINC FINGERS

Zinc finger proteins that recognize specific nucleic acid sequences are the basis of a powerful technology platform with many uses in drug discovery and therapeutics

(Jamieson *et al.*, 2003). These proteins have been employed as the nucleic acid binding domains of novel transcription factors, useful for validating genes as drug targets (Jamieson *et al.*, 2003). Analyzing gene function is an integral part of the modern drug discovery process. The completion of the human genome project has identified more than 30, 000 human genes; thousands of these genes, or their RNA transcripts, may represent potential new drug targets. Recently, synthetic zinc finger proteins have been used as a platform for the design of novel human therapeutics (Jamieson *et al.*, 2003).

1.2 rRNA SYNTHESIS IN *XENOPUS LAEVIS*

The fourth, or diplotene, stage of meiosis prophase may last for several months in developing oocytes. During this time, a phase contrast microscope may be used to observe chromosomes undergoing transcription. Such lampbrush chromosomes have been extensively studied in the oocytes of *Xenopus laevis*. At this stage, the chromosomes are still paired, the two homologues held together by chiasmata, each member of the pair consisting of two chromatids, or DNA duplexes (Adams *et al.*, 1986). The DNA duplexes run the length of the chromosome and are attached to the axial thread in a series of loops giving the structure the appearance of a lampbrush, diagramed in Figure 5 (Adams *et al.*, 1986). The loops are the site of transcriptional activity and the DNA in the loops may be only partly condensed into nucleosomes (Adams *et al.*, 1986).

The study of eukaryotic RNA polymerase activity has been enhanced by the development of systems in which enzymes correctly transcribe specific genes *in vitro*.

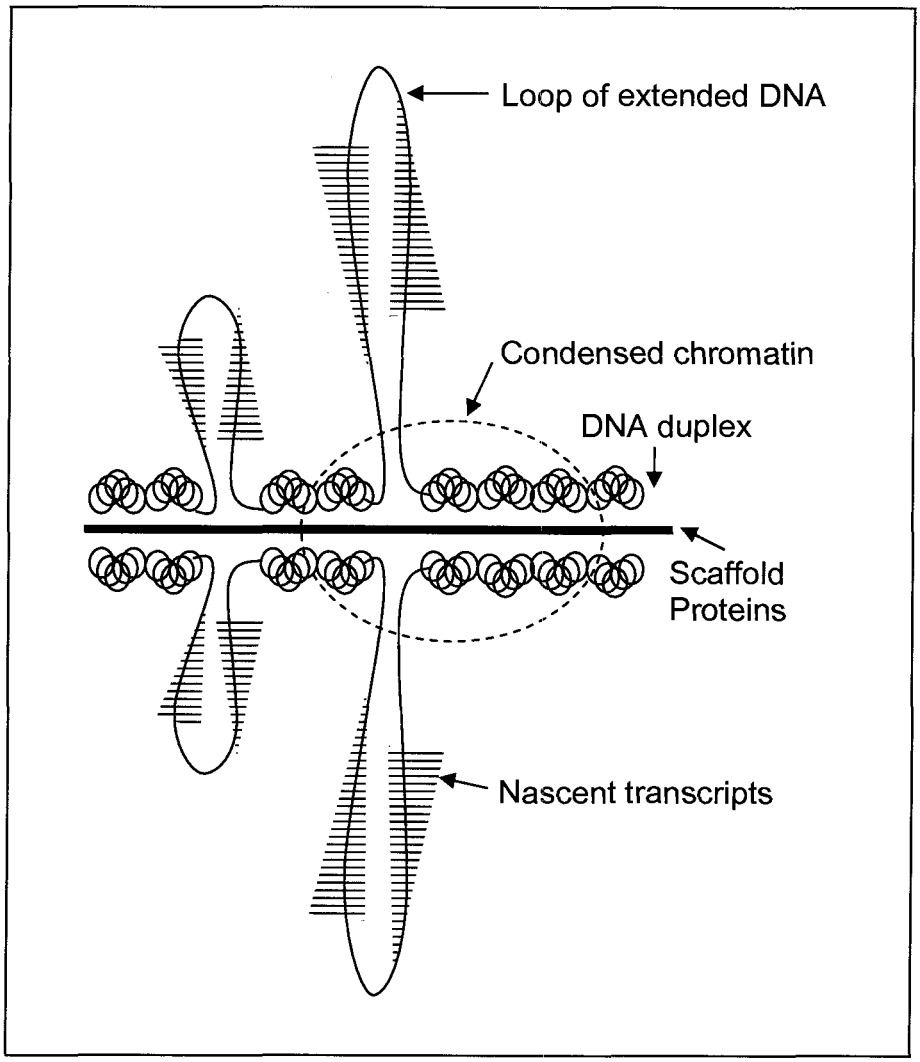

Figure 5. Diagram of part of a lampbrush chromosome showing the paired loops of extended DNA and the effect produced by the nascent transcription of RNA. Adapted from Adams (1986).

The first of these was a transcription system for RNA polymerase III (Wu, 1978). This led to the use of extracts of *Xenopus* oocytes as a major system to study transcription by RNA polymerase III (Wiel *et al.*, 1979, Birkenmeier *et al.*, 1978). The promoters for the genes transcribed by RNA polymerase III lie within the coding region of the gene itself (reviewed by Brown, 1984). The promoter is known as the internal control region or ICR. The ICR is required and sufficient for transcription. TFIIIA binds the ICR, followed sequentially by TFIIIC and TFIIIB; the entire complex is required for recognition by RNA polymerase (Bieker *et al.*, 1984). Incidentally, TFIIIA binds four times more strongly to the ICR region of somatic 5S rRNA genes than to that of oocyte 5S rRNA genes (Brown & Schissel, 1985), possibly explaining the preferential expression of somatic 5S genes over oocyte 5S genes in somatic cells (Honda & Roeder, 1980).

1.2.1 5S rRNA AND *XENOPUS* DEVELOPMENT

The *rrn* genes encode the RNA molecules used in the ribosome. These genes are present in anywhere from 8 copies per genome, as in *E. coli*, to thousands of copies in higher eukaryotes, yet are unique in that they are among only a handful of genes that do not encode protein. The family of oocyte-specific 5S rRNA genes comprises 0.7 % of total genomic DNA and is the largest family of 5S rRNA genes, present in almost all types of ribosomes (Brown *et al.*, 1971, Szymanski *et al.*, 2003). 5S rRNA is absent from the mitochondrial ribosomes of some fungi, verebrates and most protists (Szymanski *et al.*, 2003). Up to 24,000 copies of these genes occur per haploid *Xenopus* chromosome and are organized as tandemly repeated units separated by AT rich spacers (Brown, 1971 *et al.*, Federoff & Brown, 1978). Each tandem repeat contains one active gene followed

by a pseudogene, which duplicates the first 101 base pairs of the active gene (Federoff & Brown, 1978). Degradation of the pseudogene transcript by endogenous RNase activity plays a role in 5S rRNA turnover (Federoff & Brown, 1978).

Oocyte-specific 5S rRNA accumulates during early oogenesis due to the activation of the *rrn* gene family. Up to 75 % of the total cellular RNA of previtellogenic (early oogenesis) oocytes consists of 5S rRNA and tRNA (Mairy & Denis, 1971). In the vitellogenic period, tRNA is released into the cytoplasm and 5S rRNA is incorporated into the 60S large ribosomal subunit (Mairy & Denis, 1972, Szymanski *et al.*, 2003). The nucleolus is the site of ribosome assembly within the nucleus. RNA polymerase I transcribes all ribosomal RNA genes except the 5S gene into a single transcript. This transcript is further processed to yield the mature 28S, 18S and 5.8S ribosomal RNAs. All rRNAs are required in roughly equal copy number, yet the method of co-regulation of the large pre-rRNA transcript and the 5S rRNA transcript remains unknown. The precise role of 5S rRNA in ribosome function is not fully understood. Its importance for protein biosynthesis was demonstrated in *E. coli*, in which a deletion of one 5S rRNA gene greatly impaired the growth rate (Ammons *et al.*, 1999).

1.2.2 STORAGE OF 5S rRNA

Unlike somatic cells, previtellogenic oocytes of amphibian and fish store large amounts of both tRNA and 5S rRNA complexed to proteins (Joho *et al.*, 1990). These complexes accumulate as the 7S and 42S ribonucleoprotein (RNP) particles in the cytoplasm for use later in oogenesis and embryonic development (Joho *et al.*, 1990, Zang & Romaniuk, 1995). Both RNP particles serve as storage complexes for 5S rRNA prior

to ribosome assembly, which occurs later in oocyte development (Zang & Romaniuk, 1995).

The cartoon in Figure 6 illustrates the proteins that associate with 5S rRNA. In *Xenopus laevis*, the 7S RNP is composed of one molecule of oocyte-specific 5S rRNA and one molecule of transcription factor IIIA (TFIIIA) (Brown *et al.*, 1990, Zang & Romaniuk, 1995). TFIIIA is a 38 kDa zinc finger protein that interacts not only with 5S rRNA, but also with the 60-bp internal control region (ICR) of 5S rRNA genes, defining the first step in the formation of an active transcription complex (Joho *et al.*, 1990, Darby & Joho, 1992, Pieler, 1994, Zang & Romaniuk, 1995).

The 42S RNP particle is found in immature oocytes as a tetrameric complex, and contains the proteins p48 and p43, tRNA and 5S rRNA in a molar ratio of 2:2:3:1 (Joho *et al.*, 1990, Zang & Romaniuk, 1995). Historically, the 42S particle was referred to as a thesaurisome, and the proteins p48 and p43 were known respectively as thesaurins a and b (Joho *et al.*, 1990). p48 has been characterized as a diverged form of the elongation factor EF-1α that binds to a variety of aminoacyl-tRNA molecules (Joho *et al.*, 1990).

1.2.3 *XENOPUS LAEVIS* AS A MODEL SYSTEM

Xenopus laevis, the African clawed frog, derives its name from the keratinous claws that cover its medial toes and from its geographic range, which spans much of southern Africa. *Xenopus* is aquatic and bears several adaptations for this environment, including a dorsoventrally flattened body, dorsally directed eyes, the presence of a lateral line system throughout life, and large muscular hindlimbs. These

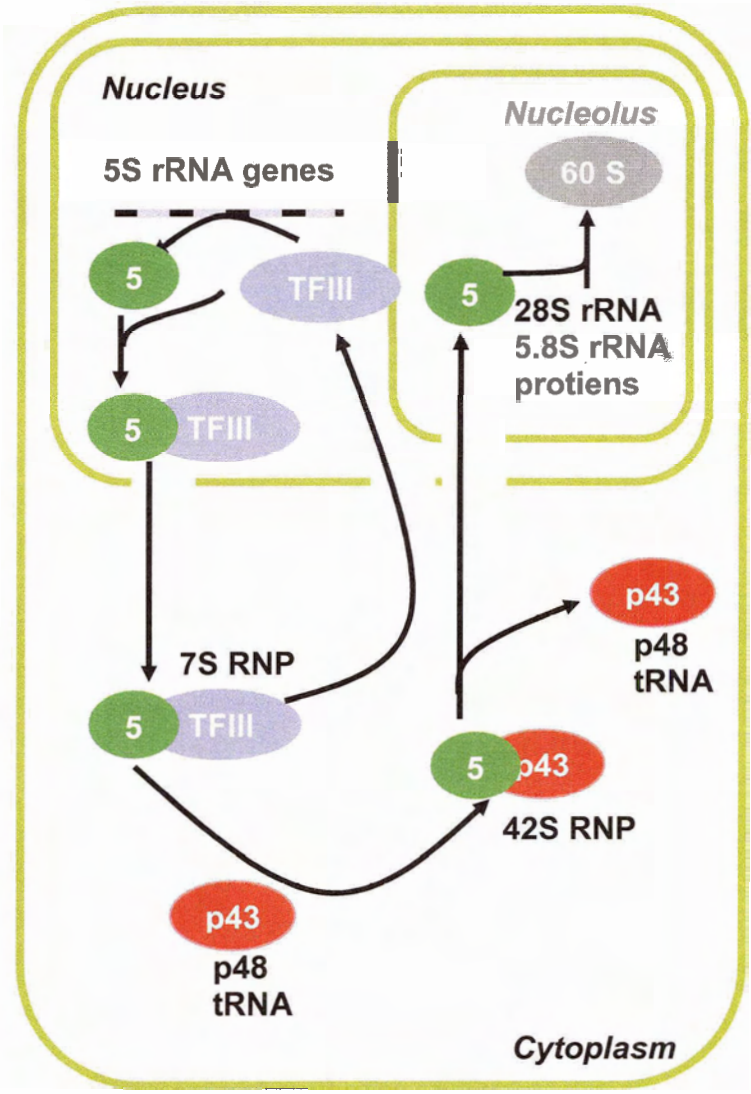

Figure 6. Proteins that interact with 5S rRNA. 5S rRNA genes are transcribed by RNA polymerase III. TFIIIA is involved in transcription initiation. It binds 5S rRNA, and is exported from the nucleus to the cytoplasm as the 7S RNP. 5S rRNA can be exchanged from the 7S RNP to form the 42S RNP, or a 5S RNP complex with ribosomal protein L5 that is imported to the nucleus and then to the nucleolus, where it is incorporated into the large ribosomal subunit, synthesized and accumulated in oocytes far in excess of the amounts found in somatic cells. Adapted from Joho *et al.*, 1990.

frogs are considered unique in that they lack tongues, vocal sacs, and vocal chords (De Sa & Hillie, 1990).

Xenopus is a member of Family Pipidae and was traditionally regarded as occupying a basal position within this family. Subsequent phylogenetic analyses indicated that *Xenopus* is the most recent common pipoid ancestor of two sub-families, the Pipinse, which encompasses the genera *Pipa, Hymenochirus* and *Pseudohymenochirus*, and the Xenopodinae, made up of the sister taxa *Silurana* and *Xenopus* (De Sa & Hillie, 1990).

Since the 1930s *Xenopus* has been used extensively as a laboratory organism for physiological research; but more recently, it also has become popular for developmental and genetic studies (Cannatella and De Sa, 1993). The usefulness of *Xenopus* as a model organism is due largely to the ease of maintaining breeding populations in the laboratory (Cannatella and De Sa, 1993).

1.3 THE ZINC FINGER PROTEINS EXPLOITED IN THIS STUDY

1.3.1 p43 AND TFIIIA

The 42S RNP component of interest in this project is the protein p43 (reviewed by Szymanski *et al.*, 2003). p43 cDNA was initially cloned from a *Xenopus* oocyte cDNA λ-g11 expression library using an anti-p43 antibody (Joho *et al.*, 1990). p43 is encoded by a single genomic gene that is transcribed abundantly in immature oocytes (Joho *et al.*, 1990). This 5S rRNA binding protein is structurally similar to TFIIIA, containing nine zinc finger domains, seven of which are exactly the same size as their TFIIIA

counterparts (Joho *et al.*, 1990, Zang & Romaniuk, 1995). The 33 % amino acid sequence identity between these two proteins is due to the amino acid residues characteristic of the zinc finger structure (Joho *et al.*, 1990, Zang & Romaniuk, 1995). The amino acid sequences of the two proteins differ extensively throughout the zinc fingers and are completely different at both their amino- and carboxyl-termini beyond the zinc fingers (Joho *et al.*, 1990). Both proteins are basic overall, and their charge distribution is similar (Joho *et al.*, 1990). Atomic absorption spectroscopy determined that a single molecule of p43 contains a minimum of four zinc atoms (Joho *et al.*, 1990). Most of the zinc fingers of p43 lack the aromatic amino acid residue that typically precedes the cysteine in each finger of TFIIIA (Joho *et al.*, 1990). This aromatic amino acid is predicted to form a hydrogen bond with another conserved aromatic amino acid at position 10 of the finger (Joho *et al.*, 1990). p43 also lacks the conserved linker polypeptide TGEK that is found in many zinc finger proteins, including zinc finger 1-3 of TFIIIA (Joho *et al.*, 1990, Ryan & Darby, 1998). Despite its abundance in immature oocytes, purification of p43 was complicated by its affinity for p48 and its insolubility as a free polypeptide (Joho *et al.*, 1990).

In addition to the structural differences between p43 and TFIIIA, a key functional difference exists between the proteins: p43 binds specifically to 5S rRNA, while TFIIIA binds both the 5S rRNA gene and its transcript (Joho *et al.*, 1990, Zang & Romaniuk, 1995). This difference in binding specificity provides an excellent model system for investigating the differences in the molecular basis for RNA and DNA recognition (Ryan & Darby, 1998).

A BLAST search was performed with the protein sequence of p43. While *Xenopus* TFIIIA from shares only 37 % amino acid identity with *Xenopus* p43, several proteins in the NCBI database were observed to share greater p43 sequence identity. A 367 amino acid protein from *Tetraodon nigroviridis* (Genoscope sequence ID: SCAF15054), shares 39 % identity. Three proteins share 38 % amino acid identity: a 363 amino acid human DNA/RNA-binding protein fragment similar to *Xenopus* TFIIIA encoded by SwissProt Accession Number P03001 (Drew et al., 1995), mouse TFIIIA (Hanas et al., 2002) and a chicken DNA/RNA binding protein predicted by automated computational analysis (Accession # XP_417125).

1.3.2 THE WILMS' TUMOR SUPPRESSOR PROTEIN, WT1

The Wilms' tumour gene, *WT1*, encodes a four C2H2 zinc-finger transcription factor with a high degree of structural homology to the early growth response family of transcription factors (Wagner *et al.*, 2003). This gene is mutated in a proportion of embryonic kidney cancers termed Wilms' tumours (Wagner *et al.*, 2003). Wilms' tumour is the most common genitourinary malignancy in children, accounting for 95 % of malignancies affecting the genitourinary tract and 8 % of childhood malignancies (Wagner *et al.*, 2003). In addition to its function as a tumour suppressor, WT1 has multiple roles during development of the kidney and gonad (Nachtigal *et al.*, 1998). Hence, mutations in WT1 are found in a variety of pediatric disease phenotypes that share a high incidence of urogenital defects (Nachtigal *et al.*, 1998), including Denys-Drash and Frasier syndromes (Wagner *et al.*, 2003). Additional studies have linked WT1 mutations to malignancies such as leukemia, breast cancer, lung cancer and

retinoblastoma (Wagner *et al.*, 2003). WT1 is expressed in many mammalian tissues during embryonic development, including the urogenital system, spleen, spinal cord, mesothelial organs and diaphragm (Wagner *et al.*, 2003). WT1 is also expressed in certain fully differentiated cells, including glomerular podocytes in the kidney, where WT1 is required for maintenance of kidney function (Wagner *et al.*, 2003).

The human WT1 gene consists of 10 exons (Wagner *et al.*, 2003). Exon 9 is alternatively spliced to yield a product that has either omitted or included a tripepetide KTS sequence between the third and fourth zinc finger (Wagner *et al.*, 2003). Consequently, isoforms lacking the KTS sequence are referred to as WT1 (-KTS) whereas those containing the sequence are called WT1 (+KTS) (Wagner *et al.*, 2003). Mutations that interfere with the ratio of WT1 (+KTS) to WT1 (-KTS) lead to Frasier syndrome, indicating the importance of the ratio of these variants (Wagner *et al.*, 2003). WT1 (+KTS) products have a much higher affinity for RNA that for DNA and are thought to play a role in RNA processing (Wagner *et al.*, 2003). The importance of WT1 (+KTS) in sex determination has been demonstrated in the gonads of mice that lack the +KTS isoform and develop solely as females (Wagner *et al.*, 2003). None of the WT1 isoforms have a binding affinity for 5S rRNA (Hamilton *et al.*, 2001).

1.4 GENERAL FEATURES OF RNA

1.4.1 SECONDARY STRUCTURE OF RNA

RNA has a variety of functions within the cell; for each function, a specific type of RNA with a secondary and tertiary structure unique to that molecule is required. While

RNA molecules do not possess the interstrand hydrogen-bonded structure of DNA, they can still form double-helical regions. RNA helices are frequently found between two segments of the same chain folded back to form an intrastrand base-paired stem (Adams *et al.*, 1986). This helical secondary structure is analogous to the A form of DNA with tilted bases, however the 2'OH of the ribose hinders B structure formation (Adams *et al.*, 1986). Helical regions formed by intrastrand base-pairing are seldom regular; often, opposing segments on the chain do not have entirely complementary sequences, so non-bonded residues project out of the structure as loops. In some RNA molecules, 70 % of the bases are involved in secondary structure interactions (Adams *et al.*, 1986).

In addition to the expected A:U and G:C base pairs, RNA molecules frequently show unusual G:U base pairing (Adams *et al.*, 1986). Formation of a stable duplex, however, requires at least three conventional base pairs and the stability of this duplex depends on three factors that must be satisfied before confidence can be placed in predictions of secondary structure for RNA:

1. The various base pairs have differing stability that is modified by the nature of the adjacent base pairs and the presence of interruptions of the duplex region. The most stable base pairs are C:G or G:C base pairs following a G:C base pair (Tinoco *et al.*, 1973);
2. Along a duplex region, unpaired bases may form bulges or short loops. These have a strong destabilizing effect on the duplex region (Adams *et al.*, 1986);
3. At one end of an intrastrand base-paired stem, there is a hairpin loop consisting of a minimum of three unpaired nucleotides. Hairpin loops with

six unpaired bases are the most stable, but even these reduce the stability of the duplex region. With shorter loops, steric hindrance and base-stacking interactions destabilize the loop. Yet the greater the distance between self-complementary regions, the less likely it becomes that duplex regions will be formed. If the stem-loop region is more stable than $\Delta G = -40\ kJ/mol^{-1}$, there is a possibility that such regions will exist *in vivo* (Woese *et al.*, 1980, Atmadja *et al.*, 1984).

1.4.2 THE TERTIARY STRUCTURE OF RNA

X-ray crystallographic data of many small RNA molecules show that extensive folding of partially duplex arms occurs (Adams *et al.*, 1986). The subsequent hydrogen bonding of those bases not already involved in secondary structure formation is important in stabilizing the folds. The type of hydrogen bonding involved is frequently not that found in the conventional Watson-Crick pair. In addition, short, triple-stranded regions can occur in which two of the chains run parallel with one another.

1.4.3 STRUCTURAL FEATURES OF 5S rRNA

An attempt to discover the function of any macromolecule invariably leads to a study of its structure. Rosset and Monier discovered 5S rRNA a short time after the discovery of the ribosome in 1963, and due to its small size (120 nucleotides), a wealth of sequence information became rapidly available. Initial analysis of the primary structure shows a good deal of complementation along certain stretches of the primary sequence, which form stem-loop structures.

Unlike transfer RNA (tRNA) and other non-coding RNA molecules, individual bases in 5S rRNA are rarely modified, however the helices are often distorted by a G:U base pair. Initially thought to form non-canonical Watson-Crick pairs, it is now established that the guanosine and uracil residues do not pair at all; their purpose in most RNA molecules appears to be the destabilization of the helical structure (Szymanski *et al.*, 2003). In yeast cells, for example, a G:U base pair in the acceptor stem of the alanine-tRNA is sufficient for recognition by the alanine aminoacyl synthetase (Szymanski *et al.*, 2003). G:U bases are also thought to play an important role in the splicing of group I introns. In the case of 5S rRNA of eukaryotes, it was established by Szymanski (2000) that the helical distortions introduced by this mispairing can be minimized by a purine upstream of the guanosine, but the majority of eukaryotic sequences had cytosine or uracil upstream of the mismatch. The conserved locations of the G:U pairs and subsequent loops indicate that this motif is used as a recognition site for proteins and possibly RNAs associated with 5S rRNA.

1.4.4 SECONDARY STRUCTURE OF 5S rRNA

The 5S rRNA molecule is approximately 120 nucleotides long, with a molecular mass of approximately 40 kDa (Szymanski *et al.*, 2003). A comparison of compensating base changes in more than 700 5S rRNA primary sequences has been used to establish a universal secondary structure for this RNA (Pieler, 1994). The common secondary structure is illustrated in Figure 7 and consists of five helices (I-V), separated by internal loops (B and E) or closed by hairpin loops (C and D) and a hinge region (A) (Pieler, 1994). Primary sequence conservation is usually higher in loops than in the centre of

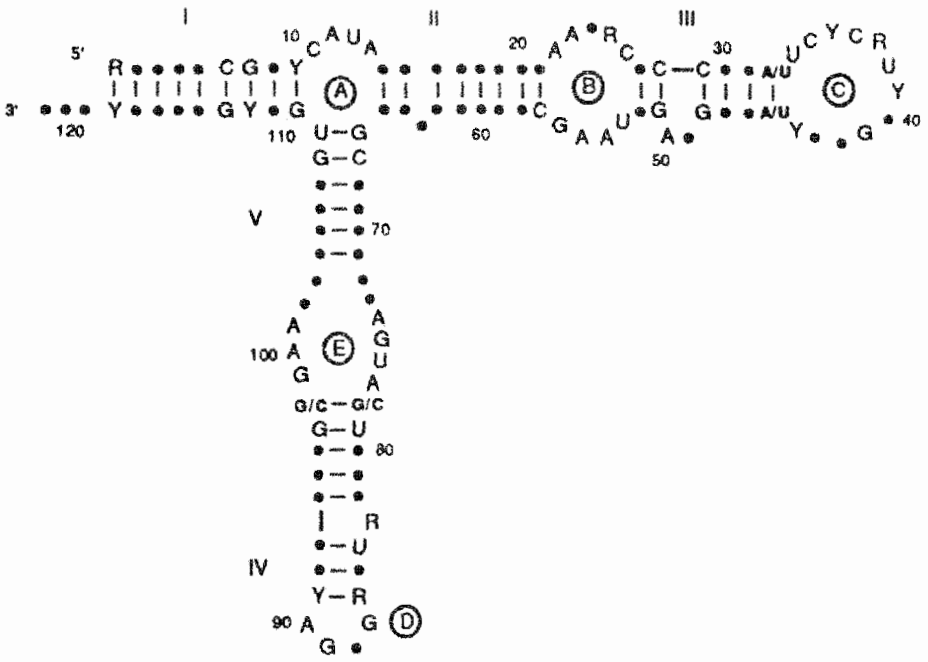

Figure 7. General eukaryotic consensus sequence for 5S rRNA (Romaniuk, 1989).

base-paired elements (Pieler, 1994). The crystal structure of a large ribosomal subunit from *Halobacterium marismortui* allowed verification of the secondary structure of 5S rRNA that had been inferred from both phylogenetic analysis and structural studies. Most of the base pairs predicted in the structural analysis were detected in the crystal structure (Ban *et al.*, 2000).

1.4.5 TERTIARY STRUCTURE OF 5S rRNA

A tertiary structure for the 5S rRNA molecule in its entirety is not yet available, despite the crystallization of whole ribosomes at relatively high resolutions. An obstacle to obtaining a 5S rRNA structure is the significant conformational change that the molecule undergoes upon incorporation into the large ribosomal subunit. Although the tertiary structure of 5S rRNA is not known, the secondary structure depicts the shape of 5S rRNA predicted by the molecular model of Westhof and Leontis (1998).

The crystal structure of helix I from *Talaromyces flavus* 5S rRNA was solved at a high resolution. Water molecules form a hydrogen bond network that maintains the tertiary structure of the helix, which deviates slightly from a canonical A-RNA helix (Betzel *et al.*, 1994). Helix II forms a binding site for ribosomal proteins and TFIIIA and has a conserved single-nucleotide bulge, which affects the protein-binding site (Scripture *et al.*, 1995). Helix III contains a nucleotide bulge in its 3' portion that is well conserved in both prokaryotes and eukaryotes (Szymanski *et al.*, 2003). Helix IV contains tandem G:U pairs, with the stacked guanosines located on opposite strands (Szymanski *et al.*, 2003).

In eubacteria, there is evidence that for interaction of 5S rRNA with two regions of the 23S rRNA, placing 5S near the peptidyl transferase and factor-binding sites (Dokudovskaya *et al.*, 1996). It is generally accepted that 5S rRNA is important in stabilizing the entire ribosomal complex (Holmberg & Nygard, 2000).

The tertiary folding of RNA can provide local environments where it is possible to titrate protons at basic pH values (Zang & Romaniuk, 1995). Some of the most solvent accessible nucleotides of an RNA molecule are be found in the single-nucleotide loops (Zang & Romaniuk, 1995). Each single-stranded loop of *Xenopus* 5S rRNA has a mixture of accessible and inaccessible nucleotides, reflecting the highly structured nature of each loop (Zang & Romaniuk, 1995).

Single unpaired bases have proven to be very important in some RNA-protein interactions (Peattie *et al.*, 1981). It has been suggested that such bulged nucleotides could constitute the protein binding sites or result in conformational change within the RNA molecule necessary for protein interaction (Peattie *et al.*, 1981). However, binding analysis shows that deletion of the bulged nucleotide within the 5S rRNA has no effect on the interaction between p43 and 5S rRNA (Zang & Romaniuk, 1995).

1.4.6 INTERACTION BETWEEN p43 AND 5S rRNA

Sands and Bogenhagen (1991) identified the location of p43 on the 5S rRNA by ribonuclease footprinting of the p43-5S rRNA complex. Nuclease protection data suggest that the p43 interacts with helices I, II, IV and V of 5S rRNA. Both TFIIIA and p43 protect sites in all three helical stems of 5S rRNA and both proteins are closely associated with the central portion of 5S rRNA located around the junction of helices I, II and IV.

Darby and Joho (1992) employed deletion analysis to identify peptide fragments of p43 that retained RNA binding activity and determined that zinc fingers at the amino terminus of p43 are essential for binding 5S rRNA and that carboxyl-terminus zinc fingers have little affinity for RNA in isolation. The amino-terminal zinc fingers of p43 may have evolved as a structure optimal for RNA binding, whereas the equivalent TFIIIA zinc fingers may represent a compromise between RNA- and DNA-binding ability (Ryan & Darby, 1998).

Zang and Romaniuk (1995) determined details of the sequence and structural requirements for the binding of 5S rRNA to full-length p43. Recombinant p43 was overexpressed and purified from *E. coli* and a nitrocellulose filter-binding assay was used to study the specificity of the *in vitro* RNA binding activity of the protein under a variety of incubation conditions (Zang & Romaniuk, 1995). The experimental conditions necessary for the formation of the p43-5S rRNA complex *in vitro* include: pH 7.0, 0.1 M KCl and incubation at 22 °C (Zang & Romaniuk, 1995). Under these conditions, the apparent association constant for the complex is 1.61 nM^{-1} (Zang & Romaniuk, 1995). The affinity of TFIIIA for 5S rRNA under similar assay conditions is virtually identical (1.4 nM^{-1}), consistent with the observation that 5S rRNA stored in the cytoplasm of immature oocytes is equally distributed between the 7S and 42S RNPs (Zang & Romaniuk, 1995). The p43 binding affinity of a series of 5S rRNA deletion and substitution mutants was also determined (Zang & Romaniuk, 1995). The primary contact points for p43 include the sequences and structures of stems II, V and loop D of 5S rRNA (Zang & Romaniuk, 1995). The results of these experiments are summarized in Figure 8. The driving force for p43-5S rRNA complex formation is entropy, and may

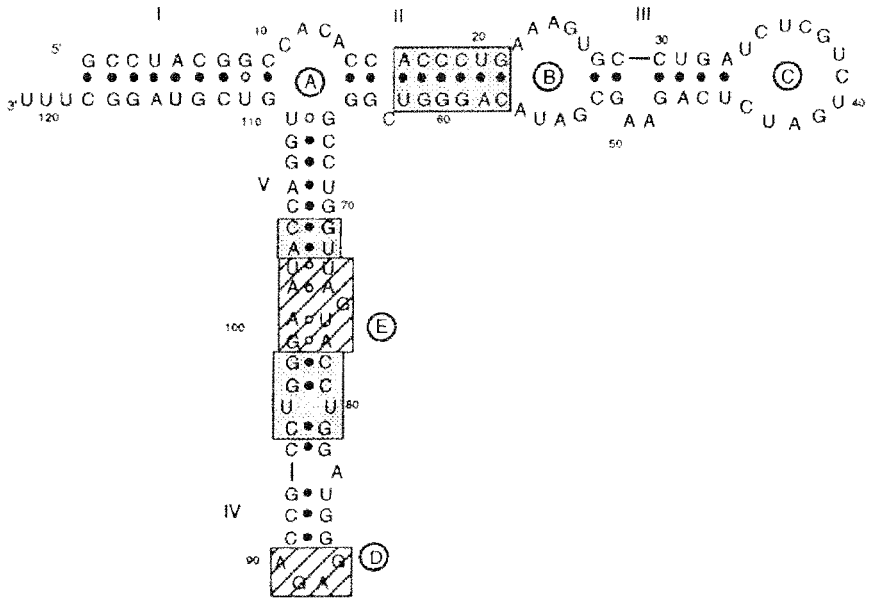

Figure 8. Recognition elements for p43-5S rRNA binding. Grey boxes indicate regions where helical structure of the 5S rRNA molecule alone contributes to p43 binding. Striped boxes indicated regions where nucleotide sequence and/or local conformation contribute to p43 binding. Stippled boxes indicate regions where both helical structure and base-pair sequence of the 5S rRNA molecule contribute to p43 binding. From Zang & Romaniuk, 1995.

reflect the release of counter ions and ordered water molecules from the individual components as a consequence of binding (Zang & Romaniuk, 1995).

1.4.7 INTERACTION BETWEEN TFIIIA AND 5S rRNA

Systematic analysis of the 5S rRNA binding properties of TFIIIA mutants showed that the interaction depends primarily on the three middle fingers, 4-6, with the first three fingers making very little contribution to binding (Theunissen *et al.*, 1992). Barciszewska and colleagues (2000) demonstrated that a peptide composed of the first three fingers of TFIIIA could bind 5S rRNA and protect helices IV, V and part of II from nuclease digestion. Successive addition of zinc fingers revealed that finger 4 interacts with helix II, fingers 5 and 6 interact with helices I and II and fingers 7-9 cover part of helix II, loop B and helix III. These results agree with those from McBryant and colleagues (1995), wherein zinc fingers 4-7, from the core region of TFIIIA, bound to a central region of the 5S rRNA molecule that consists of loops A and B and helices II and V with high affinity.

Mutations in stems II and V of 5S rRNA, which disrupted the double helix significantly, reduced the binding of TFIIIA (You & Romaniuk, 1990). These results are corroborated by evidence that TFIIIA does not make any strong sequence-specific contacts with the 5S rRNA (You *et al.*, 1990). The most important structural element of 5S rRNA required for TFIIIA binding is loop A; changes to the nucleotides in the region greatly affect protein binding (Theunissen *et al.*, 1998). Baudin and colleagues (1991) created 5S rRNA mutants containing all possible nucleotide substitutions at three positions in loop A. Results from these experiments indicated that the junction of the three helical domains is critical for protein recognition. Thus the central portion of 5S

rRNA, including loops E and A and helices II, IV and V, is thought to be the most important for the interaction with TFIIIA (Lu *et al.*, 2003). Conversely, zinc fingers 4-6 of TFIIIA are thought to be particularly necessary for 5S rRNA binding (Lu *et al.*, 2003).

1.4.8 NUCLEIC ACID BINDING PROPERTIES OF WT1

The DNA binding of the –KTS form of WT1 has been thoroughly characterized *in vitro* (Borel *et al.*, 1996). Under certain conditions, a recombinant peptide consisting of the four zinc fingers of WT1-KTS binds to the DNA consensus sequence 5'-GCGT-GGGCGTGT-3' with an apparent dissociation constant of 1.14 nM (Hamilton *et al.*, 1995). In a separate study, the interaction of the zinc finger peptide with DNA was also determined by experiments that deleted or disrupted a portion of each zinc finger. This study found that zinc finger 1 is not necessary for DNA binding, while fingers 2-4 are crucial (Bardessy & Pelletier, 1998). *In vitro*, the –KTS form of WT1 binds to two DNA ligands: a GC-rich motif similar to the EGR-1 binding sequence, 5'-GG/YGTGGGCG-3' and a motif containing a TCC repeat (Bardessy & Pelletier, 1998). The DNA binding properties of the +KTS form of WT1, however, are not well understood, mainly due to the failure to detect affinity-specific binding sites. Ladomery and collegues (2003) investigated whether the +KTS form of WT1 has any natural DNA ligands *in vivo*. The ability of both +KTS and -KTS isoforms to locate intranuclear structures *in vivo* was assessed by expressing tagged proteins in both mammalian cells and *Xenopus* oocytes. Only WT1+KTS accumulated in B-snurposomes, particles that correspond to components of the interchromatin granules of somatic nuclei also described as

trancriptosomes. Results from these experiments suggested that WT1 has acquired the ability to interact with transcripts and splice factors through the +KTS isoform.

Both the +KTS and the –KTS isoforms of WT1 have *in vitro* RNA binding specificity that is mediated by the four zinc fingers (Caricasole *et al.*, 1996). The dissociation constants for these interactions have been determined to be higher than those for the interactions between WT1 and DNA (Zhai *et al.*, 2001). The theory that the +KTS isoform of WT1 is involved in RNA metabolism is supported by the observation that this isoform binds to RNA *in vitro*. Furthermore, it has been suggested by experiments that deleted or disrupted a portion of each zinc finger that zinc finger 1 plays a key role in RNA binding (Caricasole *et al.*, 1996).

1.5 *IN VITRO* ASSAYS FOR INVESTIGATING MOLECULAR INTERACTIONS

Any ribonucleoprotein complex coexists in solution with a population of uncomplexed components that make up the RNP. This can be represented by the equilibrium equation:

$$RP \rightleftharpoons R + P$$

Where R represents the free RNA, P, the free protein and RP the RNA-protein complex for a simple bimolecular complex. At equilibrium, the distribution of the components between complexed and free states is determined by the concentrations of RNA and protein and by the equilibrium binding constant (K_d). For a simple bimolecular complex, K_d can be described by [R][P]/[RP]. K_d is expressed in molar units.

A method that distinguishes between bound and free forms of either the protein or the RNA is necessary to measure equilibrium binding constants. One such method is the nitrocellulose filter-binding assay. Another method widely employed is the gel retardation assay, which makes use of non-denaturing conditions to separate the free RNA from the RNA-protein complex. Gel retardation assays provide direct information about the stoichiometry of the binding, which must be inferred when filter-binding is employed. Both filter-binding and gel retardation are useful techniques for analyzing the interactions between p43 and 5S rRNA.

1.5.1 THE QUANTITATIVE *IN VITRO* FILTER-BINDING ASSAY

The principle behind the nitrocellulose filter-binding assay is very similar to the radioimmunoassay (RIA), a technique developed by Rosalyn Yallow that led to her Nobel Prize shared with Schally and Guillemin in 1977. Developed to study the interaction of *Xenopus* TFIIIA with 5S rRNA, RNA at a constant, low concentration is incubated with varying concentrations of protein (Romaniuk, 1985). The basis of this methodology is the observation that most proteins bind to nitrocellulose. If is protein is complexed with a nucleic acid, then the complex can also be retained by the nitrocellulose. The nitrocellulose filter retains free protein and protein-nucleic acid complex by hydrophobic interactions, while uncomplexed RNA passes through the membrane.

Because K_d = [P] when [RP] = [R], an estimate of the K_d can be obtained by determining the free protein concentration at which half of the RNA is bound. It is difficult to measure the concentration of free protein. Thus, the RNA concentration is

kept very low relative to the K_d of the complex and the concentration of free protein is approximately equal to the concentration of total protein, or [P] ~ [P] + [RP]. Assuming the percent RNA bound at the plateau represents complete binding of active RNA (Carey *et al.*, 1983), the K_d value for a simple bimolecular equilibrium can be expressed as the protein concentration at which half-saturation is achieved, provided 100 % of the protein is active. A limitation to using this type of protein titration at a fixed RNA concentration is that the concentration of active protein at each point in the titration must be known. This is sometimes not possible because only a fraction of the protein is active, for example when recombinant protein has been subject to denaturation during purification. Scatchard analysis can be used to confirm the level of activity obtained in the purified protein sample.

It was determined by Romaniuk (1985) that once the protein-RNA complex is bound to a nitrocellulose filter, the dissociation of bound complexes is unlikely to occur during the normal filtration of aliquots. Therefore, the filtration process does not alter the equilibrium in any way. However, incomplete retention of protein-nucleic acid complexes on the filter is a general phenomenon (Carey *et al.*, 1983).

1.5.2 QUANTIFICATION OF MOLECULAR INTERACTIONS BY SCATCHARD ANALYSIS

The interactions between protein and RNA can be quantified by Scatchard analysis, which provides a quantitative measure of affinity (K_d) and avoids the problems of protein titration when the activity of the sample is not known (Cox & Nelson, 2000). Scatchard analysis involves the titration of varying concentrations of RNA at a fixed

protein concentration. When the concentrations of free and bound RNA are determined, the K_d can be estimated using Scatchard analysis, which uses the following rearrangement of the equilibrium binding equation:

$$B/F = (-1/ K_d)B + (P_T/ K_d)$$

Where B is the concentration of RNA in the bound form, F is the concentration of free RNA and P_T is the total concentration of active protein in the reaction mixture, assuming the protein and RNA bind with a 1:1 ratio. When B/F is plotted against B, the slope of the line is equal to the negative reciprocal of the dissociation constant. The active protein concentration is obtained from the x-intercept.

2. INVESTIGATING INTERACTIONS BETWEEN p43 AND 5S rRNA USING THE YEAST THREE-HYBRID SYSTEM

2.1 INTRODUCTION TO THE YEAST-THREE-HYBRID SYSTEM

Yeast is widely studied because many of the genes that control its function have homologues that are also important in humans. The organism has been used to investigate the detailed functions of proteins such as mammalian transcription factors and nuclear hormone receptors. The accessibility of the yeast genome for genetic manipulation and techniques to introduce exogenous DNA into yeast cells has led to the development of methods for analyzing proteins from many organisms. Where RNA-protein interactions have been historically studied using *in vitro* biochemical assays such as RNA bandshifts, footprinting, and RNA-protein crosslinking, the yeast three-hybrid molecular interaction assay provides a system to study RNA-protein interactions *in vivo* and purification of recombinant protein is not required (Jaeger *et al.*, 2004, Zhu & Hannon, 2000).

Transcription regulators possess two distinct functions: DNA binding and transcription activation or repression (Zhu & Hannon, 2000). These different roles are performed by two discrete domain structures; the two domains are physically separable and function independently (Zhu & Hannon, 2000). This understanding of transcription regulators was followed by the inception of the yeast two-hybrid system by Fields (1989) and refinements that led to the establishment of the three-hybrid system via simultaneous experiments by SenGupta (1996) and Putz (1996). The three-hybrid system has been used both to detect specific RNA-binding proteins and to analyze the structural specificity of RNA-protein interactions (Putz *et al.*, 2000).

Several requirements must be met in order for a successful assay (Putz *et al.*, 2000):

1. The interaction of the two hybrid proteins and the hybrid RNA must be capable of occurring in the nucleus;
2. None of the hybrids alone or in any combination with a second hybrid may give rise to activation of reporter gene expression;
3. The domains of each hybrid must be accessible to allow proper interaction, and secondary and tertiary structures of RNA must be able to form when expressed as part of an RNA hybrid.

2.1.1 PRINCIPLE OF THE YEAST THREE-HYBRID SYSTEM

The three-hybrid system is an *in vivo* assay carried out in the yeast *Saccharomyces cerevisiae*. This assay involves the expression of three chimeric, or hybrid, molecules which assemble in order to activate two reporter genes (Figure 9, Jaeger *et al.*, 2004). This system uses the transactivator protein, LexA, which recruits the transcriptional machinery and triggers transcription of genes (Jaeger *et al.*, 2004). LexA consists of a DNA binding domain (DBD) and an activation domain (AD); these two domains are functionally independent, meaning that they can be fused to other molecules and still retain their activity.

The protein and RNA of interest are encoded on two separate plasmids, and are co-transformed into yeast. cDNA that codes for the RNA of interest is cloned into a vector so that it can be transcribed as a fusion to MS2 RNA. The RNA hybrid interacts with the LexA DBD-MS2 coat protein hybrid, encoded in the yeast genome, via

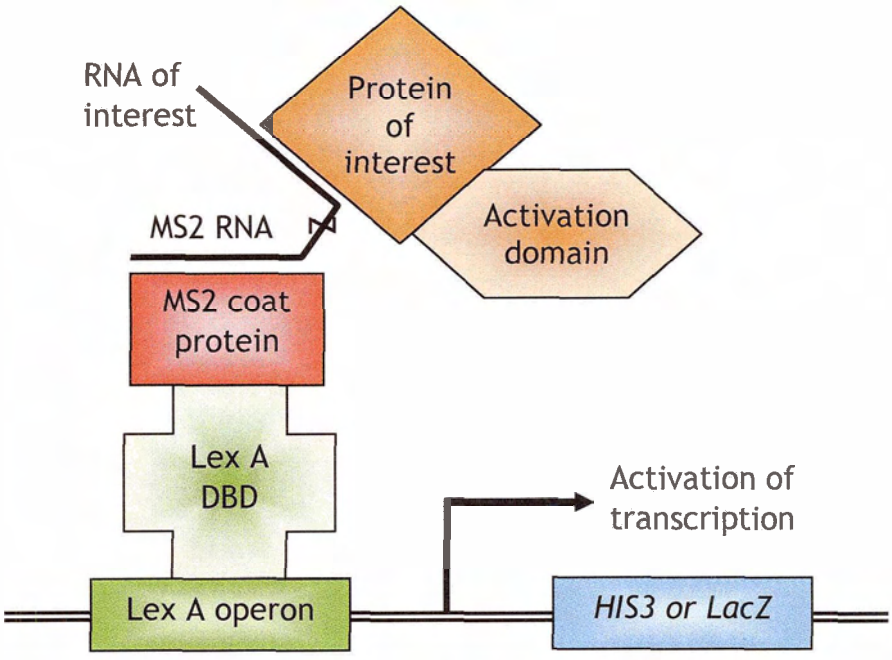

Figure 9. The yeast three-hybrid system: protein and RNA components. The LexA DBD-MS2 coat protein hybrid is encoded in the genome of the yeast strain L40uraMS2. The RNA and protein hybrids are encoded by a set of plasmids constructed by the user.

the MS2 RNA binding site. The MS2 coat protein binds to MS2 RNA with high specificity at a 33-nucleotide recognition site that forms a hairpin loop structure (Lowary and Uhlenbeck, 1987, Uhlenbeck, 1983). The cDNA that encodes the protein of interest is cloned into a vector so that it can be transcribed as a fusion to the LexA AD (Jaeger *et al.*, 2004).

The yeast strain contains two reporter genes (*lacZ* and *HIS3*) whose expression is regulated by LexA operator sequences. The LexA DBD specifically recognizes and binds to the LexA binding sites upstream of the HIS3 and lacZ reporters. Interaction between the three-hybrid molecules in the nucleus results in the assembly of the activation domain and the LexA DBD and subsequent transcriptional activation of the two reporter genes. The expression level of the *lacZ* gene can be determined in one of two ways: *in vitro* by measuring the β-galactosidase activity; or *in vivo* by plating the yeast transformants on media supplemented with X-Gal (5-bromo-4-chloro-3-indolyl-β-D-galactopyranoside, Jaeger *et al.*, 2004).

2.1.2 THE THREE-HYBRID SYSTEM AS A TOOL TO DISSECT RNA-PROTEIN INTERACTIONS

The three-hybrid system has been used to test the interaction of previously known or suspected interactors. In addition, the minimal binding domains of a RNA or protein of interest have been determined by deletion and mutational analysis and screening with the three-hybrid system (Jaeger *et al.*, 2004). The yeast three-hybrid system has been used to isolate and analyze proteins binding to the hairpin structure at the 3' end of animal replication-dependent histone mRNAs (Wang *et al.*, 1996), to the 3' UTR of the fem-3

mRNA that controls sexual cell fate in *C.elegans* (Zhang *et al.*, 1997), and of nanos mRNA in *Drosophila* (Dahanukar *et al.*, 1999).

With a randomly mutagenized RNA or protein library, the binding specificity of the molecule of interest can be analyzed. This strategy has been used extensively to study the binding of histone-binding protein (HBP) to the 3' UTR hairpin of replication-dependent histone mRNA (Martin *et al.*, 2000). Using the three-hybrid system, single mutations in HBP were selected that abolished binding to the wild-type histone hairpin mRNA. The system was subsequently used to select for intragenic mutations in HBP that restored the binding between the protein and histone hairpin mRNA.

2.2 CREATING MUTANTS RANDOMLY BY ERROR-PRONE PCR

Error-prone PCR is a random mutagenesis technique for introducing amino acid changes into proteins. Mutations are deliberately introduced during PCR through the use of error-prone DNA polymerases and reaction conditions. Randomized DNA sequences are cloned into expression vectors and the resulting mutant libraries are screened for altered protein activity. In this experiment, error-prone PCR was employed to generate a pool of randomly mutated p43 genes that were subsequently screen by yeast three-hybrid assay. Error-prone PCR methods commonly employ *Taq* DNA polymerase, as it lacks proofreading activity and is inherently error-prone (Daugherty *et al.*, 2000). Useful mutation frequencies are achieved by enhancing the error rate of *Taq* DNA. Reaction buffers containing magnesium and unbalanced dNTP concentrations (Vartanian *et al.*, 1996, Shafikhani *et al.*, 1997) can increase the error rate. These changes can lead to lower PCR product yields and a bias (e.g., As and Ts) in mutations produced (Wan *et al.*, 1998).

2.3 NEGATIVE MUTANT SELECTION IN THE PROTEIN p43 USING THE YEAST THREE-HYBRID SYSTEM

The strategy outlined by Martin and colleagues (2000) in their study of histone-binding protein was adopted to dissect the molecular interactions between p43 and 5S rRNA. The non-proofreading DNA polymerase from *T. aquaticus* was exploited to generate a randomly mutagenized p43 cDNA library. This p43 library was subsequently introduced into *S. cerevisiae* L40uraMS2 cells containing a plasmid encoding the 5S rRNA cDNA fused to the MS2 RNA hairpin gene, pRH5'-5S (Figure 10) and a gapped plasmid to which the p43 cDNA would be introduced by homologous recombination, pYESTrp2: p43 (Figure 11). The pYESTrp2: p43 sequence included a nuclear localization signal so that the first requirement for a successful yeast three-hybrid interaction is satisfied. Transformants were grown on a synthetic medium lacking uracil, histidine and tryptophan for the selection of the *URA3*, *HIS3* and *TRP2* marker genes, respectively. Colonies that appeared three days later were analyzed further for LacZ expression by performing a filter-lift assay with X-Gal. White colonies appearing among the vast majority of blue colonies were further analyzed. Mutant p43 plasmids from the white colonies were isolated and subjected to a second screening in L40uraMS2 cells to confirm the apparent loss of 5S rRNA binding activity and the sequence of the p43 cDNA insert was then determined. Finally, the effect of the mutation on the binding activity was determined by nitrocellulose filter-binding assay. It is hypothesized that specific amino acid residues are involved in 5S rRNA binding. It should be possible to employ the yeast three-hybrid assay to screen randomly generated p43 mutants. The p43

Figure 10. Multiple cloning site of pRH5'-5S plasmid showing 5S rRNA cDNA cloned into the Avr II and Xma I sites. The MS2 RNA is fused to the 5' end of the 5S rRNA cDNA.

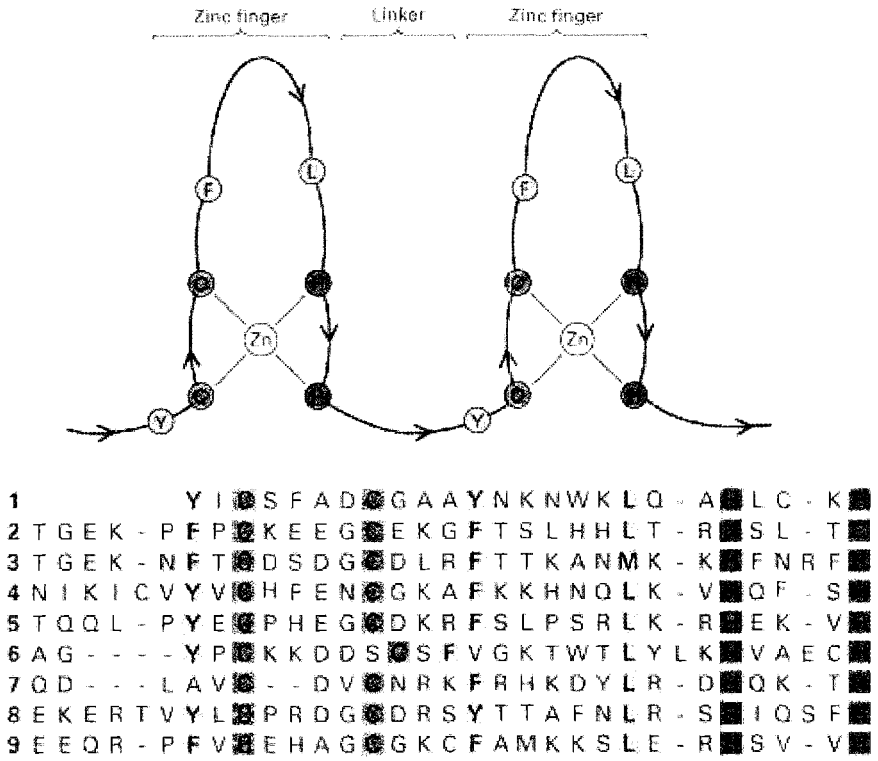

Figure 1. Amino acid sequence of the *Xenopus* zinc finger protein TFIIIA. The repeat of approximately 30 amino acids that comprises the consensus sequence for each of the nine zinc fingers is illustrated. The conserved cysteine and histidine ligands that make up a zinc-binding motif are highlighted in green and blue respectively. Adapted from Stryer (1996).

mutants identified by this method will contain mutations at amino acid residues critical for the protein-RNA interaction.

2.4 METHODS

2.4.1 CLONING VECTORS AND STRAINS

p43 cDNA was amplified by error-prone PCR from a pET16b plasmid (Clontech Laboratories, Inc, Palo Alto, California). Vectors containing recombinant protein cDNA were cloned in *E. coli* DH5α (Invitrogen, Carlsbad, California). A linker with the sequence 5'-AGCTCCATATGG-3' (Invitrogen) was ligated into Hind III (NEB, Beverly, Massachusetts) cut empty pYESTrp2 (Invitrogen) to facilitate construction of the yeast hybrid full-length p43 control plasmid. p43 cDNA was cloned into the Bam HI (NEB) and Nde I (NEB) sites of the modified pYESTrp2 (Invitrogen). The 5S rRNA encoding plasmid pRH5'-5S was provided by Dr. Romaniuk. pRH5'-5S was generated by cloning the 5S rRNA cDNA from the plasmid pXlo into the Avr II and Xma I sites of the plasmid pRH5' (Invitrogen).

2.4.2 EXPRESSION VECTORS AND STRAINS

Full-length p43 was overexpressed from a pET16b plasmid (Clontech). The putative mutant p43 proteins identified in the three-hybrid assay were overexpressed from a pET30a plasmid (Clontech). All proteins were overexpressed and purified from the *E. coli* strain BL21 (DE3) (Invitrogen).

2.4.3 ERROR-PRONE PCR

Point mutations were randomly introduced along the gene of the wild type p43 cDNA in a 50 μL PCR reaction. Approximately 10 ng of pYESTrp2: p43 plasmid DNA was used as the template. The upstream (5'-GAAGCGGTGTTAACGATACC-3') and downstream (5'-GGGCGTGAATGTAAGCGTGAC-3') primers (Invitrogen) were added to a concentration of 0.3 μM each. The PCR reaction mixture contained: three deoxynucleotide triphosphates (Invitrogen) at 1 mM and the fourth deoxynucleotide triphosphate (Invitrogen) at 0.2 mM, 5 μL of 10X PCR buffer, 1.5 mM $MgCl_2$, 0.05 mM $MnCl_2$ (BDH, Toronto, Ontario), and 1 unit of *Taq* DNA polymerase (Invitrogen). The reaction was amplified in a thermal cycler (Biometra, Göttingen, Germany) with a denaturation step at 94 °C for 1.5 min, an annealing step at 55 °C for 1.5 min and a 3 min elongation at 72 °C; these steps were repeated 29 times. The amplified 1500 nucleotide sequence contained all of the p43 gene as well as 5' and 3' ends compatible to BamHI and HindIII restriction sites of the pYESTrp2 plasmid. The presence of the correct product was verified by electrophoresis on a 1 % agarose gel in TBE buffer (45 mM Tris-borate (Roche Diagnostics, Indianapolis, Indiana), 1 mM EDTA (Sigma, Oakville, Ontario)) at 100 V. The PCR reaction for each of the four nucleotides was pooled, and this unpurified mixture was used to transform competent yeast cells.

2.4.4 YEAST TRANSFORMATION

A single isolated colony of *S. cerevisiae* L40uraMS2 (Invitrogen) was inoculated into 10 mL YC medium (0.12 % yeast nitrogen base, 0.5 % ammonium sulphate, 1 % succininc acid, 2 % glucose, 0.01 % adenine, arginine, cysteine, leucine, lysine,

threonine, tryptophan and uracil, 0.005 % aspartic acid, histidine, isoleucine, methionine, phenylalanine, proline, serine, tyrosine and valine, all Sigma) and incubated for 16 h at 30 °C in a water bath shaking at 250 rpm. The overnight culture was diluted into fresh YC medium to an A650 of 0.4 and incubated for a further 3 h. The cells were pelleted at 3000 rpm in a clinical centrifuge at room temperature for 5 min and washed with 40 mL sterile TE buffer pH 7.4 (10 mM Tris-HCl, Roche), 1 mM EDTA, Sigma). The cells were pelleted again at 3000 rpm in a clinical centrifuge at room temperature for 5 min and then resuspended in 2 mL sterile 100 mM lithium acetate (Sigma) pH 7.5 and 0.5X TE buffer and incubated at room temperature for 10 min.

The competent yeast cells were used immediately for transformations. The transformation mixtures consisted of 100 µL competent yeast cells, 40 µL error prone PCR mixture, 100 µg sheared denatured salmon sperm carrier DNA (Clontech) and 150 ng BamHI/HindIII linearized pYESTrp2. The transformed yeast cells were plated onto YC agar plates lacking uracil, tryptophan and histidine (YC-UWH) for selection in incubated at 30 °C for 3 days or until 1-2 mm colonies formed.

2.4.5 β-GALACTOSIDASE ASSAY

A colourimetric filter lift assay was employed to detect β-galactosidase activity in putative p43 mutants. Dry 0.45 µM pore size nitrocellulose filters (Schleicher & Schuell , Keene, New Hampshire) cut to fit Petri plates were laid onto yeast colonies growing on the YC-UWH plates. The filter was immersed in liquid nitrogen for approximately 30 s. After returning to 22 °C, the filter was placed colony side up onto a piece of filter paper in a Petri dish containing 1.5 mL Z buffer pH 7.0 (60 mM Na_2HPO_4, 40 mM NaH_2PO_4,

10 mM KCl, 1 mM $MgSO_4$, all EMD, Gibbstown, New Jersey and 1.5 mg X-gal, Sigma). The plates were incubated at 30 °C in the dark for approximately 2 h. White colonies identified as possible mutants were grown on a fresh YC-UWH plate, incubated at 30 °C for two days and re-assayed as described above. A single isolated colony of the mutants that maintained a strong white phenotype in the second β-galactosidase assay were inoculated into 10 mL YC-UWH and incubated for 16 h at 30 °C in a water bath shaking at 250 rpm. Samples of these cultures were stored as glycerol stocks at –70 °C.

2.4.6 WESTERN BLOT

Western blotting was performed to identify the yeast transformants that were expressing p43. One mL of a 16 h yeast culture was pelleted and resuspended in 100 uL 1X SDS-PAGE sample buffer. After boiling for 5 min, 15 μL of the sample was separated by SDS-PAGE and electrophoretically transferred at 100 V to nitrocellulose membranes. The protocol followed was described in the WesternBreeze Novex chemiluminescent Western blot immunodetection kit instructions (Invitrogen). Briefly, blotted membranes were incubated in 10 mL blocking solution (buffered saline solution containing detergent and Hammersten casein solution, Invitrogen) on a rotary shaker set at 1 rev/s for 30 min. The membrane was rinsed twice with 20 mL water and then incubated with 10 mL primary antibody, anti-V5 epitope mouse monoclonal (Invitrogen) diluted 1:5000 in blocking solution, for 1 h and then washed for 4X 5 min with 20 mL antibody wash (buffered saline solution containing detergent, Invitrogen). The membrane was incubated with secondary antibody solution from the WesternBreeze (Invitrogen) kit (solution of alkaline phosphatase-conjugated affinity purified goat anti-mouse IgG) for 30

min and then washed for 4X 5 min with 20 mL antibody wash. After 3X 5 min rinses with 20 mL water, the membrane was placed on a clean sheet of transparency plastic. 2.5 mL of the chemiluminescent substrate (2.375 mL CDP-Star, Invitrogen, with 0.125 mL Nitro-Block II, Invitrogen) was applied evenly to the membrane surface. Once the reaction had developed for 5 min, the membrane was exposed to x-ray film (Kodak, Rochester, New York) for 4 - 6 min. Plasmids from yeast expressing protein with an apparent molecular weight equal to that of full length p43 expressed in yeast were purified and sequenced as indicated in sections 2.4.7-.9

2.4.7 PURIFICATION OF MUTANT PLASMID FROM *S.CEREVISIAE*

The plasmids containing mutated p43 cDNAs were purified from yeast expressing full-length p43 according to a previously published method (Robzyk and Kassir, 1992). A single colony was inoculated into 10 mL YC-UWH and incubated in a shaking water bath for 16 h at 30 $^{\circ}$C and 250 rpm. The overnight culture was pelleted in a microcentrifuge at 14,000 rpm for 1 min. Once the supernatant was decanted, the cells were resuspended in 500 µL RIPA buffer pH 7.5 (50 mM Tris-Cl (Roche), 150 mM NaCl (EM, Darnstadt, Germany), 1 % NP-40 (Sigma), 0.5 % sodium deoxycholate (Sigma), 0.1 % SDS (Fisher Scientific)). 200 mg of acetone-washed glass beads were added to the sample and a bead beater was used to break open the cells with 5X one min cycles with a two min incubation on ice between cycles. The cell lysates were pelleted in a microcentrifuge at 14,000 rpm for 1 min. Two-hundred µL of 0.2 M NaOH (EMD) and 1 % SDS was incubated with the lysate supernatants for 5 min at 22 $^{\circ}$C. Subsequently, 150 µL ice cold 3 M NaOAc (Caledon, Georgetown, Ontario) was added and the lysates were incubated

on ice for 10 min. The preparations were pelleted in a microcentrifuge at 14,000 rpm for 10 min. The resulting supernatants were incubated with 1 μL 10 mg/mL RNAse A (Sigma) for 30 min at 37 °C. The plasmid was extracted twice with phenol-saturated chloroform (Invitrogen), once with chloroform and then precipitated with three volumes of ice cold 95 % ethanol. The purified plasmid was air-dried and resuspended in 50 μL of 50 mM Tris pH 7.4. The plasmid preparations obtained from the yeast cells were a mixture of the two plasmids originally transformed into the yeast for the three-hybrid experiment. To acquire a clean preparation of pYESTrp2 encoding each putative p43 mutant, 20 μL of the plasmid mix purified from yeast was used to transfect 100 μL of chemically competent cloning strain of *E. coli*, DH5α.

2.4.8 COLONY PCR

To determine which plasmid had transfected each colony, colonies were picked and lysed by heating at 94° C in a PCR tube for 5 min. p43 cDNA was then amplified in a 10 μL PCR reaction. The upstream (5'-GAAGCGGTGTTAAC GATACC-3') and downstream (5'-GGGCGTGAATGTAAGCGTGAC-3') primers (Invitrogen) were added to a concentration of 0.3 μM. The PCR reaction mixture contained 1 μL of 10x PCR buffer, the four deoxynucleotide triphosphates to a final concentration of 1 mM each, 1.5 mM $MgCl_2$, and 1 unit of *Taq* DNA polymerase. The reaction was amplified in a thermal cycler with a denaturation step at 94 °C for 20 s, an annealing step at 55 °C for 20 s and a 30 s elongation at 72 °C; these steps were repeated 40 times. The primers annealed adjacent to the pYESTrp2 insert site. Thus 1500 nucleotide target sequence was only amplified from the pYESTrp2 plasmid, allowing for identification of the pYESTrp2:p43

transfected DH5α colonies. The presence of the correct product was verified by electrophoresis on a 1 % agarose gel in TBE buffer at 100 V.

Plasmids that had been passed through DH5α were purified as described above for yeast except that *E. coli* cell lysis was achieved by incubation in 100 μL ice cold lysis buffer pH 8.0 (50 mM glucose (Roche), 25 mM Tris-Cl, 10 mM EDTA). The pYESTrp2 containing preparations were used to repeat the yeast transformation as described previously. β-galactosidase assays were performed as described above on the resulting yeast colonies to confirm the white phenotype of the mutants.

2.4.9 DYE-TERMINATION SEQUENCING

Sequencing reactions were carried out using the DYEnamic ET Terminator Cycle Sequencing Kit (Amersham Biosciences, Piscataway, New Jersey). To generate a sequence that spanned the p43 molecule, two upstream primers (5'-GAAGCGGTG-TTAACGATACC-3' complementary to pYEST plasmid upstream of p43 insert and 5'-AGAGGTTACCGCTGCTCC-3' corresponding to base pairs 521-538 of GenBank XELFINAC sequence) and three downstream primers (5'-GGGCGTGAATGTAAG-CGTGAC-3' complementary to the pYESTrp2 plasmid downtream of the p43 insert, 5'-TCAAGCCTTGGAGCGGTG-3' complementary to base pairs 1180-1197 of GenBank XELFINAC and 5'-ACTGGCCTTCTTGAATGG-3' complementary to p43 cDNA 30 bases downstream of Sac II site at end of finger 7) were used. The 20 μL sequencing reactions contained 0.4 pmol template DNA, 6 pmol primer and 8 μL sequencing reagent premix (Amersham Biosciences). The reaction was amplified in a thermal cycler with a denaturation step at 95 ^{o}C for 20 s, an annealing step at 50 ^{o}C for 15 s and a 60 s

elongation at 60 °C; these steps were repeated 25 times. The reaction was precipitated with 95 % ethanol, washed with 70 % ethanol and dried in a speed-vac at 22 °C. The pellet was dissolved in 4 μL formamide dye (Amersham Biosciences) and vortexed vigorously for 20 s. The samples were run on an ABI 377 instrument. Each PCR reaction resulted in sequence that was between 400 and 700 bases in length.

2.4.10 TRANSFORMATION INTO EXPRESSION STRAIN

Following confirmation of the white phenotype, the putative p43 mutant cDNA was ligated into the Bam HI/HindIII site of the plasmid pET30a. Fifteen μL of each ligation was transformed into 100 μL of chemically competent *E. coli* BL21 (DE3). The transformation mixture was incubated on ice for 5 min, heat shocked for 2 min, and returned to ice for 5 min. The culture was then incubated with 800 μL LB at 37 °C for 1 h, following which 200 μL were plated on the appropriate selective medium. The plates were incubated at 37 °C for 16 h.

2.4.11 OVEREXPRESSION AND PURIFICATION OF RECOMBINANT PROTEINS

Expression and purification of recombinant *Xenopus* p43 was performed using a modified protocol by Del Rio and Setzer (1991) describing the purification of recombinant TFIIIA. Chemically competent *E. coli* BL21 (DE3) was transfected with pET30a containing the correct mutant construct. The cells were plated on LB plates containing 50 mg/ml of ampicillin (Sigma) and incubated for 16 h at 37 °C. A single colony from each transfection was incubated in 5 ml of LB media with 50 mg/ml of

ampicillin at 37 °C for 16 h, shaking at 250 rpm. A 500 mL volume of TFB media (5g NaCl, 10 g yeast extract (DIFCO, Detroit, Michigan), 20 g casein hydrolysate (DIFCO) in 1 L dH2O containing 50 mg/mL ampicillin was inoculated with 5 mL of the overnight culture of *E. coli* BL21 (DE3) containing the pET16b:p43 expression plasmid. The culture was grown at 37 ° C, shaking at 250 rpm to an A650 of between 0.4 and 0.6. p43 protein synthesis was induced with addition of IPTG (Sigma) to a 1 mM final concentration. The cells were harvested 6 h after induction by centrifugation at 7000 rpm for ten min in a Beckman JA-16 rotor and resuspended in 10 mL of TABP (20 mM Tris pH7.4, 5 mM $MgCl_2$, 5 mM DTT (Sigma), 50 μM $ZnSO_4$ (Sigma), 10 % glycerol (EMD), 250 mM NaCl and 1 mM PMSF (Sigma)).

The cells were disrupted with a microtip sonicator (Heat Systems-Ultrasonics W-385) at setting 5 and 50 % duty cycle for five 1 min intervals with 2 min cooling between pulses. During sonication, the sample was cooled in an ethanol and ice slurry. All subsequent sample handling was performed at 4 ° C unless otherwise stated. This was followed by centrifugation at 10,000 rpm in a Beckman JA-20 rotor. The pellet was resuspended in 2 mL TABUP (20 mM Tris pH7.4, 5 mM $MgCl_2$, 5 mM DTT, 50 μM $ZnSO_4$, 10 % glycerol, 250 mM NaCl, 1 mM PMSF and 7 M urea (Roche)) and mixed gently by end-over-end rotation for 16 h.

The urea-solubilized sample was centrifuged in a microcentrifuge at 14,000 rpm fro 20 min. TABUP saturated with $(NH_4)_2SO_4$ (EM) at 4 ° C was added to the supernatant to bring the sample to 40 % (v/v) saturation. This sample was then mixed by end-over-end rotation for 1 h. Precipitated proteins were pelleted by further centrifugation for 20 min at 12,000 X g in a Beckman JA-20 rotor. Ammonium sulfate saturated TABUP was

added to the supernatant to achieve 80 % (v/v) saturation followed by rotation for 1 h. The crude protein preparation was pelleted by centrifugation for 20 min at 12,000 X g in a Beckman JA-20 rotor and the supernatant was discarded. The protein pellet was dissolved in 5 mL TABU (20 mM Tris pH 7.4, 5 mM $MgCl_2$, 5 mM DTT, 50 μM $ZnSO_4$, 10 % glycerol, 250 mM NaCl and 7 M urea).

The crude protein solution was applied to an 800 uL BioRex 70 (BioRad, Hercules, California) cation exchange column pre-equilibrated with TABU. The sample was washed with 5 mL TABU and 2 mL TABU containing 400 mM NaCl. p43 was eluted from the column with 2 mL TABU containing 600 mM NaCl and stored at 4 °C. The nucleic acid binding activity gradually decreased over one week and had an optimal binding activity within four days of purification (Veldhoen, 1995). Alternatively, the purified protein fraction was aliquoted and stored at –70 °C, where its nucleic acid binding activity remained more stable. Protein concentration and purity were determined by the method of Bradford (1976), with bovine serum albumin as a standard, and by 15 % SDS-PAGE, respectively.

Expression and purification of recombinant p43 mutants generated by error-prone PCR was performed using a modified protocol for the purification of recombinant TFIIIA described by Del Rio and Setzer (1991). A 500 mL volume of TFB media containing 50 mg/mL kanamycin (Sigma) was inoculated with 5 mL of an overnight culture of *E. coli* BL21 (DE3) containing the pET30a:p43 mutant expression plasmid. The protein was purified as described for recombinant p43 and the concentration of protein purified from this method ranged from 10 to 22 μM.

2.4.12 RADIOLABELLING OF 5S rRNA

Xenopus oocyte-type 5S rRNA was radiolabelled with [5'-^{33}P]-GTP for subsequent *in vitro* assays. The plasmid pXlo was digested with Dra I (NEB) and purified using a QIAquick PCR Purification Kit (Qiagen, Mississauga, Ontario), and then utilized directly as a template in an *in vitro* transcription reaction. The 20 μL labeling reaction contained 1X T7 RNA polymerase buffer, 2 mM NTPs (Invitrogen), 20 μCi [5'-^{33}P]-GTP (Dupont NEN, Wilmington, Delaware), 15 U RNA guard (Pharmacia, New York, New York), 2 μg BSA (Sigma), 3 to 5 μg Nde I (NEB) linearized pXlo plasmid and 30 units T7 RNA polymerase (NEB). The sample was incubated at 37 °C for 4 h. Labeled RNA was separated by electrophoresis at 400 V on an 8 % denaturing polyacrylamide gel (29:1 acrylamide: bis, 16 cm x 16 cm x 0.75 mm) followed by incubations of excised bands in elution buffer (1 mM EDTA, 0.6 M NH_4OAc, 0.1 % SDS) and ethanol precipitation (Sambrook *et al.*, 1989). The efficiency of radiolabel incorporation was measured using a LKB 1214 Rackbeta Scintillation counter. 1 μL of purified RNA was added to 1 mL of scintillation fluid (Sigma).

2.4.13 NITROCELLULOSE FILTER-BINDING ASSAY

The standard TK buffer for the filter-binding assay was 20 mM Tris, 100 mM KCl, 100 μg/ml BSA, 1 mM DTT, adjusted to pH 7.5 at 22 °C. The TMK buffer for the TFIIIA control was 20 mM Tris, 5 mM $MgCl_2$, 100 mM KCl, 100 μg/ml BSA, 1 mM DTT, adjusted to pH 7.5 at 22 °C. The proteins were serially diluted in the appropriate buffer from 400 to 0.04 nM. 5000 cpm RNA and 0.2 μg poly [d (I-C)] (Roche) was added to each dilution to reduce the non-specific interactions between the RNA and the

protein. The reactions were incubated for 90 min at 22 °C and then applied with a vacuum to a nitrocellulose membrane (Schleicher & Schuell) that had been hydrated in water for 7 min. The nitrocellulose membrane was exposed to a phosphorimager cassette for 16 h.

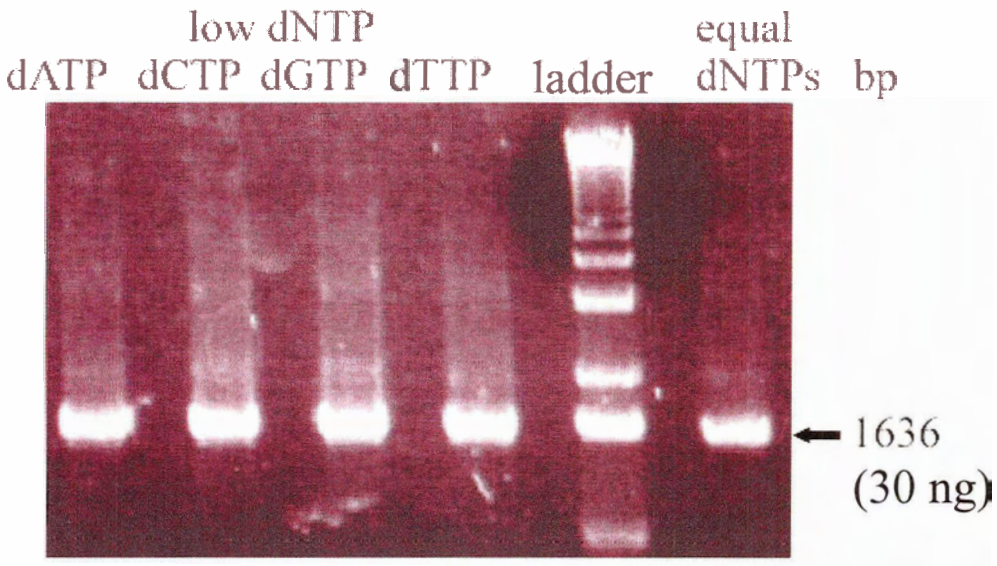

Figure 12. Products of error prone PCR amplification of p43 cDNA. 4 µL of PCR product was visualized by Ethidium bromide staining following electrophoresis on a 1 % agarose gel in TBE buffer at 100V.

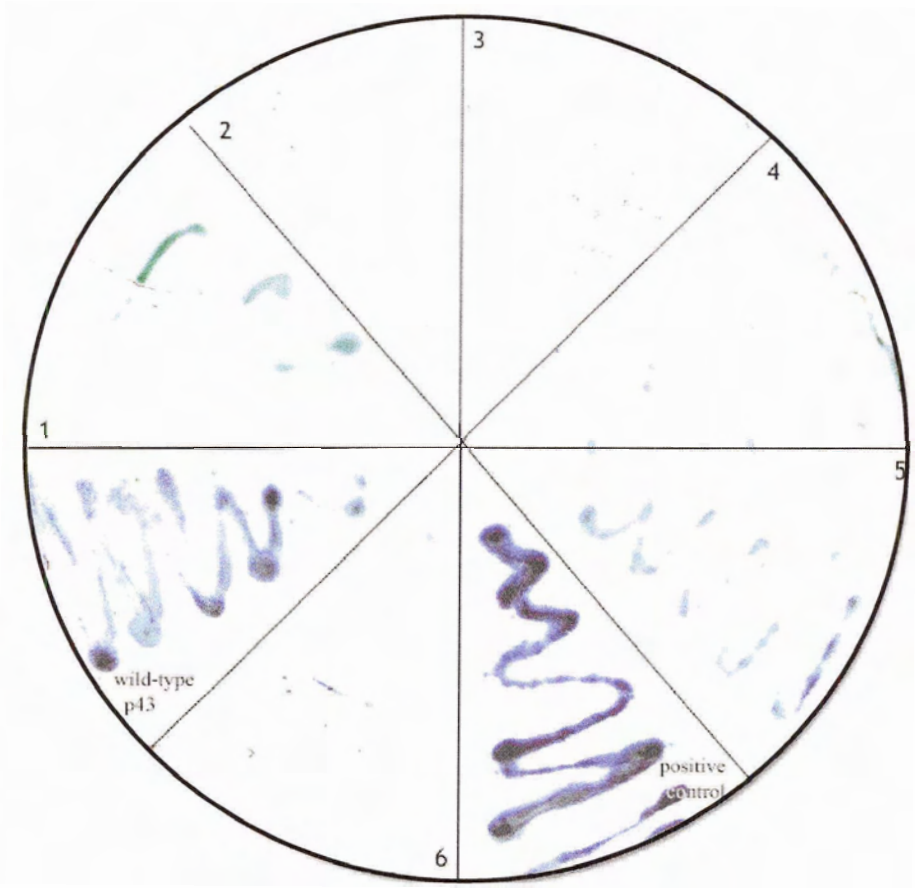

Figure 13. Beta-galactosidase filter lift assay. Developed in Z-buffer plus X-gal for 1 h at 37° C. Segments 1 - 6 show putative mutants demonstrating a loss of activity, or white phenotype. The wild-type p43 and positive control assays are indicated.

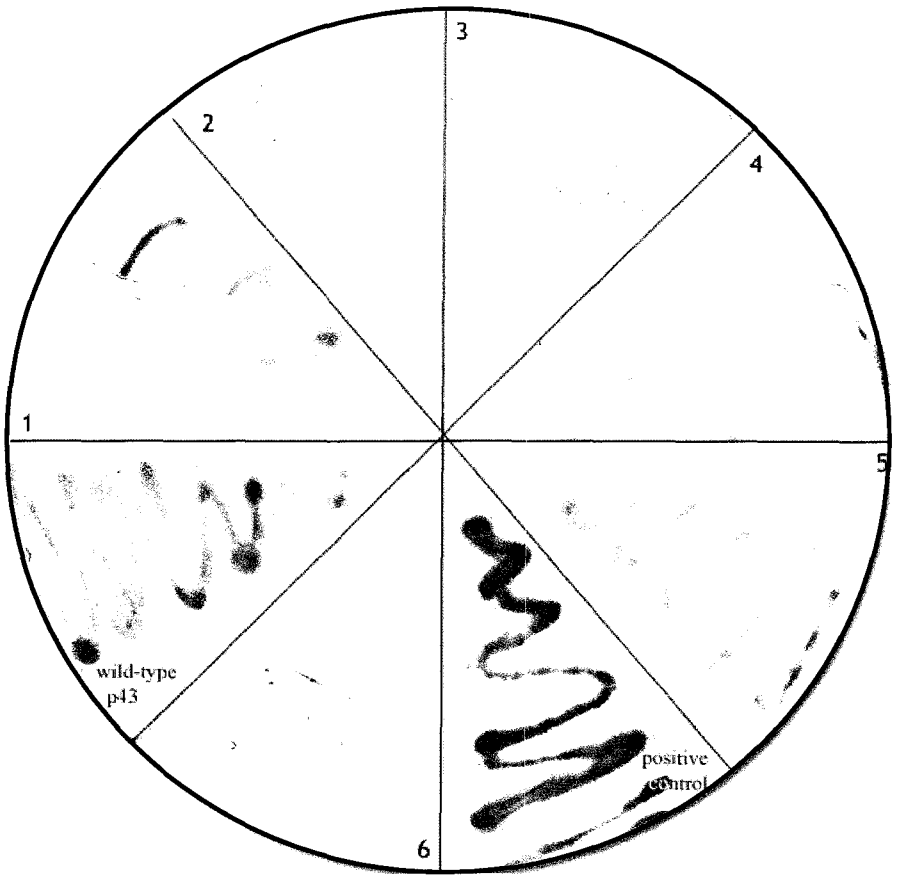

Figure 13. Beta-galactosidase filter lift assay. Developed in Z-buffer plus X-gal for 1 h at 37° C. Segments 1 - 6 show putative mutants demonstrating a loss of activity, or white phenotype. The wild-type p43 and positive control assays are indicated.

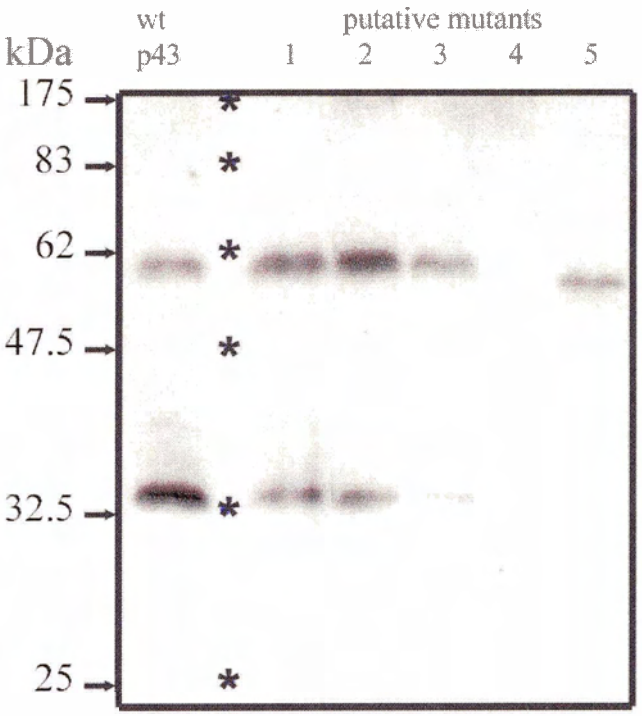

Figure 14. Western blot of full-length putative p43 mutants. Each sample was separated on a 12.5 % acrylamide gel at 200 V for 90 min and then transferred to nitrocellulose at 100 V for 1 h. The primary antibody used was a mouse monoclonal against the V5 epitope and was diluted 1/5000. The broad range prestained protein marker (*) contained the following proteins that ran with the apparent molecular weights: MBP-beta-galactosidase (175 kDa), MBP-paramyosin (83 kDa), glutamic dehydrogenase (62 kDa), aldolase (47.5 kDa), triosephosphate isomerase (32.5 kDa) and beta-lactoglobulin A (25 kDa). The blot was developed with chemiluminescent substrate (Invitrogen) and exposed to X-ray film for 8 min.

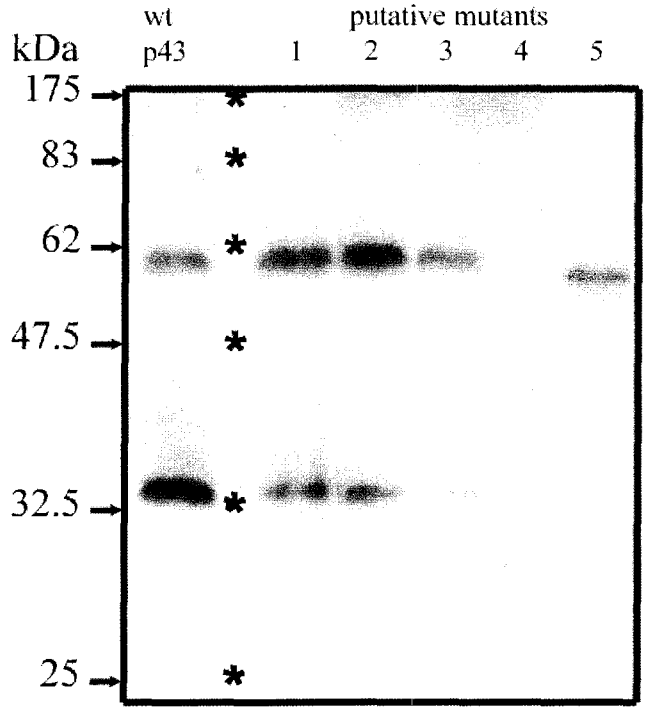

Figure 14. Western blot of full-length putative p43 mutants. Each sample was separated on a 12.5 % acrylamide gel at 200 V for 90 min and then transferred to nitrocellulose at 100 V for 1 h. The primary antibody used was a mouse monoclonal against the V5 epitope and was diluted 1/5000. The broad range prestained protein marker (*) contained the following proteins that ran with the apparent molecular weights: MBP-beta-galactosidase (175 kDa), MBP-paramyosin (83 kDa), glutamic dehydrogenase (62 kDa), aldolase (47.5 kDa), triosephosphate isomerase (32.5 kDa) and beta-lactoglobulin A (25 kDa). The blot was developed with chemiluminescent substrate (Invitrogen) and exposed to X-ray film for 8 min.

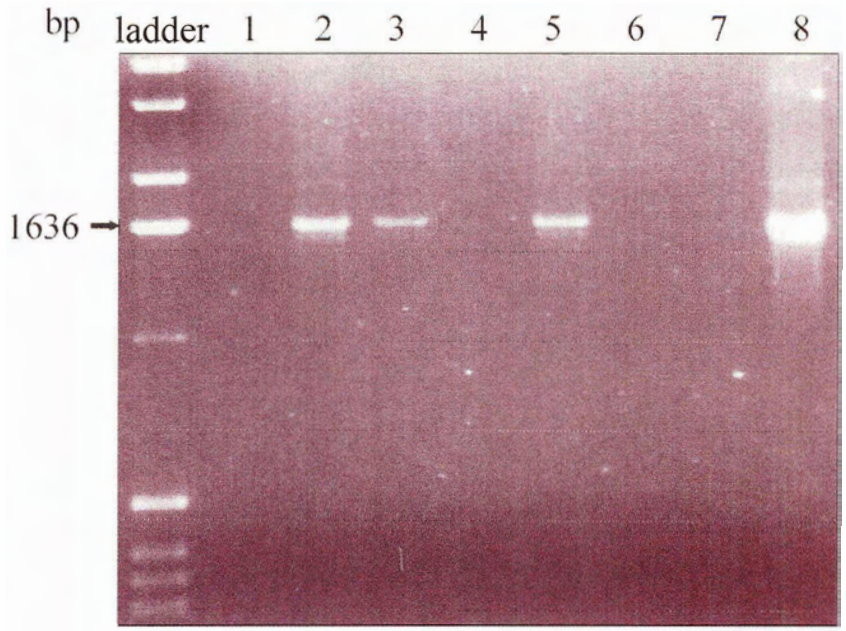

Figure 15. Identification of pYESTrp2:p43 transfected DH5α colonies by PCR. Lanes 1, 4, 6 and 7 show the negative reaction that occurred when pRH5'-5S was the plasmid contained by the DH5α colony. Lanes 2, 3 and 5 show plasmids containing the putative p43 mutants. Lane 8 shows the positive control, pYESTrp2: p43, and the resulting 1630 bp product. The product was visualized by Ethidium bromide staining following electrophoresis on a 1 % agarose gel in TBE buffer at 100 V.

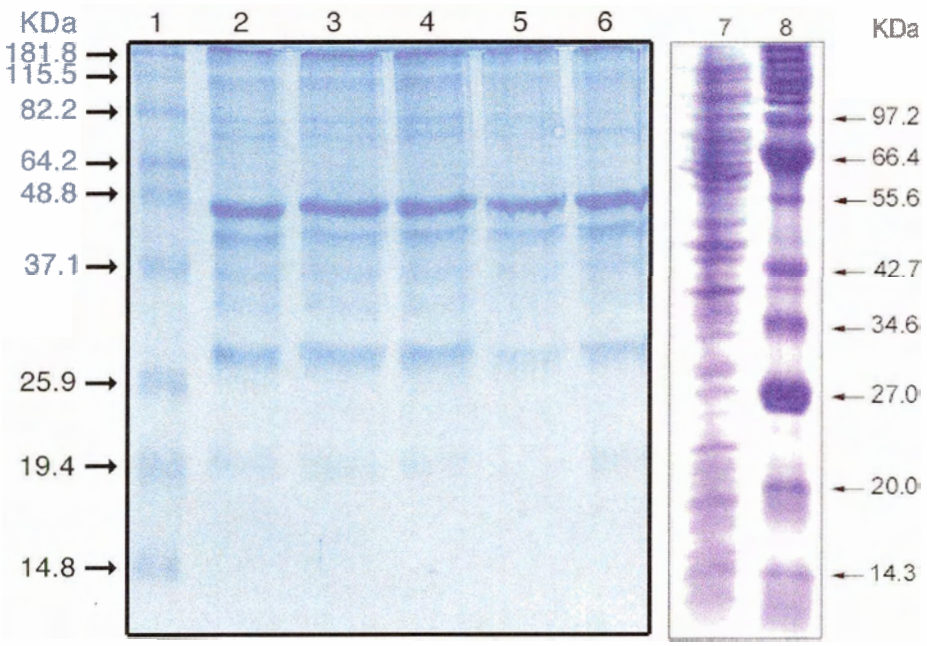

Figure 16. SDS-PAGE of purified randomly generated p43 mutants screened by yeast three-hybrid assay. 10 µL of each protein sample was separated on a 12.5 % acrylamide gel at 200 V for 90 min. Lane 1: protein ladder, lane 2: wild type p43, lane 3: mutant i, lane 4: mutant g, lane 5: mutant e, lane 6: mutant b, lane 7: a 50 µL cell pellet of uninduced *E.coli* at A650 = 0.480. The Benchmark Pre-Stained Protein Ladder (Invitrogen) molecular weight standard in lane 1 contained proteins that ran with the apparent molecular weights noted: 181.1 kDa, 115.5 kDa, 82.2 kDa, 64.2 kDa, 48.8 kDa, 37.1 kDa, 25.9 kDa, 19.4 kDa and 14.8 KDa. The Broad Range Protein Marker (NEB) molecular weight standard in lane 8 contained proteins that ran with the apparent molecular weights noted: 97.2 kDa, 66.4 kDa, 55.6 kDa, 42.7 kDa, 34.6 kDa, 27.0 kDa, 20.0 kDa and 14.3 kDa.

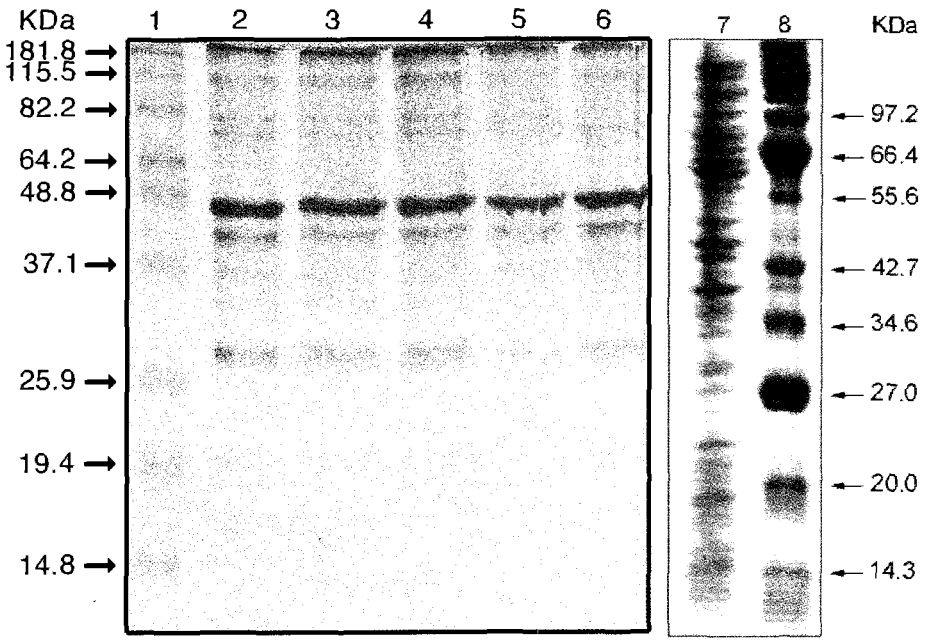

Figure 16. SDS-PAGE of purified randomly generated p43 mutants screened by yeast three-hybrid assay. 10 μL of each protein sample was separated on a 12.5 % acrylamide gel at 200 V for 90 min. Lane 1: protein ladder, lane 2: wild type p43, lane 3: mutant i, lane 4: mutant g, lane 5: mutant e, lane 6: mutant b, lane 7: a 50 μL cell pellet of uninduced *E.coli* at A650 = 0.480. The Benchmark Pre-Stained Protein Ladder (Invitrogen) molecular weight standard in lane 1 contained proteins that ran with the apparent molecular weights noted: 181.1 kDa, 115.5 kDa, 82.2 kDa, 64.2 kDa, 48.8 kDa, 37.1 kDa, 25.9 kDa, 19.4 kDa and 14.8 KDa. The Broad Range Protein Marker (NEB) molecular weight standard in lane 8 contained proteins that ran with the apparent molecular weights noted: 97.2 kDa, 66.4 kDa, 55.6 kDa, 42.7 kDa, 34.6 kDa, 27.0 kDa, 20.0 kDa and 14.3 kDa.

Table 1. Protein concentrations obtained following overexpression and purification of randomly generated p43 mutants. Determined by Bradford assay (BioRad) with a standard curve generated using BSA (Sigma). Protein concentrations ranged from 10-22 μM.

p43 mutant	Protein concentration (μM)
b	10
e	18
g	17
i	22


p43 finger 1
MKNVGETGPGKCQLLRCPAAGCKAFYRKEGKLQDHMAGH
p43 finger 2
SEQKPWKCGIKDCDKVFARKRQILKHVKRH
p43 finger 3
LALKKLSCPTAGCKMTFSTKKSLSRHKLYKH
p43 finger 4
GEAVPLKCFVPGCKRSFRKKRALRRHLSVH
p43 finger 5
SNEPLSVCDVPGCSWKSSSVAKLVAHQKRH

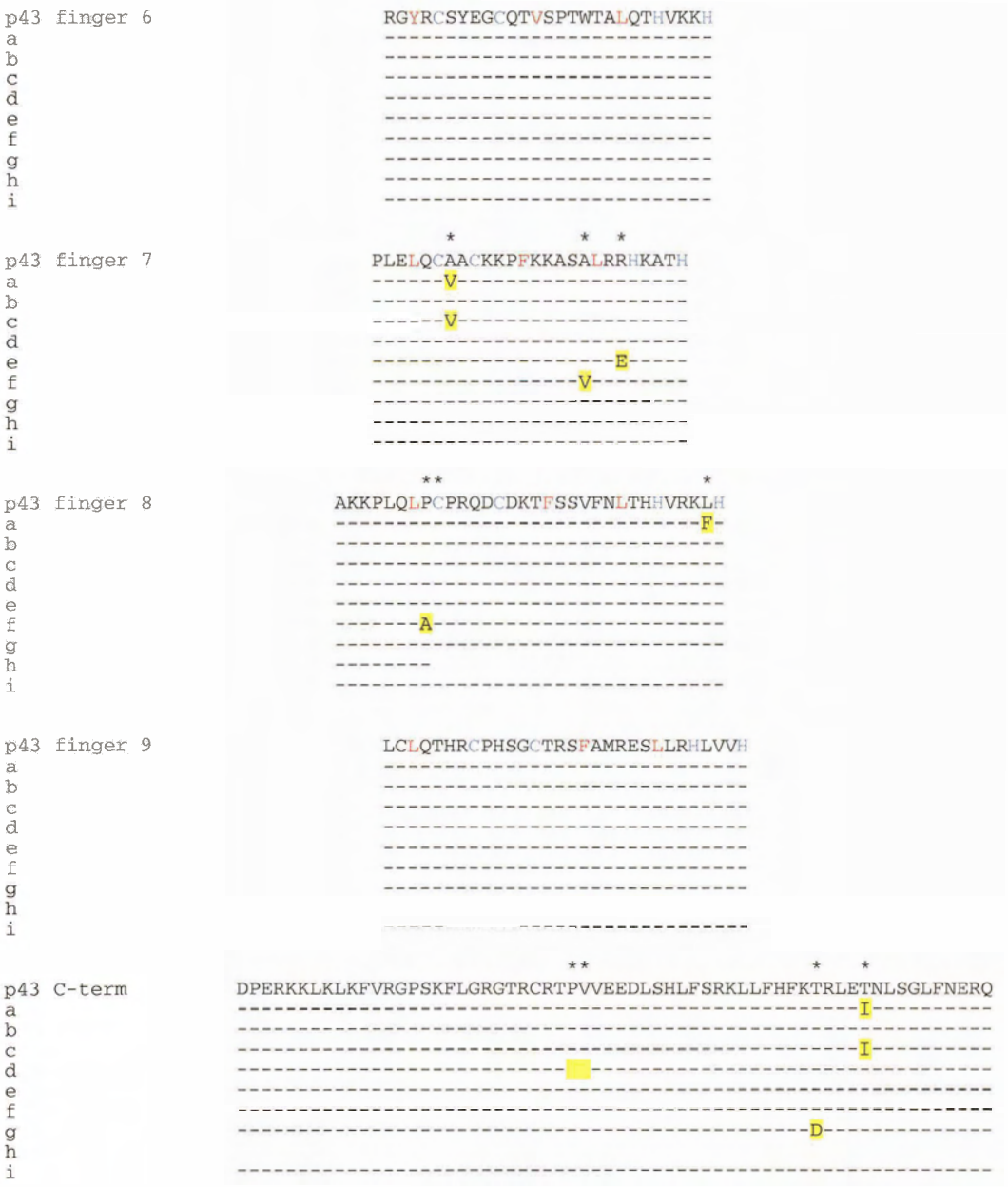
p43 finger 6
RGYRCSYEGCQTVSPTWTALQTHVKKH
a
b
c
d
e
f
g
h
i
p43 finger 7
PLELQCAACKKPFKKASALRRHKATH
a
b
c
d
e
f
g
h
i
p43 finger 8
AKKPLQLPCPRQDCDKTFSSVFNLTHHVRKLH
a
b
c
d
e
f
g
h
i
p43 finger 9
LCLQTHRCPHSGCTRSFAMRESLLRHLVVH
a
b
c
d
e
f
g
h
i
p43 C-term
DPERKKLKLKFVRGPSKFLGRGTRCRTPVVEEDLSHLFSRKLLFHFKTRLETNLSGLFNERQ
a
b
c
d
e
f
g
h
i

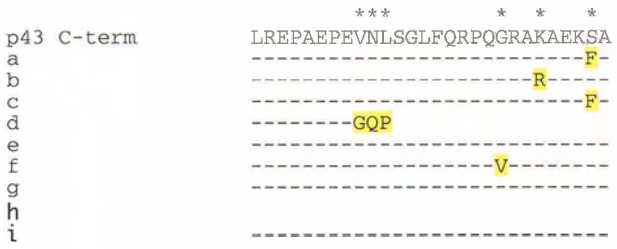

Figure 17. Amino acid sequence alignment of randomly generated p43 mutants a-i. The conserved residues that are critical for zinc ion chelation are coded as follows: blue letters denote an essential cysteine or histidine residue; red letters denote a required hydrophobic residue. Mutations are highlighted in yellow.

```
                        ***         *  *   *
p43 C-term              LREPAEPEVNLSGLFQRPQGRAKAEKSA
a                       -------------------------F-
b                       ----------------------R-----
c                       -------------------------F-
d                       --------GQP
e                       ----------------------------
f                       -------------------V--------
g                       ----------------------------
h
i                       ----------------------------
```

Figure 17. Amino acid sequence alignment of randomly generated p43 mutants a-i. The conserved residues that are critical for zinc ion chelation are coded as follows: blue letters denote an essential cysteine or histidine residue; red letters denote a required hydrophobic residue. Mutations are highlighted in yellow.

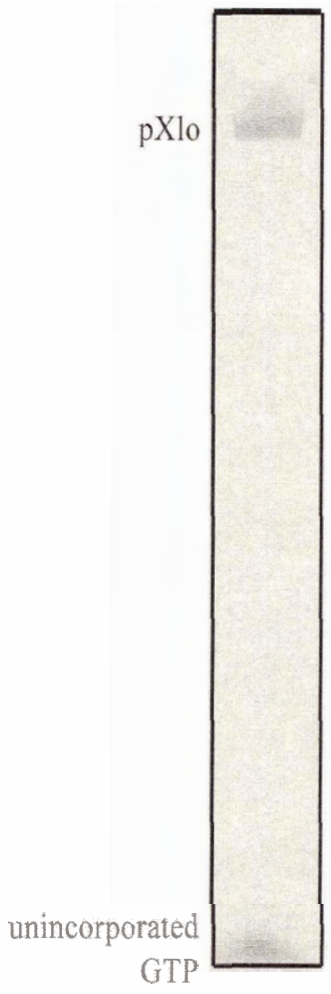

Figure 18. Autoradiogram of an *in vitro* transcription reaction. Sample separated on an 8 % denaturing acrylamide gel at 300 V for 1 h and exposed for x-ray film for 8 min..

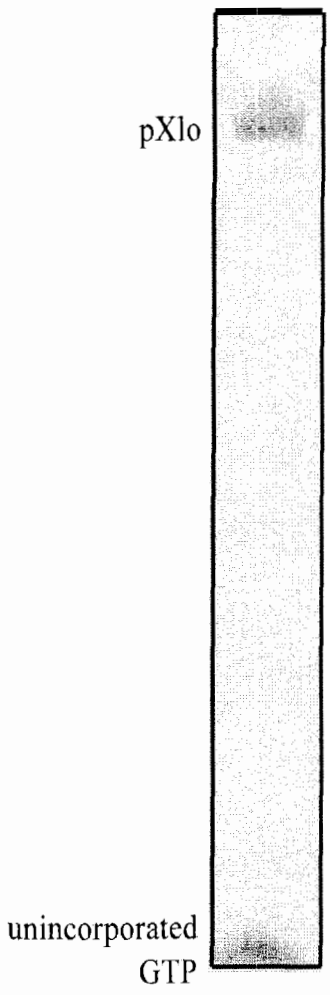

Figure 18. Autoradiogram of an *in vitro* transcription reaction. Sample separated on an 8 % denaturing acrylamide gel at 300 V for 1 h and exposed for x-ray film for 8 min..

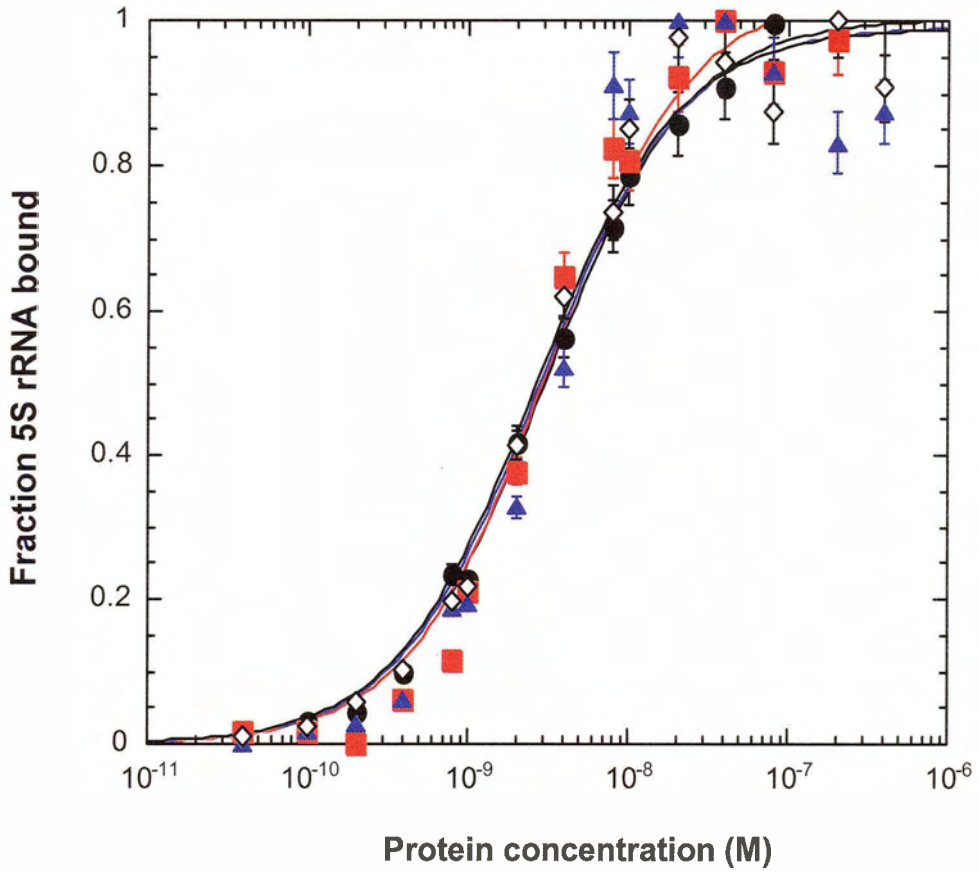

Figure 19. Sample nitrocellulose filter binding curves for randomly generated mutants. Representative curves illustrate the binding affinity of p43 (black circles), p43 mutants b (black diamonds), g (blue triangles) and e (red boxes) for 5S rRNA. Each data point is the mean of at least three independent trials with the associated standard deviations indicated by the error bars determined using Kaleidagraph software. The continuous line represents the best fit to a simple bimolecular equilibrium assuming a retention efficiency of the complex of 1.

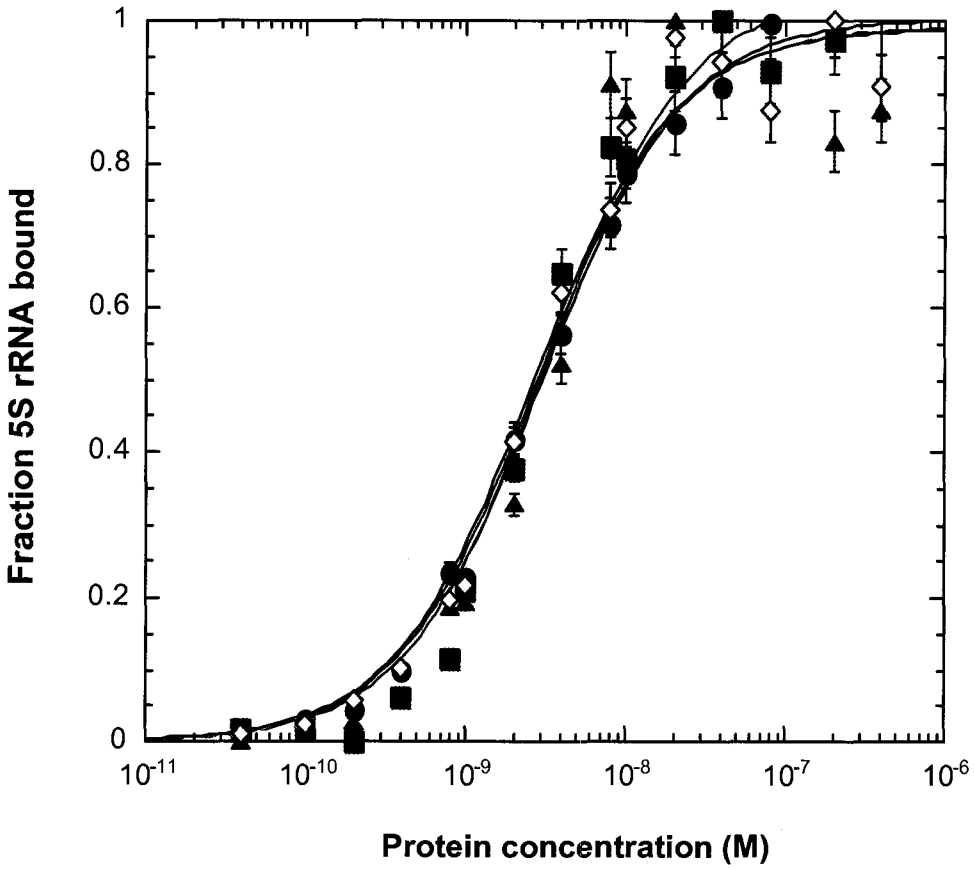

Figure 19. Sample nitrocellulose filter binding curves for randomly generated mutants. Representative curves illustrate the binding affinity of p43 (black circles), p43 mutants b (black diamonds), g (blue triangles) and e (red boxes) for 5S rRNA. Each data point is the mean of at least three independent trials with the associated standard deviations indicated by the error bars determined using Kaleidagraph software. The continuous line represents the best fit to a simple bimolecular equilibrium assuming a retention efficiency of the complex of 1.

Table 2. Affinity of randomly generated mutant p43 proteins for 5S rRNA. Apparent dissociation constants were determined by nitrocellulose filter binding assay. Relative affinities were determined by dividing the K_d for each mutant protein by the K_d for the wild-type protein. Each value represents the mean of at least three independent determinations with the associated standard deviations. P-values were determined using a Welch's t-test.

Protein	*N*	K_d (nM)	K_d relative to p43*	p-value
p43	9	2.89 (±0.99)	1	--
Mutant b	4	2.50 (±0.39)	1.16	0.3268
Mutant e	5	3.19 (±1.01)	0.91	0.6132
Mutant g	3	2.51 (±0.87)	1.15	0.5603

*Relative affinity was determined as a ratio of the dissociation constant for the wild type to the dissociation constant of the mutant, where K_d is the dissociation constant determined by regression with Kaleidagraph.

N = number of independent determinations of the K_d

2.6 DISCUSSION

In 1996, the yeast three-hybrid method, dedicated to the selection of RNA binding proteins using a hybrid RNA as bait, was conceived simultaneously by SenGupta and Putz. This method has been used successfully to dissect RNA-protein interactions. The three-hybrid method consists of the expression in yeast cells of three chimeric, or hybrid molecules, which assemble in order to activate specific reporter genes. In contrast to other methods, RNA-protein interactions are detected *in vivo* using the yeast three-hybrid system.

In the yeast three-hybrid system the LexA DNA binding domain was fused to an MS2-coat RNA binding protein. The second hybrid protein was a fusion of the LexA activation domain and the cDNA encoding p43. The two hybrids were bridged by a third hybrid RNA, the MS2 coat protein binding RNA and the 5S rRNA gene transcript. Binding of protein p43 to 5S rRNA creates a functional transactivator, which is tethered at the upstream activating sequence of two reporter genes (*HIS3* and *lacZ*) that are transcribed and expressed by yeast cells.

The observation that linear DNA fragments can efficiently stimulate recombination in *Saccharomyces cerevisiae* has led to the rapid development of powerful methods for DNA manipulation in yeast (Oldenburg *et al.*, 1997). One use for recombination-based DNA manipulation in yeast is for straightforward cloning purposes. In this case the p43 PCR product, whose ends were homologous to the pYESTrp2 vector, was ligated into the linearized vector by *in vivo* recombination, alleviating the need for an *in vitro* ligation reaction. It has been demonstrated previously that the amount of sequence identity necessary to promote efficient recombination-mediated gene disruption

in yeast is small enough to be synthesized as part of a PCR primer (Oldenburg *et al.*, 1997). The highest frequency of recombinants is obtained with at least 40 nt of homology, however, even 20 nt of homology is sufficient to mediate homologous integration (Oldenburg *et al.*, 1997). The 5' end of the p43 error-prone PCR product contained 45 nucleotides of homology with the gapped pYESTrp2 plasmid and the 3' end of the PCR product contained 131 nucleotides of homology.

The results of the yeast-three hybrid analysis of the molecular interaction between p43 and 5S rRNA are summarized as follows. Approximately 1300 yeast colonies were screened by β-galactosidase filter-lift assy. Among the vast majority of blue colonies, 152 white colonies were identified. Thus approximately 11 % of the yeast colonies appeared to have been transformed with putative p43 mutants following the initial β-galactosidase screenings. The frequency with which white colonies produced blue colonies when re-assayed by nitrocellulose filter lift was not recorded, however, these preliminary results implied that the screening of the pool of randomly generated mutants by the three-hybrid assay was successful.

Fifteen of 19 white colonies were identified by a Western blot to express wild type-sized p43. The decrease in the sample population from 19 to 15 between the colourimetric screening and the Western blot may be partially accounted for by the spontaneous insertion of premature stop codons into the p43 cDNA sequence that occurred during error-prone PCR. Indeed, one of the putative mutants expressed a protein with a higher electrophoretic mobility than the wild type-sized p43. In order for a prematurely terminated p43 peptide to permit assembly of the three-hybrid components, it must retain some 5S rRNA binding affinity. Additionally, a white colony could be a

false negative. Rationale for the occurrence of false negatives is explored in greater detail below, and may explain the lack of immunoreaction observed for the 3 remaining Western blot-screened mutants. One hundred and thirty-three out of the total 152 putative p43 mutants were not screened by Western blot.

Upon sequencing of the putative mutant p43 cDNAs, nine of these fifteen contained actual mutations, and four of these contained mutations in zinc finger 4. The six putative p43 mutants that did not contain mutations but demonstrated a white phenotype may have contained regions outside of the p43 coding sequence, but inside the regions amplified by the error-prone PCR reaction by the pYESTrp2 forward primer, that were critical to the folding of the LexA activation domain. *In vitro* 5S rRNA binding assays were completed for three of the mutants, there was no significant difference between the 5S rRNA affinity of these p43 mutants and the wild type p43 protein.

Following the sequencing of the mutant p43 cDNA, no disruptions to the conserved residues critical to the formation of zinc fingers 1, 3, 5, 6, 7, or 9 were observed. Therefore, no comments can be made about the role of these zinc fingers in 5S rRNA binding. Finger 2 of p43 mutant b was disrupted by the substitution of a conserved cysteine; this protein was not expressed and no comment can be made about the effect of this mutation on 5S rRNA binding. Finger 4 of p43 mutant a was disrupted by the substitution of a conserved leucine for a phenylalanine; this protein was not expressed and no comment can be made about the effect of this mutation on 5S rRNA binding. However, it would be expected that this mutation would have little or no effect on 5S rRNA binding affinity as the chemical properties of leucine and phenylalanine are somewhat comparable. Leucine's R-group is a nonpolar aliphatic with a hydropathy index

rating of 3.8 (Kyte & Doolittle, 1982) that stabilizes protein structure by hydrophobic interactions. Phenylalanine's R-group, while also able to participate in hydrophobic interactions, is considerably larger than the aliphatic leucine residue but has a lower hydropathy index rating of 2.8 due to electron resonance about the benzene ring (Kyte & Doolittle, 1982).

While no change in binding affinity was seen in p43 mutant e, where a single alanine was substituted to proline substitution in zinc finger 4, it is intriguing that 3 other mutants with mutations in zinc finger 4 were determined *in vivo*, by three hybrid assay, to have decreased 5S rRNA binding. The R-group of a proline residue is significantly larger than that of alanine; while this substitution did not occur at an amino acid residue critical for the formation of the zinc finger, it is possible that it interfered with the folding of zinc finger 4 in some way.

A BLAST search was employed to determine that all of the mutations described in Figure 17 occurred at residues that shared sequence identity between the three *Xenopus* species, *laevis*, *borealis* and *tropicalis* except the mutations described below. Eighty-two percent of the amino acid sequence for p43 from the three *Xenopus* species are conserved. Mutant a contained a lysine substituted by a phenylalanine in zinc finger 8. This residue is a valine in the other two *Xenopus* species, *borealis* and *tropicalis*. Mutants c and d contained a glutamine substituted by an arginine in zinc finger 1. Arginine is the residue found in the two other *Xenopus* species.

Darby and Joho (1992) assayed a series of p43 deletion mutants for their affinities fot 5S rRNA. The results of qualitative gel shift experiments showed that a truncation mutant consisting of zinc fingers 1-4 had 5S rRNA binding equal to that of full length

p43; however, deletion of zinc finger four reduced the affinity of the protein for RNA. It was proposed that zinc finger four induced a specific conformation in either the protein or the RNA that was critical for high-affinity binding. It is intriguing that four of the mutants generated by error-prone PCR and screened by yeast-three hybrid (mutants a, c, e and i) contained substitutions in zinc finger 4 and demonstrated a white phenotype in the β-galactosidase assay. It is possible that the *in vivo* yeast three-hybrid assay permitted a specific zinc finger conformation that lead to a reduction in binding affinity that was undetectable if the *in vitro* nitrocellulose filter binding assay. Three of the zinc finger 4 mutants, however, remain to be characterized *in vitro*.

None of the reductions in binding affinity observed for the randomly generated mutants b, e or g were as dramatic as desired. Previous attempts to characterize the interaction between p43 and 5S rRNA lead to the discovery that substitution with alanine of the lysine at position –1 of the alpha-helix of finger 4 of p43 decreased the 5S rRNA binding affinity by 3.5 fold (Hamilton et al., 2001). It was therefore expected that the decrease in affinity for the randomly generated mutants would be in this range upon *in vitro* characterization. Thus mutant proteins a, c, d, f, and h were not expressed and the yeast three-hybrid project was abandoned. An alternate approach to study the interactions between 5S rRNA and p43 was thus attempted and is detailed in subsequent chapters. It seems possible that mutations dramatically affecting the binding activity of p43 might have failed to precipitate the formation of the hybrid complex necessary to activate the β-galctosidase gene; this assay may have therefore been biased to select for mutations with the subtle decreases in binding affinity, such as those observed.

The three-hybrid assay has revealed aspects of an RNA-protein interaction that

are important *in vivo* even when these are problematic to detect *in vitro*. For example, avian retroviral RNA binding is conferred by the Gag protein's nucleocapsid (NC) portion. Gag mutants that were shown to perturb the interaction between these molecules in the three-hybrid assay showed parallel effects in infected cells (Lee *et al.*, 1999). In contrast, an *in vitro* gel shift assay did not detect the effect of these NC region mutants on Gag binding (Bacharach *et al.*, 1998). It is therefore a possibility that the white phenotype seen with p43 mutants b, e and g using the hybrid assay indicate an alteration in the proteins' affinity for 5S rRNA *in vivo* that was not detected with the *in vitro* filter-binding assay employed to quantify the loss of binding activity.

The *HIS3* gene encodes an enzyme that catalyses histidine catabolism, imidazoleglycerol-phosphate dehydratase (His3); its expression confers the ability to grow on medium lacking histidine. 3-amino-1,2,4-triazole (3-AT) is a competitive inhibitor of *HIS3* gene product, and cells containing more His3 can survive at higher concentrations of 3-AT in the medium (Jaeger *et al.*, 2004). Thus, the level of 3-AT resistance of the yeast cells reflects the HIS3 expression level and consequently the strength of the RNA-protein interaction in the yeast three-hybrid context (Jaeger *et al.*, 2004). This also means that the stringency of the selection can be adjusted to the type of RNA-protein couple of interest by changing the concentration of 3-AT in the medium (Jaeger *et al.*, 2004).

In the case of my experiments, mutants with decreased 5S rRNA binding activity were characterized, and 3-AT was not used. It would, however, be interesting to repeat the three-hybrid experiments using 3-AT to screen for mutations that increase the affinity of p43 for 5S rRNA from its wild type value of 1.9 nM (Zang & Romaniuk, 1995).

Indeed, 3-AT was used successfully to screen for mutant HBP molecules that bound to the target RNA with sub-nanomolar affinity (Martin *et al.*, 2000).

In the system developed by SenGupta (1996) and incorporated into the kit available from Invitrogen, the first hybrid molecule LexADB-MS2 is encoded by the genome of the yeast strain L-40 coat and the p43-Gal4AD fusion is expressed from the plasmid pYESTrp2: p43 (Figure 11). An advantage of using this plasmid is that the resulting fusion protein is localized to the nucleus, satisfying one of the requirements for a successful three-hybrid assay. However, p43 is normally localized to the cytoplasm, this change in the cellular localization of the p43 protein may highlight a disadvantage of the three hybrid system. Nuclear localization of p43 may have perturbed the interaction between this protein and its RNA ligand, and lead to the unexpected results observed upon *in vitro* characterization.

The hybrid RNA molecule is produced by RNA polymerase III leading to an RNA containing the RNAse 5' leader sequence and 3' trailer sequence leading to nuclear localization (Figure 10). One major drawback of RNA polymerase III is that stretches of four or more T residues act as transcription terminator (Jaeger *et al.*, 2004). Unfortunately, many RNA binding proteins recognize U-rich RNA targets and RNA polymerase III is not able to transcribe such RNAs (Jaeger *et al.*, 2004). The sequence of 5S rRNA, illustrated in Figure 7, contains three sequential T residues at its 3' terminus, so this issue would probably not effect 5S rRNA transcription.

In the method developed by Putz (1996) and not employed in my experiments, the three components of the system are expressed from two plasmids allowing the use of any number of yeast strains previously described for two-hybrid system that provide the two

reporter genes *HIS3* and *lacZ* under the control of *Gal4* operator (Jaeger *et al.*, 2004). With this method, the hybrid RNA molecule is transcribed by RNA polymerase II, avoiding any premature stop in the transcription of U-rich target RNAs (Jaeger *et al.*, 2004).

A drawback of the three-hybrid strategy is that the RNA-protein interaction takes place *in vivo*, where it can be in influenced by many cellular parameters (Jaeger *et al.*, 2004). This leads to false positive clone predominance that must be eliminated by additional time-consuming screening tests. False positives are interactions that register as positive, but do not in fact reflect an RNA-protein interaction in the three-hybrid assay. False positives can occur when an interaction occurs that is not biologically relevant. This type of false positive can be divided into three groups (Bernstein *et al.*, 2002):

1. High-affinity, nonspecific interactions. Although few proteins have non-specific affinities for RNA that fall in the nanomolar range, it is possible that a protein that interacts with a restricted set of RNAs in the cell can bind to many more RNAs in the three-hybrid system.
2. Bridges. A protein that appears to interact with the RNA of interest may in fact interact with a yeast cellular protein that in turn interacts with that RNA. For example, the yeast protein She3 appears to bind to a portion of the 3'UTR from ASH1 mRNA. She3 actually interacts with She2, which is capable of binding to the hybrid RNA (Long *et al.*, 2000).
3. RNA-independent interactions. The protein that is being tested in the three-hybrid assay may bind directly to the LexA/MS2 protein fusion. This is a common problem when screening for RNA-interacting proteins using a cDNA library, but

is much less common when testing a specific protein, such as in the experiments described herein.

False negatives assays can arise due to the improper expression or folding of the protein or the RNA. Expression of protein or RNA can be verified by performing either a Western blot or a Northern blot, respectively. Western blotting was used to confirm correct protein expression, but a Northern blot was not employed, and expression of 5S rRNA in the transformed yeast cells was not verified. It is therefore possible that the white phenotype observed for the loss of binding affinity p43 mutants could have occurred in cells where the 5S rRNA was either not being expressed properly or not being folded properly. This however is not likely as each putative mutant was screened multiple times by β-galactosidase assay to confirm the white phenotype.

Unfortunately, the three-hybrid strategy can be useless for some RNA-protein couples. Since protein and RNA partners are expressed as chimeric molecules, the folding or the accessibility of the bait might be disturbed by the other moiety of the molecule (Jaeger *et al.*, 2004). The hybrid RNA might also be altered in the nucleus by yeast processing machinery leading to truncated hybrid RNA, useless for the three-hybrid strategy (Jaeger *et al.*, 2004). It is suspected that the lack of success of this project had to do with the first of the above reasons. The binding of 5S rRNA to p43 is highly conformation-dependent (Zang & Romaniuk, 1995) and if the 5S rRNA folding was perturbed by the MS2 fusion, its binding affinity to p43 would be altered. This possibility could have been examined with greater scrutiny by creating a labeled RNA that contained 5S rRNA sequence transcribed from the three-hybrid plasmid. Such a transcript would include the MS2 RNA 5' to the 5S rRNA sequence. A comparison of the binding

affinities for the two transcripts for both wild-type p43 and the mutants might have shown whether the results obtained were an artifact of a conformational change in the 5S rRNA brought about by its fusion to the MS2 RNA. In addition, the localization of p43, normally found in oocyte cytoplasm, to the nucleus of the yeast may have perturbed the RNA-protein interaction.

2.7 PROSPECTS

Future developments of the hybrid screenings will be to select protein partners binding to bait consisting of RNP complexes, for example the 42S particle. This has already been done in the case of the hunchback mRNA (Sonoda & Wharton, 2001) and could be applied to many other complexes. By varying the stringency of the selection, characterization of different protein partners binding tightly or weakly will be possible (Jaeger *et al.*, 2004). Most of RNP complexes consist of a core composed of strong interactors surrounded by weak interactors modulating the activity of the RNP (Jaeger *et al.*, 2004). Three-hybrid screens will enable to select proteins binding to RNA at different steps of their function (Jaeger *et al.*, 2004). Once the proteins are characterized one can analyze the RNA-protein complexes by making positive and negative selections on randomly mutated libraries of the two partners (Jaeger *et al.*, 2004).

3. INVESTIGATING INTERACTIONS BETWEEN p43 AND 5S rRNA USING PCR DIRECTED MUTAGENESIS

3.1 CREATING MUTANTS BY SITE-DIRECTED MUTAGENESIS

In vitro mutagenesis makes it possible to systematically alter the nucleotide sequence of a cloned gene. With PCR-based mutagenesis, mutant primers are added to a PCR reaction in which the gene, or a segment thereof, is amplified. The mutant primers contain sequence that has been specifically designed to introduce a directed change at a particular place in the nucleotide sequence of the gene being amplified. Mutant versions of the gene can then be cloned and expressed to determine any effects of the mutation on the function of the gene product. As specific amino acid residues of p43 are thought to be involved in 5S rRNA binding, site directed mutagenesis could be employed to change these residues. Mutations that retain the C2H2 zinc finger domain structure yet reduce the protein's affinity for its RNA ligand could lead to the identification of the amino acid residues of p43 critical to specific 5S rRNA binding.

Finger-swap and C- terminal deletion mutants of p43, illustrated in Figure 20, were constructed by PCR directed mutagenesis, illustrated in Figure 21. cDNA encoding WT1 zinc fingers 1-4 was substituted for either the first four or the last four zinc fingers of p43. As WT1 has no 5S rRNA binding affinity (Hamilton *et al.*, 2001), the finger swap mutants would allow for a determination of the importance of either the N- or C-terminal zinc fingers in RNA binding. While the 5S rRNA binding of each eight zinc finger peptide will be altered, the structure of the tandem array of zinc fingers will be maintained. Thus any observed decrease in 5S rRNA binding can be attributed to the

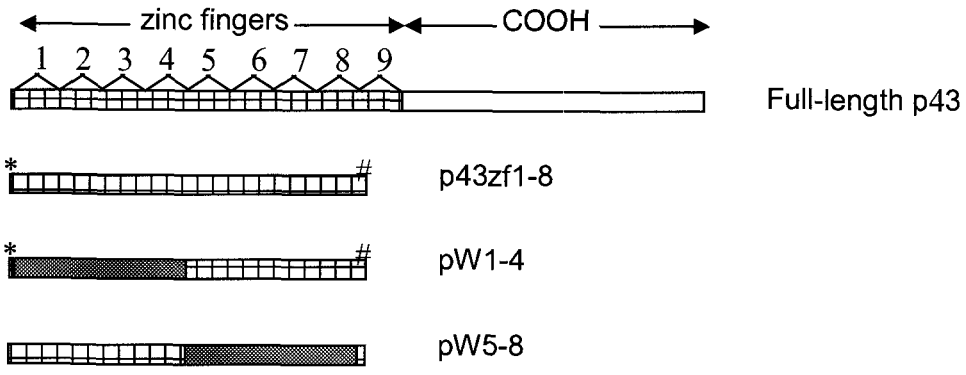

Figure 20. p43 deletion and finger swap mutants. A schematic representation of p43 cDNA and the chimeric cDNAs is shown. Small boxes depict regions of the cDNAs that encode wild-type p43 zinc finger sequences; stippled boxes represent regions of the cDNAs which encode donor WT1 sequences. Restriction enzyme sites used to clone the cDNAs into the vector pET30a are shown above the mutant p43 cDNAs; the Nco I cut site is indicated by the asterix (*) and the Eco RI cut site is indicated by the number sign (#).

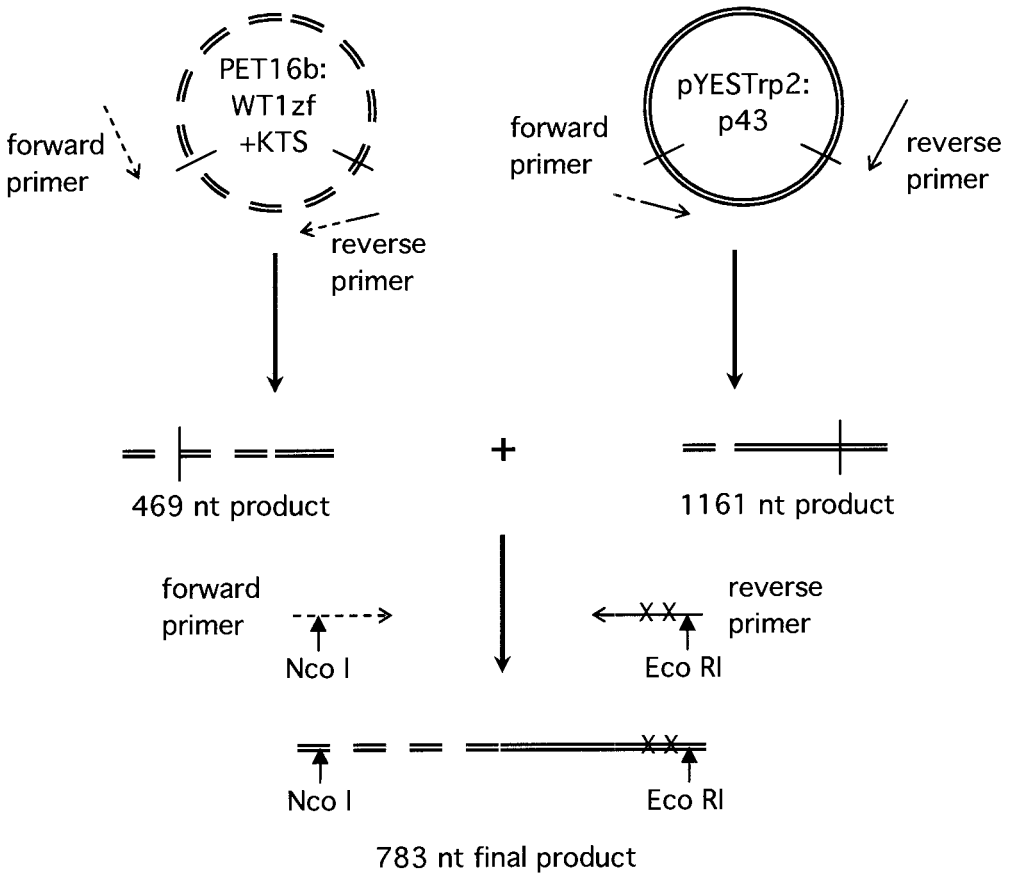

Figure 21. PCR strategy for constructing the p43 mutant pW1-4. In order to generate the WT1 zinc finger half reaction, primers annealed upstream of the WT1 cDNA and downstream to add a p43 zinc finger 5 homology region to the 3' end of the WT1 zinc finger sequence. In order to generate the p43 zinc fingers 5-8 half reaction, primers were designed to add a WT1 zinc finger 4 homology region. Primers annealed downstream of the p43 cDNA and upstream of the zinc finger 5 sequence. The final reaction fused the half reactions and generated a product with Nco I and Eco RI sites to facilitated cloning and two stop codons immediately downstream of the p43 zinc finger 8 sequence.

change in amino acid sequence. The p43 mutant pW1-4 was constructed by swapping zinc fingers 1-4 of p43 with the four zinc fingers from WT1. The p43 mutant pW5-8 was constructed by swapping the four WT1 zinc fingers with fingers 5-8 of p43.

The effect of each mutation was to be determined by nitrocellulose filter-binding assay and in those mutants showing a significant decrease in binding affinity, by Scatchard analysis. Previous attempts to characterize full-length p43 in non-denaturing gel separations met with limited success due to the relative insolubility of the full-length p43 molecule. This property of p43 is attributed to the C-terminal tail, which is thought to be involved in interactions with other protein components of the 42 S RNP. Therefore, a C-terminal truncation mutant, p43zf1-8, consisting of the first eight zinc fingers of the protein was cloned for use as a positive control for Scatchard analysis.

3.2 METHODS

3.2.1 CLONING VECTORS AND STRAINS

p43 cDNA was amplified by from the pYESTrp:p43 plasmid. WT1+KTS zinc finger cDNA was amplified from the pET16b:WT1+KTSzf plasmid provided by Dr. Romaniuk. Vectors containing recombinant protein cDNA were cloned in *E. coli* DH5α (Invitrogen).

3.2.2 EXPRESSION VECTORS AND STRAINS

The mutant p43 proteins cloned by site-directed mutagenesis were overexpressed from a pET30a plasmid (Clontech). All proteins were overexpressed and purified from the *E. coli* strain BL21 (DE3) (Invitrogen).

3.2.3 DELETION MUTAGENESIS PCR

The C-terminal tail p43 deletion mutant, p43zf1-8 was constructed as follows. The mutant was introduced at targeted locations in wild type p43 cDNA in a 20 μL PCR reaction. Approximately 10 ng of pYESTrp2: p43 plasmid DNA was used as the template. All of the primers in section 3.2.3 were synthesized by Invitrogen. The upstream primer (5'-CGTTCACCATGGCGAATGTTG GTGAGACTG-3') was designed to insert an Nco I restriction site upstream of the p43 cDNA. The downstream primer (5'-GCAGCGGAATTCATTAACACAGGTGGAG-3') was designed to insert tandem stop codons directly after zinc finger 8, and an Eco RI restriction site. The primers were added to a final concentration of 0.3 μM each. The PCR reaction mixture

contained 4 μL of 10X PCR buffer, deoxynucleotide triphosphates to a final concentration of 1 mM each, 1 mM $MgSO_4$, and 1 unit of *Pfx* DNA polymerase (Invitrogen). The reaction was amplified in a thermal cycler with an initial denaturation step at 94 °C for 5 min, followed by a denaturation step at 94 °C for 20 s, an annealing step at 55 °C for 20 s and a 1 min elongation at 68 °C; these three steps were repeated 34 times. The amplified 765 nucleotide sequence contained p43 cDNA encoding the 8 zinc fingers of the protein as well as 5' and 3' ends compatible to Eco RI and Nco I restriction sites of the pET30a plasmid. The presence of the correct product was verified by electrophoresis on a 1.5 % agarose gel in TBE buffer (45 mM Tris-borate, 1 mM EDTA) at 100 V. The PCR reaction product was purified using a PCR Purification column (Qiagen).

3.2.4 FINGER SWAP MUTAGENESIS PCR

The p43 mutant pW1-4 was constructed such that the four zinc fingers of WT1 were substituted for the N-terminal four zinc fingers of p43. This was carried out with three 20 μL PCR reactions. The first reaction amplified the WT1 zinc finger sequence with a region homologous to p43 zinc finger 5 directly downstream of WT1 zinc finger 4. Approximately 10 ng of pET16b: WT1+KTSzf plasmid DNA was used as the template. . All of the primers in section 3.2.4 were synthesized by Invitrogen. The upstream primer (5'-CGGCGGTGTGAGCGGATAACAATTCCC-3') was a universal forward primer for the vector pET16b and the downstream primer (5'-GTCACAAACAGACAGAGGC-TCTCTCTGATGCATGTTGTG-3') was a reverse primer with the first 21 nucleotides complementary to the start of finger 5 in p43 and the last 18 nucleotides complementary

to the end of finger 4 of WT1. The primers were added to a final concentration of 0.3 μM each. The PCR reaction mixture contained 4 μL of 10X PCR buffer, deoxynucleotide triphosphates to a final concentration of 1 mM each, 1 mM $MgSO_4$, and 1 unit of *Pfx* DNA polymerase. The reaction was amplified in a thermal cycler with an initial denaturation step at 94 °C for 5 min, followed by a 20 s denaturation at 94 °C, an annealing step at 55 °C for 20 s and a 1 min elongation at 68 °C; these three steps were repeated 34 times. The amplified 469 nucleotide sequence contained cDNA encoding the four zinc fingers of WT1 in addition to a region homologous to zinc finger 5 of p43. The presence of the correct product was verified by electrophoresis on a 1.5 % agarose gel in TBE buffer (45 mM Tris-borate, 1 mM EDTA) at 100 V. The PCR reaction product was purified using a Qiaquick PCR Purification column.

The second reaction leading to the construction of the mutant pW1-4 was an amplification of p43 cDNA encoding zinc fingers 5-8. Approximately 10 ng of pYESTrp2:p43 plasmid DNA was used as the template. The upstream primer (5'-GA-GCCTCTGTCTGTTTGTG-3') was complementary to zinc finger 5 of p43 cDNA and the downstream primer (5'-GGGCGTGAATGTAAGCGTGAC-3') was complementary to a region of the pYESTrp2 plasmid downstream from the p43 insert. The primers were added to a final concentration of 0.3 μM each. The PCR reaction mixture contained 4 μL of 10X PCR buffer, deoxynucleotide triphosphates to a final concentration of 1 mM each, 1 mM $MgSO_4$, and 1 unit of *Pfx* DNA polymerase. The reaction was amplified in a thermal cycler with an initial denaturation step at 94 °C for 5 min, followed by a denaturation step at 94 °C for 20 s, an annealing step at 55 °C for 20 s and a 1 min elongation at 68 °C; these three steps were repeated 34 times. The amplified 1161

nucleotide sequence contained cDNA encoding the C-terminal half of p43. The presence of the correct product was verified by electrophoresis on a 1.5 % agarose gel in TBE buffer at 100 V. The PCR reaction product was purified using a Qiaquick PCR Purification column.

The final reaction leading to the construction of the mutant pW1-4 fused the two half-reaction products. The templates for the reaction were 1/100 dilutions of each of the column-purified half-reaction PCR products. The upstream primer (5'-CGTTCACCAT-GGGACGTGTGCCTGG-3') was designed to insert an Nco I restriction site upstream of the WT1 cDNA. The downstream primer (5'-GCAGCGGAATTCATTAACACAGGT-GGAG-3') was designed to insert an Eco RI restriction site downstream of tandem stop codons at the end of p43 zinc finger 8. The primers were added to a final concentration of 0.3 μM each. The PCR reaction mixture contained 4 μL of 10X PCR buffer, deoxynucleotide triphosphates to a final concentration of 1 mM each, 1 mM $MgSO_4$, and 1 unit of *Pfx* DNA polymerase. The reaction was amplified in a thermal cycler with an initial denaturation step at 94 °C for 5 min, followed by a three-step cycle of a 20 s denaturation step at 94 °C, an annealing step at 55 °C for 20 s and a 1 min elongation at 68 °C; this cycle repeated 34 times. The amplified 783 nucleotide sequence contained cDNA encoding the four zinc fingers of WT1 followed by zinc fingers 5-8 of p43 in addition to 3' and 5' end compatible to the Nco I and Eco RI restriction sites of the pET30a plasmid. The presence of the correct product was verified by electrophoresis on a 1.5 % agarose gel in TBE buffer at 100 V. The PCR reaction product was purified using a Qiaquick PCR Purification column.

The p43 mutant pW5-8 was constructed such that the four zinc fingers of WT1 were substituted for zinc fingers 5-8 of p43. This was carried out with three PCR reactions. The first reaction introduced a region homologous to WT1 zinc finger 1 directly downstream of p43 zinc finger 4. Approximately 10 ng of pYESTrp2:p43 plasmid DNA was used as the template. The upstream primer (5'-GAAGCGG-TGTTAACGATACC-3') was complementary to the plasmid pYESTrp2 upstream of the p43 insert and the downstream primer (5'-GCAGCCTGGGTAAGCACAAACAGACA-GAGGCTC-3') was designed to insert a WT1 zinc finger 1 homology region directly downstream of zinc finger 4 of p43. Primers were added to a final concentration of 0.3 μM each. The PCR reaction mixture contained 4 μL of 10X PCR buffer, deoxynucleotide triphosphates to a final concentration of 1 mM each, 1 mM $MgSO_4$, and 1 unit of *Pfx* DNA polymerase. The reaction was amplified in a thermal cycler with an initial denaturation step at 94 °C for 5 min, followed by a denaturation step at 94 °C for 20 s, an annealing step at 55 °C for 20 s and a 1 min elongation at 68 °C; these three steps were repeated 34 times. The amplified 486 nucleotide sequence contained cDNA encoding the first four zinc fingers of p43 with a region homologous to zinc finger 1 of WT1. The presence of the correct product was verified by electrophoresis on a 1 % agarose gel in TBE buffer (45 Mm Tris-borate, 1 mM EDTA) at 100 V. The PCR reaction product was purified using a Qiaquick PCR Purification column.

The second reaction leading to the construction of the mutant pW5-8 introduced a region homologous to p43 zinc finger 4 directly upstream of WT1 zinc finger 1. Approximately 10 ng of pET16b: WT1+KTSzf plasmid DNA was used as the template. The upstream primer (5'-GAGCCTCTGTCTGTTTGTGCTTACCCAGGCTGC-3') was

designed to insert a WT1 zinc finger 4 homology region directly upstream of zinc finger 5 of p43. The downstream primer (5'-AGCTCTATCAAAGCGCCAGCTGGAG-3') was designed to anneal downstream of WT1 zinc finger 4 in the pET16 sequence. The primers were added to a final concentration of 0.3 μM each. The PCR reaction mixture contained 4 μL of 10X PCR buffer, deoxynucleotide triphosphates to a final concentration of 1 mM each, 1 mM $MgSO_4$, and 1 unit of *Pfx* DNA polymerase. The reaction was amplified in a thermal cycler with an initial denaturation step at 94 °C for 5 min, followed by a three-step cycle of a denaturation step at 94 °C for 20 s, an annealing step at 59 °C for 20 s and a 1 min elongation at 68 °C; this cycle was repeated 34 times. The amplified 469 nucleotide sequence contained cDNA encoding the four zinc fingers of p43 with a 3' region homologous to zinc finger 1 of WT1. The presence of the correct product was verified by electrophoresis on a 1 % agarose gel in TBE buffer at 100 V. The PCR reaction product was purified using a Qiaquick PCR Purification column.

The final reaction leading to the construction of the mutant pW5-8 fused the two half-reaction products and introduced 5' and 3' restriction sites to facilitate cloning into the pET30a vector. The templates for the reaction were 1/100 dilutions of each of the column-purified half-reaction PCR products. The upstream primer (5'-GTTCACCAT-GGCGAATGTTGGTGAGACTG-3') was designed to insert an Nco I restriction site upstream of the p43 cDNA. The downstream primer (5'-CAGTCCGAATTCCTATC-AAAGCGCCAGCTGGAG-3') was designed to insert tandem stop codons and an Eco RI restriction site downstream of WT1 zinc finger 4. The primers were added to a final concentration of 0.3 μM each. The PCR reaction mixture contained 4 μL of 10X PCR buffer, deoxynucleotide triphosphates to a final concentration of 1 mM each, 1 mM

$MgSO_4$, and 1 unit of *Pfx* DNA polymerase. The reaction was amplified in a thermal cycler with an initial denaturation step at 94 °C for 5 min, a denaturation step at 94 °C for 20 s, an annealing step at 55 °C for 20 s and a 1 min elongation at 68 °C; these last three steps were repeated 34 times. The amplified 865 nucleotide sequence contained cDNA encoding the first four zinc fingers of p43 followed by the four zinc fingers of WT1 in addition to 3' and 5' ends compatible to the Nco I and Eco RI restriction sites of the pET30a plasmid. The presence of the correct product was verified by electrophoresis on a 1.5 % agarose gel in TBE buffer at 100 V. The PCR reaction product was purified using a Qiaquick PCR Purification column.

3.2.5 TRANSFORMATION INTO EXPRESSION STRAIN

Following confirmation of the expected PCR product size by electrophoresis, the cDNAs encoding the p43 mutants p43zf1-8, pW1-4 and pW5-8 were ligated in-frame into an open reading frame that introduced a six-histidine repeat at the N-terminus of each insert at the Eco RI/ Nco I site of the plasmid pET30a. 20 uL of each ligation was transformed into 100 μL of chemically competent *E. coli* DH5α. The transformation mixture was incubated on ice for 5 min, heat shocked for 2 min, and returned to ice for 5 min. The culture was then incubated with 800 μL LB at 37 °C for 1 h, following which 200 μL were plated on the appropriate selective medium. The plates were incubated at 37 °C for 16 h.

3.2.6 COLONY PCR

To screen for successful transfections of each p43 mutant into *E. coli* DH5α, colonies were picked and lysed by heating at 94 °C in a PCR tube for 5 min. p43 cDNA was then amplified in a 10 μL PCR reaction. The upstream primer (5'-TAATACGA-CTCACTA TAGGG-3') was complementary to T7 promoter sequence of pET30a. The downstream primer (5'-TAGTTATTGCTCAGCGGTGG-3') was complementary to the T7 terminator sequence in pET30a. The primers were added to a final concentration of 0.3 μM each. The PCR reaction mixture contained 1 μL of 10X PCR buffer, the four deoxynucleotide triphosphates to a final concentration of 1 mM each, 1.5 mM $MgCl_2$, and 1 unit of *Taq* DNA polymerase. The reaction was amplified in a thermal cycler with an initial denaturation step at 95 °C for one min, a denaturation step at 95 °C for 20 s, an annealing step at 55 °C for 20 s and a 30 s elongation at 72 °C; these steps were repeated 40 times. This PCR reaction only yielded a product of the expected size when the vector contained the desired insert. The presence of the expected product was verified by electrophoresis on a 1 % agarose gel in TBE buffer at 100 V. Plasmids were purified by Qiagen mini-prep kit and the presence of an insert of correct size was verified by a digestion check with Eco RI/ Nco I (both NEB).

3.2.7 OVEREXPRESSION AND PURIFICATION OF RECOMBINANT PROTEINS

Expression and purification of the recombinant p43 mutants generated by site-directed mutagenesis was performed using a modified laboratory protocol for the purification of recombinant WT1. Chemically competent *E. coli* BL21 (DE3) was

transformed with pET30a containing the correct mutant construct. The cells were plated on LB plates containing 50 μg/ml of kanamycin and incubated for 16 h at 37 °C. A single colony from each transfection was incubated in 5 ml of LB media with 50 μg/ml of kanamycin at 37 °C for 16 h, shaking at 250 rpm. The following day, the 2.5 ml of the overnight culture was subcultured into 250 ml of TFB media containing 50 μg/ml of kanamycin and incubated at 37 °C for approximately 3 h, shaking at 250 rpm. Once the absorbance at 650 nm had reached between 0.4 and 0.6, the plasmid was induced with 1 mM isopropyl-β-D-thiogalactopyranoside or IPTG. The cells were harvested 6 h later by centrifugation at 7000 rpm in a Beckman JA-16 rotor. The cell pellets were washed with 10 ml of buffer A (10mM Tris-HCl, pH 7.5, 5 mM $MgCl_2$, 250 mM NaCl, 10 mM PMSF, 10 % glycerol, 5mM DTT, 5mM imidazole (Roche)) and resuspended in 10 ml of the same buffer. The cells were disrupted with a microtip sonicator (Heat Systems-Ultrasonics W-385) at setting 5 and 50 % duty cycle for five 1 min intervals with 2 min cooling between pulses. During sonication, the sample was cooled in an ethanol and ice slurry. All subsequent sample handling was performed at 4 ° C unless otherwise stated. The sonicated sample was centrifuged at 10,000 rpm in a Beckman JA-20 rotor and the pellet was resuspended in 2 ml buffer G (buffer A plus 5 M Guanidine-HCl (Sigma)), and rotated for 16 h at 4 °C.

The following day, the crude lysate was pelleted again at 15, 000 rpm and the supernatant was applied to a 1.5 ml Ni-NTA column (Qiagen). The column was washed with 2 ml of buffer B (buffer A plus 5 M Urea and 50mM imidazole) The protein was then eluted with 1 ml of buffer B plus 150 mM imidazole and 1ml of buffer B plus 250 mM imidazole. The protein concentrations were then determined using the Bradford

method with BSA as the standard. Purity was tested by running the column fraction on a 15 % SDS-PAGE gel. Protein purified by this method ranged from 45-93 μM and ran between 32 and 35 kDa on a 15 % SDS-page gel.

3.2.8 SEQUENCING OF MUTANT p43 cDNAs

Following the expression and purification of recombinant protein with the correct molecular weight, sequencing reactions were carried out. To generate a sequence that spanned the each mutant p43 molecule, the upstream primer (5'-TAATACGACTCACTA TAGGG-3', complementary to pET30a's T7 promoter sequence) and the downstream primer (5'-TAGTTATTGCTCAGCGGTGG-3', complementary to T7 terminator sequence in pET30a) were used. The sequencing reactions were carried out at the University of Victoria's Center for Biomedical Research Sequencing Center.

3.2.9 RADIOLABELLING OF 5S rRNA

Xenopus oocyte-type 5S rRNA was radiolabeled with ^{33}P-GTP for subsequent *in vitro* assays as described in section 2.4.12.

3.2.10 NITROCELLULOSE FILTER-BINDING ASSAY

The nitrocellulose filter-binding assay was carried out as described previously in section 2.4.13.

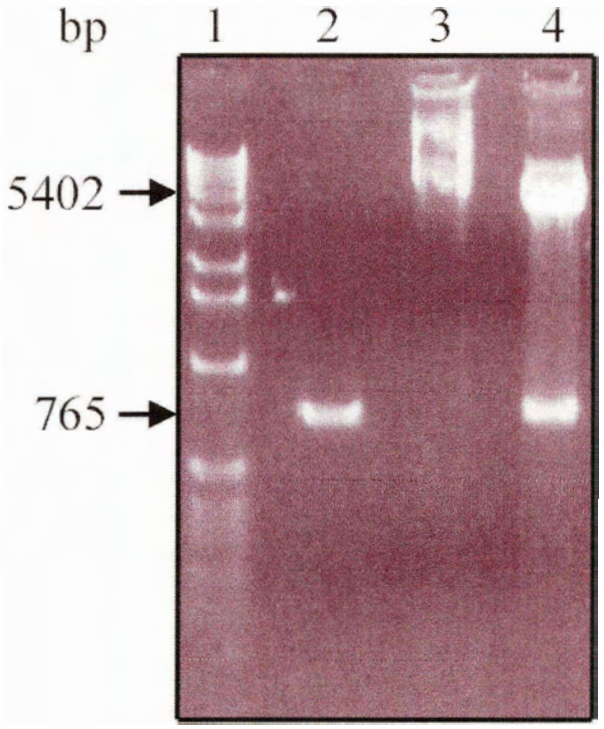

Figure 22. Cloning of p43 mutant p43zf1-8. Lane 1: 1 Kb ladder (Invitrogen), lane 2: PCR product, lane 3: undigested pET30a:p43zf1-8 plasmid, lane 4: pET30a:p43zf1-8 Eco RI / Nco I restriction fragments. The products were visualized by Ethidium bromide staining following electrophoresis on a 1.5 % agarose gel in TBE buffer at 100 V.

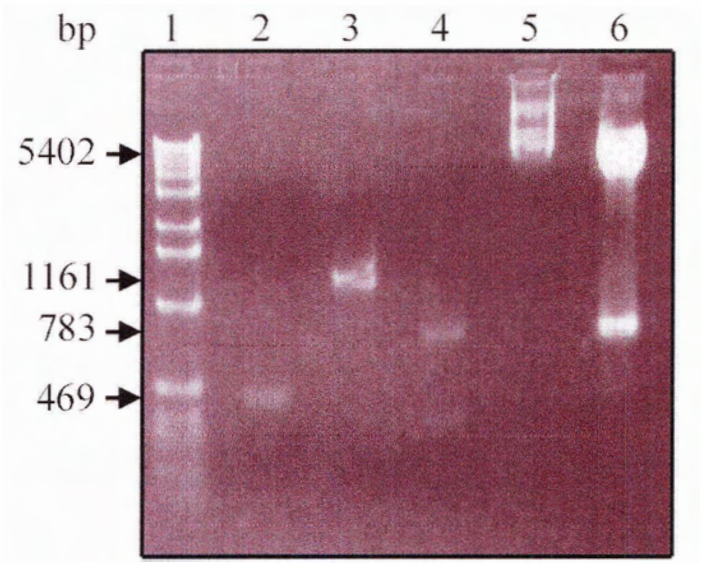

Figure 23. Cloning of p43 mutant pW1-4. Lane 1: 1 Kb ladder (Invitrogen), lane 2: PCR product amplified from pET16b:WT1+KTS template, lane 3: PCR product amplified from pYESTrp2:p43 template, lane 4: final pW1-4 PCR product, lane 5: undigested pET30a:pW1-4 plasmid, lane 6: pET30a:pW1-4 Eco RI / Nco I restriction fragments. The products were visualized by Ethidium bromide staining following electrophoresis on a 1.5 % agarose gel in TBE buffer at 100 V.

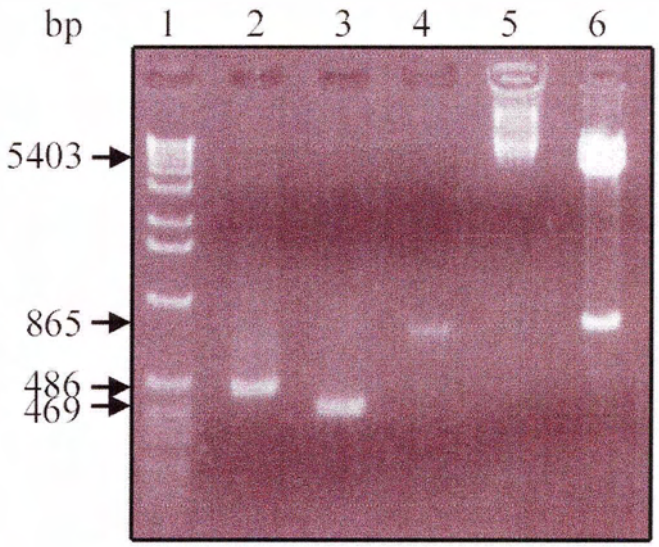

Figure 24. Cloning of p43 mutant pW5-8. Lane 1: 1 Kb ladder (Invitrogen), lane 2: PCR product amplified from pYESTrp2:p43 template, lane 3: PCR product amplified from pET16b:WT1+KTS template, lane 4: final pW5-8 PCR product, lane 5: undigested pET30a:pW5-8 plasmid, lane 6: pET30a:pW5-8 Eco RI / Nco I restriction fragments. The products were visualized by Ethidium bromide staining following electrophoresis on a 1.5 % agarose gel in TBE buffer at 100 V.

In an approach similar to that used to construct the pW1-4 mutant, mutant pW5-8 was constructed in three steps: two PCR half-reactions and a final reaction to fuse the two half reactions. The PCR product for the first half reaction was amplified from the full-length p43 cDNA template, was the expected 486 base pair size, shown in lane 2 of Figure 24. The PCR product for the second half reaction, shown in lane 3 of Figure 24, was amplified from the WT1 zinc finger cDNA template and was the expected 469 base pair size. The final PCR reaction resulted in a 803 base pair product and of consisted a cDNA encoding zinc fingers 1-4 of p43 followed by the four WT1 zinc fingers, bounded at the 5' and 3' end by an Nco I restriction site and an Eco RI restriction site, respectively. The correct cloning of this product was confirmed following ligation into the pET30a vector, transfection into *E. coli* DH5α, plasmid isolation and digestion with both Eco RI and Nco I. The result of the digestion, in lane 6 of Figure 24, confirms that an insert equal to the size of the original PCR product was successfully ligated into the pET30a vector.

3.3.2 OVEREXPRESSION AND PURIFICATION OF SITE DIRECTED MUTANTS

The p43 mutant proteins, p43zf1-8, pW1-4 and pW5-8, were overexpressed and purified from *E. coli* BL21 (DE3) cells. Following elution from the Ni-NTA (Qiagen) nickel affinity column, the concentration of each fraction was determined by Bradford assay and the purity of each fraction was verified by SDS-PAGE. The fractions containing the highest protein concentration were pooled. Figure 25 shows an SDS-PAGE of the pooled fractions for wild type p43 and p43 mutants p43zf1-8, pW1-4 and pW5-8.

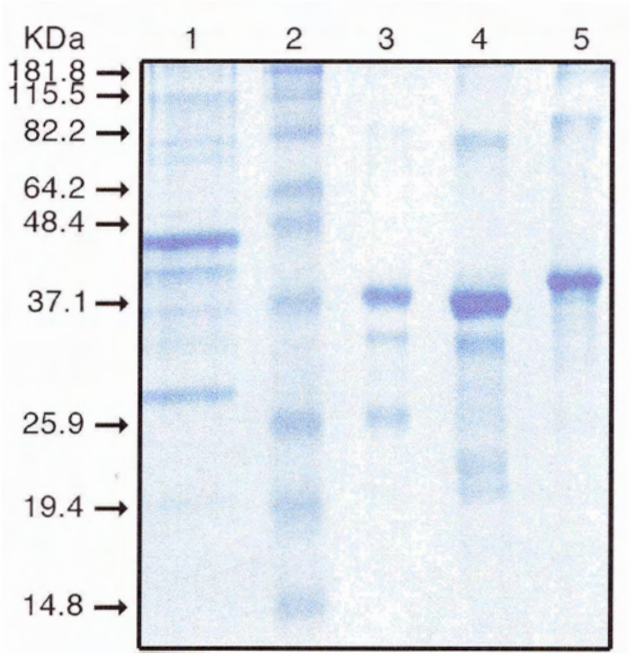

Figure 25. SDS-PAGE of purified p43 mutants p43zf1-8, pw1-5 and pW5-8. The purified protein samples were separated on a 15 % acrylamide gel at 200 V for 90 min. Lane 1: full-length p43, lane 2: protein molecular weight ladder, lane 3: p43zf1-8, lane 4: pW1-4, lane 5: pW5-8. The Benchmark Pre-Stained Protein Ladder (Invitrogen) molecular weight standard contained the following proteins that ran with the apparent molecular weights noted: 181.1 kDa, 115.5 kDa, 82.2 kDa, 64.2 kDa, 48.8 kDa, 37.1 kDa, 25.9 kDa, 19.4 kD and 14.8 KDa.

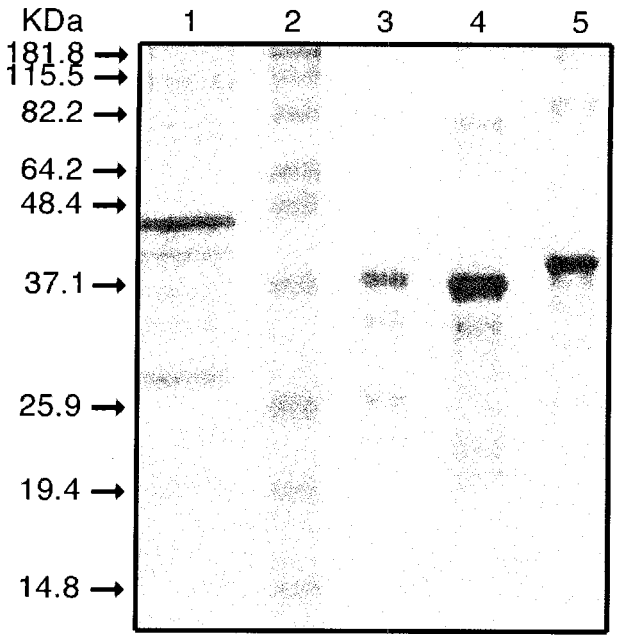

Figure 25. SDS-PAGE of purified p43 mutants p43zf1-8, pw1-5 and pW5-8. The purified protein samples were separated on a 15 % acrylamide gel at 200 V for 90 min. Lane 1: full-length p43, lane 2: protein molecular weight ladder, lane 3: p43zf1-8, lane 4: pW1-4, lane 5: pW5-8. The Benchmark Pre-Stained Protein Ladder (Invitrogen) molecular weight standard contained the following proteins that ran with the apparent molecular weights noted: 181.1 kDa, 115.5 kDa, 82.2 kDa, 64.2 kDa, 48.8 kDa, 37.1 kDa, 25.9 kDa, 19.4 kD and 14.8 KDa.

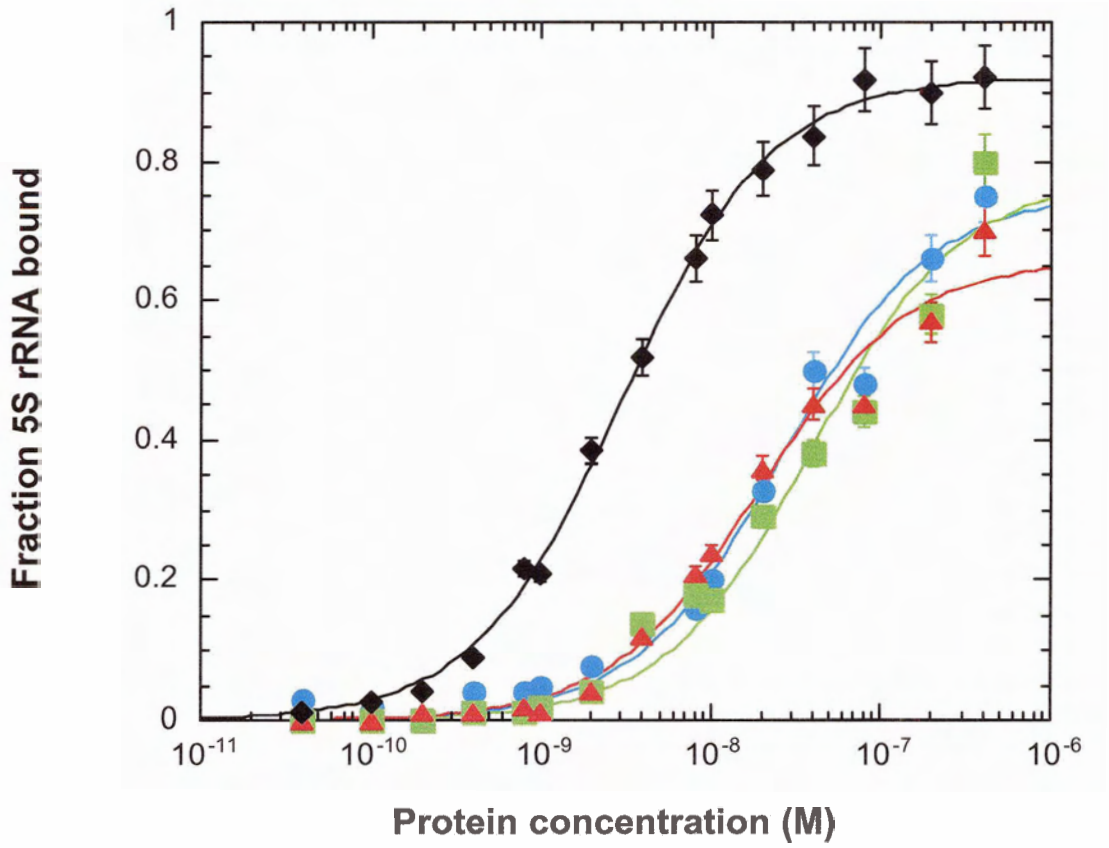

Figure 26. Sample nitrocellulose filter-binding curves for site directed p43 mutants. Representative curves illustrate the binding affinity of full-length p43 (black), p43 mutants p43zf1-8 (blue), pw1-4 (green) and p4w5-8 (red) for 5S rRNA. Each data point is the mean of 3 independent trials with the associated standard deviations indicated by the error bars determined using Kaleidagraph software. The continuous line represents the best fit to a simple bimolecular equilibrium assuming a retention efficiency of the complex of 1

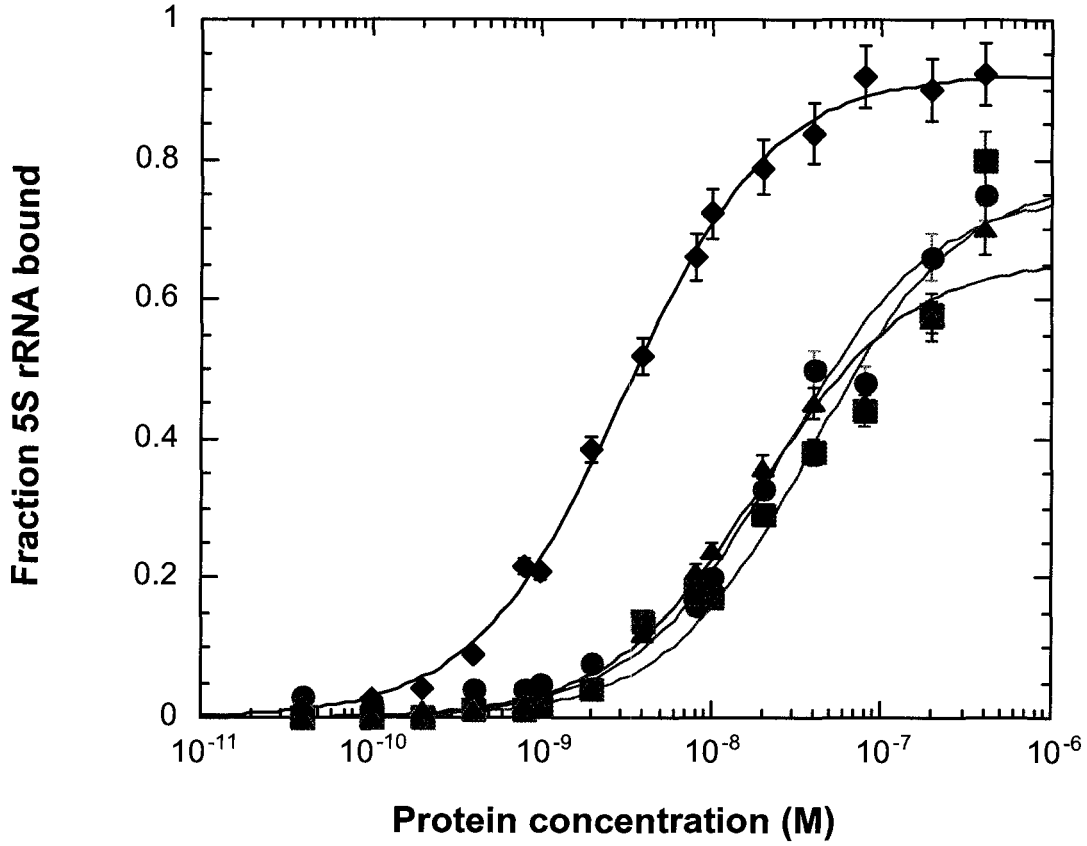

Figure 26. Sample nitrocellulose filter-binding curves for site directed p43 mutants. Representative curves illustrate the binding affinity of full-length p43 (black), p43 mutants p43zf1-8 (blue), pw1-4 (green) and p4w5-8 (red) for 5S rRNA. Each data point is the mean of 3 independent trials with the associated standard deviations indicated by the error bars determined using Kaleidagraph software. The continuous line represents the best fit to a simple bimolecular equilibrium assuming a retention efficiency of the complex of 1.

Table 3. Affinity of deletion and finger swap mutants of p43 for 5S rRNA. Apparent dissociation constants were determined by nitrocellulose filter-binding. Relative affinities were determined by dividing the K_d for each mutant protein by either the K_d for the wild-type protein or the K_d for the protein p43zf1-8. Each value represents the mean of four or more independent determinations with the associated standard deviations. P-values were determined using a Welch's t-test.

Protein	*N*	K_d (nM)	K_d relative to p43*	p-value relative to p43	K_d relative to p43zf1-8*	p-value relative to p43zf1-8
Full-length p43	9	2.89 (±0.99)	1.00	--	--	--
p43zf1-8	3	30.0 (±14.6)	0.10	0.085	--	--
pW1-4	3	36.2 (±91.1)	0.08	0.094	0.83	0.6818
pW5-8	6	26.6 (±9.6)	0.13	0.00395	1.33	0.4857

*Relative affinity was determined as a ratio of the dissociation constant for the wild type to the dissociation constant of the mutant, where K_d is the dissociation constant determined by regression with Kaleidagraph.

$^{\#}N$ = number of independent determinations of the K_d

With respect to p43zf1-8, pW1-4 and pW5-8 were determined to have relative binding ratios of 0.83 and 1.33 respectively. Following a Welch's t-test, however, neither mutant had a significant decrease in 5S rRNA binding. It was therefore determined that the difference between the binding affinities, given the standard deviation of the input K_d values, were not statistically significant and Scatchard analysis was not required.

3.4 DISCUSSION

The difficulties experienced in early p43 studies due to the insolubility of the p43 molecule and its high affinity for other components of the 42 S RNP were solved by the cloning of p43 cDNA into a pET expression vector (Zang & Romaniuk, 1995). This cloning resulted in recombinant p43 produced in quantities sufficient for subsequent characterization experiments. A similar approach was used successfully in the experiments described in this chapter to generate a deletion mutant containing the first eight zinc fingers of p43 and two WT1 finger swap mutants.

Nitrocellulose filter-binding showed that only pW5-8 bound 5S rRNA with a statistically significant lower affinity than wild type p43 of nearly 10-fold. pW5-8 bound to 5S rRNA with approximately twice the affinity of p43zf1-8, but when the error was taken into account, this difference was not significant. The former result described above was unexpected, as the interaction between p43 and 5S rRNA is generally thought to occur via the protein's nine zinc fingers, and not via the C-terminal region. The results of this research suggest that the C-terminal tail, and possibly zinc fingers 5-9 of p43 play an important role in 5S rRNA binding. This could have been confirmed by characterizing the 5S rRNA binding properties of an N-terminal deletion mutant consisting of the amino

acid sequence from zinc finger 5 to the end of the protein. It is possible that the C-terminal tail adds stability to the zinc finger region of the p43 molecule and favors a conformation that is better able to bind the RNA ligand. The decrease in affinity may, however, be due to a difference in fractional activity between the different protein preparations or to the contribution of the C-terminal region of full-length p43.

The binding affinity indicated that p43zf1-8 and pW1-4 both bound to 5S rRNA with a similar efficiency. The results for pW1-4 were not expected as the first four zinc fingers of p43 were previously determined to be particularly critical for 5S rRNA binding (Darby & Joho, 1992). A possible explanation for the unexpected results could be that the charge on the histidine tag employed for protein purification had perturbed the interaction between the mutant p43s and the 5S rRNA. The six histidine repeats would have increased the positive charge of the mutant proteins. This may have altered the proteins' affinity for the negatively charged RNA ligand.

An additional reason for the observed changes in binding affinity that were not statistically significant could have been the inclusion of the nonspecific competitor, poly [d (I-C)]. Poly [d (I-C)] is generally included in a binding reaction when the target nucleic acid binding sequence is GC-rich (Roche, 2003). With purified nucleic acid binding proteins, no or low concentrations of nonspecific competitor is required (Roche, 2003). If used, the amount of competitor used should be carefully titrated. A titration was not performed in this thesis work, but as the full-length p43 protein bound to its RNA ligand with the expected affinity, it is not expected that the inclusion of poly [d (I-C)] into the reaction mixture altered the results obtained.

As shown previously in the lab where my research was carried out, WT1 has no 5S rRNA binding affinity (Hamilton *et al.*, 2001). Therefore, the finger swap mutants should have allowed for a determination of the importance of either the N- or C-terminal zinc fingers in RNA binding. A filter-binding curve for the lack of interaction between WT1 and 5S rRNA would consist of an exponential curve, with the fraction of RNA bound very close to zero, until the concentration of protein entered the millimolar range. The asymptote would indicate the point at which non-specific interactions between the protein and RNA begin to occur. This type of curve does not allow for the determination of K_d. A negative control such as this was not performed in this thesis work; had the differences in binding between mutant and wild type p43 been statistically significant, it would have been challenging to make a valid conclusion. Future experiments involving finger swap mutations should include the protein from which the non-RNA binding zinc fingers come as a negative control.

Darby and Joho (1992) set out to determine the relative affinities for groups of zinc fingers from both p43 and TFIIIA for 5S rRNA. The results published for TFIIIA have subsequently been contradicted by several reports. A qualitative gel shift assay was employed to determine whether RNA affinity changed towards the C-terminus of TFIIIA. N-terminal binding was compared to the abilities of other four zinc finger segments to bind RNA. TFIIIA zinc fingers 1-4, 3-6 and 6-9 had similar affinity for 5S rRNA and the investigators concluded that all zinc fingers could contribute to RNA binding, but that a slight preference for the C-terminal fingers was observed. RNA affinity appeared to be dependant on the number of zinc fingers tested; wild-type binding required the five carboxyl terminus zinc fingers, while the four N-terminal zinc fingers bound to 5S rRNA

with lower affinity. Darby and Joho concluded that all zinc fingers of TFIIIA participate in 5S rRNA binding, but C-terminally located zinc fingers have the highest affinity for the RNA molecule. As all zinc finger segments from TFIIIA had some affinity for 5S rRNA, the existence of an affinity gradient was proposed, with the C-terminal zinc fingers contributing slightly more to RNA binding.

Darby and Joho then constructed a series of p43 carboxyl- and amino- terminal mutants to determine how the RNA-binding region of p43 compared to that of TFIIIA. The evidence presented by Darby and Joho for the binding 5S rRNA by TFIIIA has since been contradicted by the studies of Setzer (1996) and Hamilton (2001), described in greater detail below. However, the Darby and Joho study is the most recent attempt to study the interaction between p43 and 5S rRNA and further investigation into this interaction had been neglected until now. The results of the study by Darby and Joho into the interaction 5S rRNA binding by p43 will be described and compared to the results obtained by characterizing the mutants p43zf1-8, pW1-4 and pW5-8.

Darby and Joho deleted zinc finger four of p43 to the carboxyl terminus. The results of qualitative gel shift experiments showed that this deletion had no effect on 5S rRNA binding; however deletion of zinc finger four reduced the affinity of the protein for RNA. It was proposed that zinc finger four induced a specific conformation in either the protein or the RNA that was critical for high-affinity binding. In contrast to their results for TFIIIA, the two N-terminal zinc fingers of p43 were insufficient for binding to 5S rRNA and the C-terminal zinc fingers 5-9 appeared to have very weak RNA binding. These results lead to the conclusion that the zinc fingers from the N-terminus of p43 are essential for binding 5S rRNA. It was observed that the C-terminal fingers bind with

greater affinity when attached to the N-terminal fingers; Darby and Joho therefore concluded that p43 uses its N-terminal zinc fingers to initiate RNA binding even though all zinc fingers contribute to the overall binding affinity. N-terminal zinc fingers are therefore required in order for the C-terminal zinc fingers to make their contacts.

Further mutational evidence with respect to the interaction between TFIIIA and 5S rRNA that arose from investigations by both Hamilton's (2001) and Setzer's (1996) groups contradicted the TFIIIA-5S rRNA binding results published earlier by Joho and Darby (1992). It was shown that zinc fingers 4 - 7 of p43 could be exchanged for fingers 4-7 of TFIIIA without affecting TFIIIA's ability to bind 5S rRNA. However this study also revealed that a peptide containing p43 fingers 4 - 7 was not sufficient to elicit 5S rRNA binding (Hamilton *et al.*, 2001). These results raised the question of whether a strong interaction between one, or a combination of, zinc fingers 1 - 3, 8 or 9 in full-length TFIIIA are capable of preventing the interaction between zinc fingers 4 - 7 and the 5S rRNA. Indeed, this may be an explanation for the results of the quantitative assays with the mutants pW1-4 and pW5-8. It is possible that swapping the non-5S rRNA binding zinc fingers from WT1 for either the N- or C-terminal zinc fingers of p43 ablates the finger-finger interactions between the first and last four zinc fingers. This could permit the remaining p43 zinc fingers to contact the 5S rRNA in a novel manner not seen when all eight zinc fingers of p43 are presented to the RNA. This new mode of binding could explain the relative increase in binding affinity seen in the mutant pW5-8.

This rationalization is similar to a model for TFIIIA-5S rRNA binding proposed by Setzer and colleagues (1996), in which finger-finger interactions within the TFIIIA molecule prevent zinc fingers 1-3 from interacting strongly with the 5S rRNA. Setzer

suggested that energetically unfavourable interactions between individual zinc fingers in TFIIIA might play a role during interaction between the protein and 5S rRNA. In order to determine the type of functional interaction that might exist during 5S rRNA recognition, two peptides consisting of TFIIIA zinc fingers 1-3 and zinc finger 4-9 were analyzed with respect to their 5S rRNA binding affinities. The results revealed an unexpected level of complexity in the formation of the TFIIIA-5S rRNA complexes. Subsets of TFIIIA zinc fingers were uncovered that bound specifically to 5S rRNA in a structurally and kinetically unique manner. Surprisingly, the peptide containing the N-terminal zinc fingers of TFIIIA bound with a higher affinity than that observed for the full-length protein, indicating that the two ends of the protein interfere with one another in some way. Thus, in the full length TFIIIA molecule, the N-terminal three zinc fingers are prevented from interacting with 5S rRNA.

Setzer proposed that a novel form of interference exists between zinc fingers in TFIIIA when the protein binds to 5S rRNA. One or more modes of 5S rRNA recognition may occur when the mode of the binding favoured by the full-length protein is compromised. When wild-type binding is disrupted, an alternative, specific, high-affinity mode of binding is mediated at least in part by TFIIIA zinc fingers 1-3.

It was argued by Setzer's group that the binding sites for the two half-molecules may overlap on the 5S rRNA even though the corresponding regions in the full-length protein must occupy different positions than when wild type TFIIIA binds. All of the results from this study pointed to the formation of a complex in which the specific alignment of the zinc fingers relative to the 5S rRNA was altered. As a consequence,

novel protein-RNA interactions occur in the mutant TFIIIA containing complexes and result in higher affinity complexes than predicted.

This model could account for the less than expected decrease seen in pW1-4 binding. The rather unremarkable effects of the WT1 zinc-finger substitution can be understood as the consequence of the protein using an alternative mode of binding when those zinc fingers crucial for mediating the wild-type binding have been mutated. It is difficult to envision how these alternative modes of binding would be relevant under physiological conditions. These alternative modes of binding of p43 might be important in providing different cellular responses based on changes intracellular concentrations of this protein.

3.5 PROSPECTS

The results of my thesis represent a starting point in the study of the interaction between p43 and 5S rRNA. Future experiments that will help to explain the interactions between 5S rRNA and p43 include the characterization of a larger panel of directed mutants. It would be of interest to assay the mutants pW1-4, pW1-5 and p43zf1-8 by the yeast three-hybrid system to see if a white phenotype is observed.

If the model proposed by Setzer with respect to the interaction between TFIIIA and 5S rRNA is to be accepted for p43-5S rRNA binding, an important question to answer will be whether p43zf1-8, pW1-4 and pW5-8 bind to the same site on the 5S rRNA. A finer series of C- and N-terminal deletion mutants would enable the determination of the minimum binding region of p43 required for 5S rRNA interaction. Additionally, linker-scanning mutagenesis could be employed to provide further

information about the contribution of individual p43 zinc fingers to 5S rRNA binding. This could lead to quantification of the contribution of individual zinc fingers to RNA binding, and might serve to either prove or disprove the application of Setzer's model to the p43 problem.

Alternatively, a panel of finger swap mutants exchanging individual zinc fingers of p43 for zinc fingers from a non-5S rRNA binding protein, like WT1, could be employed. Results from such experiments would elucidate the specific zinc finger or even amino acid residues involved in 5S rRNA interaction. Once amino acid residues critical to 5S rRNA binding have been identified, the mutants with altered amino acid sequence could be expressed *in vivo* in *Xenopus* oocytes. This would ultimately lead to observations on the effect of changes in p43's ability to compete with TFIIIA for binding of 5S rRNA on the cellular fate of 5S rRNA and oocyte development.

4. CONCLUSIONS

p43, a key protein component of the 42S RNP storage particle, employs a tandem array of nine zinc finger domains to bind 5S rRNA. The difference between the binding specificities of p43 and TFIIIA, which is well characterized, provides an excellent system for investigating the differences in the molecular basis for RNA recognition. Interaction between p43 and 5S rRNA has been examined in a limited fashion by others; studies have been predominantly qualitative in nature, relying on nuclease probing of protein-nucleic acid complexes established with wild type or deletion variants of p43. The studies involving truncation mutations of p43 may have resulted in gross changes to the protein structure. The sole quantitative study that has been performed relied on full-length wild-type protein to generate data.

The present p43-5S rRNA analyses have utilized a number of random point mutations in addition to a series of zinc finger substitution mutants in an attempt to minimize changes in overall protein conformation. Changes in 5S rRNA binding affinity were quantified using nitrocellulose filter binding assays. The data presented are not consistent with earlier results. The carboxy-terminal end of p43 appears to play the greatest role in 5S rRNA as deletion of the C-terminal region of the protein lead to a reduced RNA-binding affinity. While zinc fingers 1-4 are required for RNA binding, the effect of disrupting the zinc-chelating properties or swapping out the amino-terminal zinc fingers of this region had no significant effect. All zinc fingers, however, contribute to some degree towards the interactions of p43 with 5S rRNA. The effects of both the randomly generated point mutations and the large zinc-finger substitutions on RNA

binding may be a consequence of the protein adopting an alternative mode of binding that has been proposed previously to explain the interaction of another nine-zinc finger protein, TFIIIA, with 5S rRNA.

5. LITERATURE CITED

Adams, R.L.P., Knowler, J.T., Leader, D.P. (1986) The Biochemistry of the Nucleic Acids, 10th Ed. Chapman & Hall, New York. p. 55, 276, 353, 471.

Ammons, D., Rampersad, J., Fox, G.E. (1999) 5S rRNA gene deletion cause an unexpectedly high fitness loss in *E. coli*. *Nucl Acids Res* **27**: 537-642.

Atmadja, J., Brimacombe, R., Maden, B.E. (1984) *Xenopus laevis* 18 S ribosomal RNA: experimental determination of secondary structural elements, and locations of methyl groups in the secondary structure model. *Nucl Acids Res* **8**: 2649.

Bacharach, E., Goss, S.P. (1998) Binding of the HIV type I Gag protein to the viral RNA encapsidation signal in the yeast-three hybrid system. *J Virol* **72**: 6944-9.

Ban, N., Nissen, P., Hansen, J., Moore, P.B., Steltz, T.A. (2000) The complete atomic structure of the large ribosomal subunit at 2.4 A resolution. *Science*. **289**: 905-920.

Barciszewska, M.Z., Szymanksi, M., Erdmann, V.A., Barciszewski, J. (2000) 5S ribosomal RNA. *Biomacromolecules* **1**: 297-302.

Bardeesy, N., Pelletier, J, (1998) Overlapping RNA and DNA binding domains of the WT1 tumor suppressor gene product. *Nucl Acids Res* **26**: 1784-92.

Baudin, F., Romaniuk, P.J., Romby, P., Brunel, C., Westhof, E., Ehresmann, E., Ehresmann, C. (1990) Involvement of "Hinge" Nucleotide of *Xenopus laevis* 5S rRNA in the RNA Structural Organization and in the Binding of TFIIIA. *J Mol Biol* **218**: 69-81.

Bernstein, D.S., Buter, N., Stumpf, C., Wickens, M. (2002) Analyzing mRNA-protein complexes using a yeast three-hybrid system. *Methods* **26**: 123-41.

Betzel, C., Lorenz, S., Furste, J.P., Bald, R., Zhang, M., Schneider, T.R., Wilson K.S., Erdmann, V.A. (1994) Crystal structure of domain A of *T. flavus* 5S rRNA and the contribution of water molecules to its structure. *FEBS Lett* **351**: 159-164.

Bieker, J.J, Roeder, R.G. (1984) Physical properties and DNA-binding stoichiometry of a 5S gene-specific transcription factor. *J Biol Chem* **259**: 6158.

Birkenmeier, E.H., Brown, D.D., Jordan, E. (1978) A nuclear extract of *Xenopus laevis* oocytes that accurately transcribes 5S RNA genes. *Cell* **15**: 1077.

Bolsovel, S.R., Hyams, J.S., Shepard, E.A., White, H.A., Wiedemann, C.O. (2004) Cell Biology 2nd edition. Chapter 6: Transcription and the Control of Gene Expression. John Wiley & Sons, Inc. Online. p105-127

Borel, F., Barilla, K.C., Hamilton, T.B., Iskandar, M., Romaniuk, P.J. (1996) Effects of Denys-Drash syndrome point mutations on the DNA binding activity of the Wilms' tumor suppressor protein WT1. *Biochemistry* **35**: 12070-6.

Boysen, R.I., Hearn, M.T. (2001) The metal binding properties of the CCCH motif of the 50 S ribosomal protein L36 from *Thermus thermophilus*. *J Pept Res* **57**:19-28.

Brown, D.D., Wensink, P.C., Jordan, E. (1971) Purification and some characteristics of 5S DNA from *Xenopus laevis*. *Proc Natl Acad Sci USA* **68**: 3175-9.

Brown, D.D, (1984) The role of stable complexes that repress and activate eukaryotic genes. *Cell* **37**: 359-65.

Brown, D.D., Schissel, M.S., (1985) The transcription of *Xenopus* 5S RNA genes in chromatin: the roles of active stable transcription complexes and histone H1. *Cell* **42**: 759.

Carey, J, Lowary, P.T., Uhlenbeck, O.C. (1983) Interaction of R17 coat protein with synthetic variants of its ribonucleic acid binding site. *Biochemistry* **22**: 4723-30.

Caricasole, A, Duarte, A., Larsson, S.H., Hastie, N.D., Little, M., Holmes, G., Todorov, I., Ward, A. (1996) RNA binding by the Wilms' tumor suppressor zinc finger proteins. *Proc Natl Acad Sci USA* **93**: 7562-6.

Cox, M.M., Nelson, D.L. (2000) Principles of Biochemistry. Worth Publishers, Inc. p.107.

Dahanukar, A., Alker, J.A., Wharton, R.P. (1999) Smaug, a novel RNA-binding protein that operates a translational switch in *Drosophila*. *Mol Cell* **4**: 2009-18.

Darby, M.K., Joho, K.E. (1992) Differential binding of zinc fingers from *Xenopus* TFIIIA and p43 to 5S RNA and the 5S RNA gene. *Mol Cell Biol* **12**: 3155-64.

Das, C., Frankel, A.D. (2003) Sequence and Structure Space of RNA-Binding Peptides. *Biopolymers* **70**: 80-85.

Daugherty, P. S., Chen, G., Iverson, B. L. and Georgiou, G. (2000) Quantitative analysis of the effect of the mutation frequency on the affinity maturation of single chain Fv antibodies. *Proc Natl Acad Sci USA* **97**: 2029-34.

Del Rio, S., Setzer, D.R. (1991) High yield purification of active transcription factor IIIA expressed in *E. coli*. *Nucl Acids Res* **19**: 6197-203.

De Sa, R.O., Hillie, D.M. (1990) Phylogenetic relationships of the pipid frogs Xenopus and Silurana: an integration of ribosomal DNA and morphology. *Mol Biol Evol* **7**: 365-76.

Dokudovskaya, S., Dontsova, O., Shpanchenko, O., Bogdanov, A, Brimacombe, R. (1996) Loop IV of 5S rRNA has contacts both to domain II and to domain V of the 23 S RNA. *RNA* **2**: 146-152.

Drew, P.D., Nagle, J.W., Canning, R.D., Ozato, K., Biddison,W.E., Becker,K.G. (1995) Cloning and expression analysis of a human cDNA homologous to Xenopus TFIIIA. *Gene* **159**: 215-218

England, T.E., Uhlenbeck, O.C. (1978) Enzymatic oligoribonucleotide synthesis with T4 RNA ligase. *Biochemistry* **17**:2069-81.

El-Baradi, T. and Pieler, T. (1991) Zinc finger proteins: what we know and what we would like to know. *Mech Dev* **35**: 155.

Fedoroff, N.V., Brown, D.D. (1978) The nucleotide sequence of oocyte 5S DNA in *Xenopus laevis*. I. The AT-rich spacer. *Cell* **13**: 701-16.

Fields, S., Song, O. (1989) A novel genetic system to detect protein-protien interactions. *Proc Natl Acad Sci USA* **8**: 5703-7.

Giege, Richard (1996) Interplay of tRNA-like structures from plant viral RNAs with partners of the translation and replication machineries. *Proc Natl Acad Sci USA* **93**: 12078-81.

Hamilton T.B., Turner, J., Barilla, K., Romaniuk, P.J. (2001) Contribution of individual amino acids to the nucleic acid binding activities of *Xenopus* zinc finger proteins TFIIIA and p43. *Biochemistry* **40**: 6093-101.

Hanas, J.S., Hocker, J.R., Cheng, Y.G., Lerner, M.R., Brackett, D.J., Lightfoot, S.A., Hanas, R.J., Madhusudhan, K.T., Moreland, R.J. (2002) cDNA cloning, DNA binding, and evolution of mammalian transcription factor IIIA. *Gene* **282**: 43-52.

Holmberg, L., Nygard, O. (2000) Release of ribosome-bound 5S rRNA upon cleavage of the phosphodiester bond between nucleotides A54 and A55 in 5S rRNA. *Biol Chem* **381**: 1041-46.

Honda, B.M., Roeder, R.G. (1980) Association of a 5S gene transcription factor with 5S RNA and altered levels of the factor during cell differentiation. *Cell* **22**: 119-26.

Hermann, T. (2003) Chemical and functional diversity of small molecule ligands for RNA. *Biopolymers* **70**: 4-18.

Invitrogen (2002) RNA-Protein Hybrid Hunter Kit: A system for the *in vivo* analysis of RNA-protein interactions in the yeast, *Saccharomyces cerevisiae.* p 2.

Jaeger, S., Eriani, G., Martin, F. (2004) Results and prospects of the yeast three-hybrid system. *FEBS Letters* **556**: 7-12

Jamieson, A.C., Miller, J.C., Pabo, C.O. (2003) Drug discovery with engineered zinc-finger proteins. *Nat Rev Drug Discov* **2**: 361-8.

Joho, K.E., Darby, M.K., Crawford, E.T., Brown, D.D. (1990) A zinc finger protein structurally similar to TFIIIA that binds exclusively to 5S RNA in *Xenopus. Cell* **61**: 293-300.

Jones, S., Daley, D.T., Luscombe, N.M., Berman, H.M., Thornton, J.M. (2001) Protein-RNA interactions: a structural analysis. *Nucl Acids Res* **29**: 943-54.

Krishna, S.S., Majumdar, I., Grishin, N.V (2003) Structural classification of zinc fingers. *Nucl Acids Res* **31**: 532-550.

Kyte, J. Doolittle, R.F. (1982) A simple method for displaying the hydropathic character of a protein. *J Mol Biol* **157**: 105-32.

Ladomer, M,., Sommerville, J., Woolner, S., Slight, J., Hastie, N. (2003) Expression in *Xenpous* oocytes shows that WT1 binds transcripts *in vivo*, with a central role for zinc finger one. *J Cell Science* **116**: 1539-49.

Laity, J.H., Lee, B.M., Wright, P.E. (2001) Zinc finger proteins: new insights into structural and functional diversity. *Curr Opin Struct Biol* **11**: 39-46.

Lee, E., Yeo, A., Kraemer, B., Wickens, M., Linial, M.L. (1999) The gag domains required for avian retroviral RNA encapsidation determined by using two independent assays. *J Virol* **73**: 6282-92.

Leontis. N.B., Westhof, E. (1998) The 5S rRNA loop E chemical probing and phylogenetic data versus crystal structure. *RNA* **4**: 1134-53.

Li, Y., Altman, S. (2003) A specific endoribonuclease, Rnase P, affects gene expression of polycistronic operon mRNAs. *Proc Natl Acad Sci USA* **100**: 13213-8.

Long, R.M., Gu, W., Lorimer, E., Singer, R.H., Chartrand, P. (2000) She2p is a novel RNA-binding protein that recruits the Myo4p-She3p complex to ASH1 mRNA. *EMBO J* **19**: 6592-601.

Lowary, P. T., Uhlenbeck, O. C. (1987) An RNA mutation that increases the affinity of an RNA-protein interaction. *Nucl Acids Res* **15**: 10483-93.

Lu, D., Searles, M.A., Klug, A. (2003) Crystal strucure of a zinc-finger RNA complex reveals two modes of molecular recognition. *Nature* **426**: 96-100.

Mairy, M., Denis, H. (1971) Biochemical studies on oogenesis: RNA synthesis and accumulation during oogenesis of the South African toad *Xenopus laevis*. *Dev Biol* **24**: 143-65.

Mairy, M., Denis, H. (1972) Biochemical studies on oogenesis: Ribosome assembly during the development of oocytes in *Xenopus laevis*. *Eur J Biochem* **25**: 535-43.

Martin, F., Michel, F., Zenklusen, D., Muller, B. Schumperli, D. (2000) Positive and negative mutant selection in the human histone binding protein using the yeast three-hybrid system. *Nucl Acids Res* **28**: 1594-603.

McBryant, S.J., Veldhoen, N., Gedulin, B., Leresche, A., Foster, M.P., Wright, P.E., Romaniuk, P.J., Gottesfeld, J.M. (1995) Interaction of the RNA Binding Fingers of *Xenopus* TFIIIA with Specific Regions of 5S rRNA. *J Mol Biol* **248**: 44-57.

Miller J, McLachlan AD, Klug A. (1985) Repetitive zinc-binding domains in the protein transcription factor IIIA from *Xenopus* oocytes. *EMBO J* **4**: 1609-14.

Nachtigal, M.W., Hirokawa, Y., Enyeart-VanHouten, D.L., Flanagan, J.N., Hammer, G.D., Ingraham, H.A. (1998) Wilms' tumor 1 and Dax-1 modulate the orphan nuclear receptor SF-1 in sex-specific gene expression. *Cell* **93**: 445-54.

Oldenburg, K.R., Vo, K.T., Michaelis, S., Paddon, C. (1997) Recombination-mediated PCR-directed plasmid construction *in vivo* in yeast. *Nucl Acids Res* **25**: 451-2.

Pavletich, N.P., Pabo, C.O. (1991) Zinc-Finger-DNA recognition: crystal structure of a Zif268-DNA complex at 2.1 Å. *Science* **252**: 809-816.

Peattie, D..A., Douthwaite, S., Garrett, R.A., Noller, H.F. (1981) A bulged double helix in a RNA-protein contact site. *Proc Nat Acad Sci USA* **78**: 7731-35.

Perrotti D, Calabretta B. (2004) Translational regulation by the p210 BCR/ABL oncoprotein. *Oncogene* **23**: 3222-9.

Pieler, T. (1994) Chapter 8: Interaction of 5 S RNA with TFIIIA p. 178-188.

Putz, U., Skehel, P., Kuhl, D. (1996) A tri-hybrid system for the analysis and detection of RNA-protein interactions. *Nucl Acids Res* **24**: 4838-40.

Putz, U., Kremerskothen, J., Skehel, P., Kuhl, D. (2000) RNA-Protein Interactions Reconstituted by a Tri-Hybrid System. Yeast Hybrid Technologies. Eaton Publishing, Natick, MA.

R Development Core Team, R: A language and environment for statistical computing. R Foundation for Statistical Computing, Vienna, Austria, 2004 (http://www.R-project.org)

Ren, D. Collingwood, T.N., Rebar, E.J., Wolfee, A.P., Camp H.S. (2002) PPARγ knockdown by engineered transcription factors: exogenous PPARγ2 but not PPARγ1 reactivates adipogenesis. *Genes Dev* **16**: 27-32.

Robzyk, K, Kassir, Y. (1992) A simple and highly efficient procedure for rescuing autonomous plasmids from yeast. *Nucleic Acids Res* **20**: 3790.

DIG Gel Shift Kit, 2nd Generation. Instruction Manual. (2003) RocheApplied Science. Basel, Switzerland. p. 6, 22.

Romaniuk, P.J. (1989) The role of highly conserved single-stranded nucleotides of *Xenopus* 5S RNA in the binding of TFIIIA. *Biochemistry* **28**: 1388-95.

Romaniuk, P.J. (1985) Characterization of the RNA binding properties of TFIIIA of *Xenopus laevis* oocytes. *Nucleic Acids Res* 13: 5369-87.

Rosset, R., Monier, R. (1963) Apropos of the presence of weak molecular weight RNA in the ribosomes of *E. coli. Biochim Biophys Acta* **68**: 653-6.

Ryan, R.F., Darby, M.K. (1998) The role of zinc finger linkers in p43 and TFIIIA binding to 5S rRNA and DNA. *Nucleic Acids Res* **26**: 703-9.

Sambrook, J., Fritsch, E.F., Maniatis, T. (1989) Molecular Cloning: A Laboratory Manual. Cold Spring Harbour, Cold Spring Harbour Laboratory Press.

Sands, M.S., Bogenhagen, D.F. (1991) Two zinc finger proteins from *Xenopus laevis* bind the same region of 5S RNA but with different nuclease protection patterns. *Nucleic Acids Res* **19**: 1797-803.

Scripture, J.B., Huber, P.W. (1995) Analysis of the binding of *Xenopus* ribosomal protein L5 to oocyte 5S rRNA *J Biol Chem* **270**: 27358-365.

SenGupta, D.J., Zhang, B., Kraemer, B., Pochart, P, Fields, S., Wickens, M. (1996) A three-hybrid system to detect RNA-protein interactions *in vivo*. *Proc Natl Acad Sci USA* **93**: 8496-501.

Setzer, D.R, Menezes, S.R., Del Rio, S. Hung, V.S., Subramayan, G. (1996) Functional interactions between the zinc fingers of *Xenopus* transcription factor IIIA during 5S RNA binding. *RNA* **2**: 1254-69.

Shafikhani, S., Siegel, R. A., Ferrari, E. and Schellenberger, V. (1997) Generation of large libraries of random mutants in *Bacillus subtilis* by PCR-based plasmid multimerization. *Biotechniques* **23**: 304-10.

Sonoda, J., Wharton, R.P. (2001) *Drosophila* Brain Tumor is a translational repressor. *Genes Dev* **20**: 2212-14.

Stryer, L. (1995) Biochemistry 4th edition. W.H. Freeman & Co., New York. Media Supplement CD-ROM.

Szymanski, M., Bariszewska, M.Z., Erdmann, V.A., Baricszewski, J. (2003) 5S rRNA: structure and interactions. *Biochem J* **371**: 641-651.

Szymanski, M., Bariszewska, M.Z., Erdmann, V.A., Baricszewski, J. (2000) An analysis of G:U base pair occurrence in eukaryotic 5S rRNAs. *Mol Biol Evol* **17**: 1194-8.

Tinoco, I., Borer, P.N., Dengler, B., Levine, M.D., Uhlenbeck, O.C., Crothers, D.M., Gralla, J. (1973) Improved estimation of secondary structure in ribonucleic acids. *Nature* **246**: 40.

Theunissen, O., Rudt, F., Guddat, U., Mentzel, H, Pieler, T. (1992) RNA and DNA binding zinc fingers in *Xenopus* TFIIIA. *Cell* **71**: 679-90.

Theunissen, O., Rudt, F., Pieler, T. (1998) Structural determinants in 5S RNA in TFIIIA for 7S RNP formation. *Eur J Biochem* **258**: 758-67.

Uhlenbeck, O. C., Carey, J., Romaniuk, P. J., Lowary, P. T., and Beckett, D. (1983) Interaction of R17 Coat Protein with its RNA Binding Site for Translational Repression. *J Biomol Struct Dyn* **1**:539-552.

Uil, T.G., Haisma, H.J., Rots, M.G. (2003) Therapeutic modulation of endogenous gene function by agents with designed DNA-sequence specificities. *Nucleic Acids Res* **31**: 6064-6078.

Veldhoen, N. (1995) Studies on the nucleic acid interactions of Xenopus transcription factor IIIA. Phd Thesis.

Vartanian, J. P., Henry, M. and Wain-Hobson, S. (1996) Hypermutagenic PCR involving all four transitions and a sizeable portion of transverions. *Nucleic Acids Res* **24**: 2627-31.

Wagner, K.D., Wagner, N., Schedl, A. (2003) The complex life of WT1. *J Cell Sci* **116**: 1653-8.

Wan, L., Twitchett, M. B., Eltis, L. D., Mauk, A. G. and Smith, M. (1998) *In vitro* evolution of horse heart myoglobin to increase peroxidase activity. *Proc Natl Acad Sci USA* **95**: 12825-31.

Wang, Z.F., Whitfield, M.L., Indledue, T.C., Dominski, Z., Marzluff, W.F. (1996) The protein that binds the 3' end of histone mRNA: a novel RNA-binding protein required for histone pre-mRNA processing. *Genes Dev* **10**: 3028-40.

Weeks, K.M, Crothers, D.M. (1993) Major groove accessibility of RNA. *Science* **261**: 1574-7.

Weil, P.A., Segall, J., Harris, B., Ng, S.Y., Roeder, R.G. (1979) Faithful transcription of eukaryotic genes by RNA polymerase III in systems reconstituted with purified DNA templates. *J Biol Chem* **254**: 6463.

Woese, C.R, Magrum, L.J., Gupta, R., Siegel, R.B., Stahl, D.A., Kop, J., Crawford, N., Brosius, J., Gutreil, R., Hogan J.J., Noller, H.F. (1980) Secondary structure model for bacterial 16S ribosomal RNA: phylogenetic, enzymatic and chemical evidence. *Nucleic Acids Res*. **8**: 2275.

Wu, G.-J. (1978) Adenovirus DNA-directed transcription of 5.5S RNA *in vitro*. *Proc Natl Acad Sci USA* **75**: 2175.

You, Q, Romaniuk, P.J. (1990) The effects of disrupting 5S RNA helical structures on the binding of *Xenopus* TFIIIA. *Nucleic Acids Res* **18**: 5055-62.

You, Q., Veldhoen, N., Baudin, F., Romaniuk, P.J. (1991) Mutations in 5S DNA and 5S RNA Have Different Effects on the Binding of *Xenopus* TFIIIA. *Biochemistry* **30**: 2495-500.

Zang, W.Q., Romaniuk, P.J. (1995) Characterization of the 5 S RNA binding activity of *Xenopus* zinc finger protein p43. *J Mol Biol* **245**: 549-58.

Zarudnaya, M.I., Kolomiets, I.M., Hovorun, D.M. (2002) What nuclease cleaves pre-mRNA in the process of polyadenylation? *IUBMB Life* **54**:27-31.

Zhai, G., Iskandar. M., Barilla, K., Romaniuk, P.J. (2001) Characterization of RNA aptamer binding by the Wilms' tumor suppressor protein WT1. *Biochemistry* **40**: 2032-40.

Zhang, B., Gallegos, M., Puoti, A., Durkin, E., Fields, S., Kimble, J., Wickens, M.P. (1997) A conserved RNA binding protein that regulates patterning of sexual fates in the *C. elegans* hermaphrodite germ line. *Nature* **390**: 477-84.

Zhu, L., Hannon, G.J. (2000) Yeast Hybrid Technologies. Eaton Publishing, Biotechniques books division, Natick, MA. p103.